

Dissertation
submitted to the
Combined Faculties for the Natural Sciences and for Mathematics
of the Ruperto-Carola University of Heidelberg, Germany
for the degree of
Doctor of Natural Sciences

presented by
M.Sc. by Research, Nisit Khandelwal
born in Kolkata, India
Oral-examination:

**Identification of novel tumor-associated immune modulators
using a high-throughput RNAi screen**

Referees: Prof. Dr. Philipp Beckhove

Prof. Dr. Michael Boutros

Parts of this thesis have been published in:

N Khandelwal, M Breinig, T Speck, C Kreutzer, T Michels, A Sorrentino, L Umansky, H Conrad, I Poschke, R Offringa, H Bernhard, A Machlenkin, M Boutros, P Beckhove. A high-throughput RNAi screen for detection of immune-checkpoint molecules that mediate tumor resistance to cytotoxic T lymphocytes (*manuscript under submission*).

N Khandelwal, J Bruder, A Sorrentino, M Witzens-Harig, H Conrad, S Juenger, C Kreutzer, I Poschke, R Offringa, H Bernhardt, P Beckhove. CEACAM-6 on tumor cells inhibits anti-tumor T cell response via interaction with CEACAM-1 (*manuscript under preparation*).

M Witzens-Harig, D Hose, S Jünger, C Pfirschke, **N Khandelwal**, L Umansky, A Seckinger, H Conrad, B Brackertz, A Seckinger, T Rème, B Gueckel, T Meißner, M Hundemer, AD Ho, JF Rossi, K Neben, H Bernhardt, H Goldschmidt, B Klein and P Beckhove. Tumor cells in multiple myeloma patients inhibit myeloma-reactive T cells through carcinoembryonic-antigen-related cell adhesion molecule-6. *Blood*. 2013. 121(22): 4493-503.

N Khandelwal, M Breinig, H Conrad, T Speck, H Bernhard, L Umansky, M Boutros and P Beckhove. A high-throughput RNAi screen unravels new immune-checkpoint molecules that mediate tumor resistance to cytotoxic T lymphocytes. AACR Tumor Immunology Conference, Miami, USA. 2012. p96.

N Khandelwal, M Witzens-Harig, D. Hose, C. Pfirschke, A. Seckinger, H. Conrad, H. Bernhard, H. Goldschmidt, B. Klein, P. Beckhove. Human tumor cells inhibit T-cell responses through expression of CEACAM-6. *European Journal of Cancer*. 2012. 48: suppl. 5, S265.

N Khandelwal, P Beckhove, M Boutros, M Breinig. Patent pending at the *US Patent and Trademark Office*.

Acknowledgements

While I wrap up this beautiful journey of trial and triumph, I feel instinctively compelled to express my deepest and sincerest gratitude towards my mentor **Prof. Dr. Philipp Beckhove** whose vision and guidance has made this mountain of work possible. Your unfaltering faith in my capability to shape up this project from scratch to a story while providing your constant support and motivation has made this Ph.D. a true learning experience!

At the same time I am indebted to **Prof. Dr. Michael Boutros** for not only being my examiner, but also for his mentorship, enthusiasm and his regular feedback on the progress of the project throughout. It has been one of the most enriching collaboration I could possibly imagine.

My sincere gratitude to **Prof. Dr. Michael Kirschfink** for his valuable comments and suggestions during my Thesis Advisory Committee meetings that helped shape the project. A big thanks goes to **Dr. Marco Breinig** who helped in setting up and analyzing the RNAi screen. Without his untiring support and constructive criticism, this project would never have taken off the ground. So thanks a lot Marco for truly being there!

This work would also have been incomplete without the eager participation, earnest hard work and fruitful contributions from my Masters student and a good friend **Tobias Speck**. Special thanks goes to **Tillmann Michels** and **Antonio Sorrentino** too who have enriched this project with their individual contributions.

I couldn't imagine staying on course this long had it not being for the most warm and welcoming atmosphere in the lab thanks to the most awesome colleagues-cum-friends. So a big thanks to all of you for making this an enjoyable ride, starting with **Christoph Schlude, Felix Klug, Hans-Henning Schmidt, Maria Xydia, Jasmin Quandt, Anna-Lena Krause** and ending with **Noemi, Slava, Anchana, Diane, Lilli** and **Chih-yeh**. Special thanks to **Dr. Gerhard Moldenhauer** for providing the bi-specific antibody, **Christiane Kreutzer** for expanding the T cell clones, **Simone Jünger** and **Mariana Bucur** for their technical help and exuberant presence and **Ludmila Umansky** for performing the luminex analysis.

“Some people go to priests, others to poetry, I to my friends”, said Virginia Woolf and I couldn’t agree more. Heidelberg and this Ph.D. gave me the opportunity to meet some of the most wonderful people in my life and an opportunity to forge life-long friendships. **Taronish, Serena, Ashwin, Ivana, Andrea, Devanjali, Mudita, Vignesh, Shariq** – thanks a lot for being there! A special mention of the fellow members of the legendary PhD Student Council of 2012- **Aoife, Dharanija, Ansam, Nao and Alex** – who have made this journey extra special. Thank you guys!

Words fail when it comes to expressing my humble gratitude towards my parents who gave me the freedom to pursue my dreams and Nilay, my brother, who helped in transforming those dreams into reality. So thank you **Maa, Mom, Dad, Nilay** and **Khusbhu** for standing by my side and for having faith in my decisions because that means a world to me!

*Dedicated to my parents
and to countless others alike
for their unsurpassable strength in their grievances.....*

Summary

Immune surveillance by T cells is an important component of body's defense against infection and disease, whereas the peripheral immune tolerance is important for defense against self-reactive T cells. The fine balance between the two is skewed in cancer, whereby the tumors exploit the immune tolerance mechanisms to escape recognition and elimination by the cytotoxic T lymphocytes (CTLs). One of the major routes of immune resistance of tumor cells is mediated by cell surface bound ligands that engage immune-inhibitory receptors on T cells. Targeting these immune-checkpoint ligands that inhibit immune rejection, e.g. via blocking antibodies, can restore immune surveillance and increase the efficacy of cancer immunotherapy. However, only a few such targets have been identified so far.

The aim of this thesis was to establish a high-throughput screening assay that enables a rapid and comprehensive identification of cell surface genes with immune modulatory function in selected tumors. To this end, a tumor cell-T cell co-culture assay was established which combines siRNA-based gene knockdown with a luciferase-based assessment of T cell-mediated tumor cell killing. Applied to three independent parallel screens, this study uncovered a repertoire of novel and robust immune modulatory ligands on breast cancer cells that are also abundantly expressed by other cancer types. Amongst them, CCR9 was functionally validated as a strong inhibitor of T cell function and suppressor of T cell reactivity against breast cancer, malignant melanoma and pancreatic cancer. Knockdown of CCR9 resulted in increased tumor susceptibility towards immune lysis by antigen-experienced T cells along with the increased production of effector cytokines and cytolytic enzymes. CCR9-induced gene expression changes in the encountering T cells were consistent with an enhanced effector T cell phenotype. Mechanistically, CCR9 regulated T cell effector function through differential activation of the STAT signaling pathways, thereby representing a unique example of an alternative, TCR-independent route for effective immune suppression induced by a cell surface molecule. Additionally, the *in vivo* relevance of targeting CCR9 for adoptive cancer immunotherapy was explored in this study.

Taken together, this study describes a rapid, high-throughput, siRNA-based screening approach that allows a comprehensive identification of immune-modulatory genes which, as an entity, represents the 'immune modulome' of cancer. Screening additional tumor types for their immune modulatory signatures would help in uncovering additional targets for therapeutic inhibition.

Zusammenfassung

T-Zellen spielen eine wichtige Rolle bei der Abwehr von Pathogenen und Krankheiten, die periphere Toleranz hingegen schützt vor selbst-reaktiven T-Zellen. Das Gleichgewicht zwischen diesen beiden Mechanismen ist bei Krebserkrankungen gestört und der Tumor nutzt die Mechanismen der peripheren Toleranz, um der Erkennung und Eliminierung durch zytotoxische T-Zellen zu entgehen. Einen der wichtigsten Mechanismen stellen dabei Liganden auf der Zelloberfläche der Tumorzellen dar, die inhibitorische Rezeptoren auf T-Zellen binden. Ein Blocken dieser *immune-checkpoint*-Liganden, zum Beispiel mittels Antikörpern, kann das Erkennen des Tumors durch das Immunsystem wiederherstellen und die Effizienz von Immuntherapien erhöhen. Bisher wurden nur wenige dieser Liganden identifiziert.

Das Ziel dieser Doktorarbeit war die Entwicklung eines Hochdurchsatz-*Screens* zur schnellen und umfassenden Identifizierung von Molekülen mit immunmodulierender Wirkung auf der Oberfläche von Krebszellen. Zu diesem Zweck wurde die Kokultur von Tumorzellen und T-Zellen mit einem siRNA basiertem *knockdown* kombiniert. Das Töten der Tumorzellen durch die T-Zellen wurde dabei mit einem Luciferase-Assay gemessen. Mit Hilfe dieser Methode wurden in drei voneinander unabhängigen Screens neue immunmodulierende Liganden auf Brustkrebs-Zellen gefunden, die jedoch auch auf anderen Tumorentitäten überexprimiert sind. Von den Liganden wurde CCR9 als ein starker Inhibitor der T-Zell Antwort gegen Zellen aus Brustkrebs, malignem Melanom und Pankreaskarzinom funktional validiert. Der *knockdown* von CCR9 führt zu einer größeren Empfänglichkeit der Tumorzellen gegenüber einer Lyse durch Antigen-erfahrene T-Zellen sowie zu einer erhöhten Produktion von Effektor-Zytokinen und lytischen Enzymen der T-Zellen. Eine Genexpressions-Analyse der T-Zellen zeigt einen verstärkten Effektor-Phänotyp nach *knockdown* von CCR9 in den Krebszellen. Mechanistisch reguliert CCR9 die T-Zell Effektor-Funktionen über die differenzielle Aktivierung von STAT-Signalwegen. Dies stellt einen alternativen, von Oberflächenmolekülen aktivierten Suppressions-Mechanismus dar, der vom Signalweg des T-Zellrezeptors unabhängig ist. Zusätzlich wurde die Relevanz von CCR9 für eine adoptive Immuntherapie *in vivo* untersucht.

Diese Arbeit beschreibt einen Hochdurchsatz-*Screen* zur umfassenden Identifikation von immunmodulierenden Molekülen, die in ihrer Gesamtheit das „Immun-Modulator“ von Krebs darstellen. Die Untersuchung der immunmodulierenden Signatur weiterer Tumorentitäten kann zusätzliche Ziele für eine verbesserte Immuntherapie hervorbringen.

Table of Contents

1. Introduction	1
1.1 Cancer	1
1.2 Anti-tumor immunity	2
1.3 Cancer despite immunosurveillance: the 3E's of cancer immune-editing	4
1.4 Immune-escape pathways	5
1.4.1 Impairment of antigen-presentation by tumors	5
1.4.2 Elaboration of soluble immune-suppressive mediators	6
1.4.3 Specific recruitment of the immune-regulatory cell populations	7
1.4.4 Activation of negative co-stimulatory signals on the immune cells	9
1.4.4.1 CTLA4-CD80/CD86 axis	10
1.4.4.2 PD1-PDL1 axis	11
1.4.4.3 Other immune modulatory ligands	13
1.5 High-throughput RNAi-based screen	16
1.5.1 RNAi: principle and formats	16
1.5.2 Cell-based assays and workflow for an RNAi screen	18
1.5.3 Data analysis from RNAi screen experiments	19
1.6 Aims and objectives of the thesis	21
2. Materials	22
2.1 Chemicals, reagents and consumables	22
2.2 Assay kits	25
2.3 Buffers	25
2.4 Media and supplements	28
2.5 Cell lines	30
2.6 Antibodies	31
2.6.1 Flow cytometry	31
2.6.2 Immunoblot	32
2.6.3 Cell-based assays	32
2.7 Mice	33
2.8 Equipments	33
2.9 Additional software	34
3. Methods	35
3.1 Cell culture techniques	35
3.1.1 Tumor cell lines	35
3.1.2 Generation of stable CCR9 knockdown cell lines	35

3.2	Molecular biology techniques	36
3.2.1	RT-PCR	36
3.2.2	Protein extraction.....	37
3.2.3	Immunoblotting	37
3.2.4	Bacterial transformation and plasmid extraction.....	38
3.2.5	Reverse siRNA transfection	38
3.2.6	Plasmid Transfection	39
3.2.7	Fluorescent microscopy	39
3.2.8	Cell viability assays	39
3.2.9	Transwell migration assay	40
3.2.10	Global gene expression analysis	40
3.3	Immune-RNAi screen	41
3.3.1	Screen layout and the Luc-CTL assay.....	41
3.3.2	Data analysis.....	42
3.4	Immunological techniques.....	43
3.4.1	T cell isolation and activation.....	43
3.4.2	Rapid expansion protocol (REP) for TILs.....	43
3.4.3	⁵¹ Chromium-release Assay	44
3.4.4	ELISpot Assays	45
3.4.5	ELISA	45
3.4.6	Cytokine measurements using luminex.....	46
3.4.7	Phosphoprotein analysis	46
3.4.8	Imprinting T cells with immunosuppressive tumor supernatants.....	47
3.4.9	Flow cytometry.....	47
3.5	Mouse work	48
3.6	Statistical evaluation	49
4.	Results	50
4.1	Establishment of the Luc-CTL cytotoxicity assay for immune-RNAi screen	50
4.2	Optimization of RNAi screen parameters	52
4.3	Antigen-restricted and antigen-unrestricted T cells for the high-throughput screen ..	54
4.4	Immunosuppressive positive controls for the screen.....	57
4.5	Workflow and performance of the high-throughput RNAi screen	58
4.6	Data analysis and hit-calling parameters.....	62
4.7	Validating potential immunosuppressors in the re-run of the primary assay	63
4.8	Knockdown of CCR9 sensitizes the breast cancer cells towards immune lysis	64
4.9	Overexpression of CCR9 on breast cancer cells inhibits immune lysis	67

4.10	CCR9 inhibits the secretion of cytolytic enzymes and Th1 cytokines.....	67
4.11	CCR9 expression in melanoma inhibits the anti-tumor reactivity of TILs	68
4.12	CCR9 suppresses the tumor lysis potential of TILs in pancreatic adenocarcinoma	70
4.13	Tumor-specific CCR9 does not impair the activation of the TCR signaling.....	72
4.14	CCR9 impedes STAT signaling in antigen-specific T cells	74
4.15	Role of CCL25 in CCR9-mediated immune-suppression	76
4.16	CCR9-mediated immune suppression requires direct cellular contact with T cells.....	78
4.17	CCR9 induces immune-suppressive gene signatures in encountered T cells	79
4.18	Synergistic blockade of immunomodulators: CCR9, PD-L1 & CEACAM6.....	82
4.19	Tumor pathways modulated by CCR9	83
4.20	Blocking antibody for inhibiting CCR9's immunosuppressive effect.....	84
4.21	CCR9 inhibition results in delayed tumor growth <i>in vivo</i>	85
4.22	Extension of the screening methodology to additional tumor entities	89
5.	Discussion	92
5.1	High-throughput screening for immune modulatory genes.....	92
5.1.1	Assessment of cytotoxicity	92
5.1.2	Gene knockdown for high-throughput approaches	94
5.1.3	T cell recognition format for high-throughput assays	95
5.1.4	Performance and interpretation of the high-throughput screen	96
5.2	Functional validation of the high-throughput screen	99
5.2.1	C-C chemokine receptor 9 (CCR9)	99
5.2.2	Synergy of CCR9 with other immune-checkpoint pathways	106
5.2.3	<i>In vivo</i> relevance of CCR9 inhibition on anti-tumor immunity.....	107
5.3	Identification of tumor-associated immune activators by the RNAi screen.....	110
5.4	Outlook.....	112
6.	References:	115
7.	Appendix	132
8.	Abbreviations and definitions	134

1. Introduction

1.1 Cancer

In the present day world where at least one out of every 5 person suffers from cancer, cancer is a household subject that requires little introduction. More than 8.2 million deaths were accorded to cancer in 2012 worldwide (1). Amongst this, breast cancer, which results from the neoplasm arising from the inner linings of the milk ducts or lobules of the healthy breast tissue, has been the most frequently diagnosed form of cancer in women and the leading cause of cancer-related mortality with 522,000 deaths reported in 2012 (1). But cancer is more than just this mere representation of staggering statistics. Sun Tzu, an ancient military general and strategist, in his book titled ‘The Art of War’ said: “If you know neither the enemy nor yourself, you will succumb in every battle”. This age-old wisdom for successful combat also applies to our current fight against cancer where ‘knowing thy enemy’ would be the first milestone towards successful cancer therapy.

Cancer is the malignant transformation of a normal cell to a state of uncontrolled proliferation that is capable of propagating throughout the body, infringing on the normal functioning of healthy organs and thereby endangering the survival of the host. In 2000, Douglas Hanahan and Robert Weinberg (2) fittingly summarized the complexity of cancer to six key hallmark signatures according to which cancer cells: i) stimulate their own growth; ii) resist anti-growth signals; iii) inhibit their programmed cell death (apoptosis); iv) stimulate the growth of blood vessels in order to fetch nutrients (angiogenesis); v) multiply uncontrollably; and vi) can invade to local and distant sites (metastasis). Their oversight of the role of the immune system in shaping tumor progression was rectified in a follow-up publication a decade later (3), whereby they added two new additional hallmarks of cancer as: vii) evading the immune system; and viii) deregulating the metabolic circuitry.

Despite the fact that considerable progress has been made over the last decade in dissecting the molecular basis of cancer, a great deal of knowledge still remains to be acquired regarding the complex interplay between the tumor and the host, as well as its regulation thereof. In a broader sense, this thesis is focused on *knowing thy enemy* in which I attempt to further characterize cancer to the next level by defining its immune modulatory properties. But before

going into that, it is important to understand how the immune system plays a role in cancer development.

1.2 Anti-tumor immunity

The theory of immunosurveillance, put forward by Burnet and Thomas way back in the 1950s, underlines the fact that the host immune system is capable of recognizing the transformed self-cells right at the early stage of tumor development (4). Over time this theory has found increased experimental validation and reinforcement, with both the innate and the adaptive arms of the immune system being shown to play a role in controlling tumor outgrowth. In fact the occurrence of tumor antigen-specific T cells in the tumor microenvironment is a predictive biomarker for improved survival in cancer patients, especially for melanoma and colorectal cancer patients (5, 6). Generation of anti-tumor immunity, however, is a multi-step process described in the so-called 'Cancer Immunity Cycle' (Figure I) (7):

- i. For mounting an effective immune response, first the tumor-associated neo-antigens have to be released so that they can be captured, processed and presented by the professional antigen presenting cells (APC), such as dendritic cells (DC), present in the tumor bed. Immunogenic cell death inducers, such as certain chemotherapeutic agents and radiotherapy, aid in this antigen release process (8). Tumor-associated antigens (TAAs) that are recognized by the immune system can be broadly classified into six categories: overexpressed self antigens (such as EpCAM, survivin), cancer testis antigens (such as MAGEA1), tissue differentiation antigens (melanosome-related antigens such as MART1), chromosomal breakpoint antigens (such as BCR-ABL), mutated self-antigen (such as mutated KRAS or p53) and finally oncogenic virurs-encoded antigens (such as HPV-16 virus encoded E6 and E7). Whole genome exome sequencing has revealed that the success of generating high frequency antigen-specific anti-tumor immune response is correlative to the mutational frequency of certain tumors, especially in case of melanoma, colon and lung cancer (9, 10) which have been shown to harbor higher mutations per megabase (11).

- ii. Following the uptake of antigen, DCs undergo maturation, receiving stimulatory signals from the proinflammatory cytokines and co-signaling receptors (such as TNF- α , IFN- α , ATP from dying tumor cells, CD40/CD40L interaction). This results in mature DCs that are capable of processing and presenting the antigenic peptides on their surface bound to the MHC-I or MHC-II molecules.
- iii. MHC receptor-bound peptides are then presented by DCs to the naïve T cells in the lymph nodes to prime the T cell response against the presented antigen. The nature of the immune response is determined at this stage depending on whether immune tolerance is induced towards the presented antigen (mediated by regulatory T cell priming and expansion) or anti-tumor immunity is induced (leading to effector T cell generation).
- iv. Effector CD8⁺ T cells primed in the above stage then migrates to the tumor site by virtue of chemokine and chemokine receptors, such as CXCL9 and CXCL10 (ligands for CXCR3) or CCL5 (ligand for CCR5) among others (12).
- v. The next challenge for the immune cells is to infiltrate the tumor bed by crossing through the endothelial barrier, which is achieved via the virtue of adhesion molecules such as LFA1, ICAM1, selectins etc.
- vi. Once in the tumor microenvironment, the effector T cells then have to recognize and bind to their tumor targets through interaction between its antigen-specific T cell receptor (TCR) and the MHC-I bound cognate antigen on the tumor cell surface.
- vii. Finally, antigen-recognition and binding activates the downstream TCR signaling in these antigen-specific cytotoxic T lymphocytes (CTLs), leading to the release of effector cytokines such as interferon-gamma (IFN- γ), interleukin-2 (IL-2) and cytolytic granules containing enzymes such as granzyme-B and perforin. These effector mechanisms not only bring about the tumor lysis, but also result in the release of fresh antigens that can be taken up by surrounding APCs for re-initiating the immune response cycle.

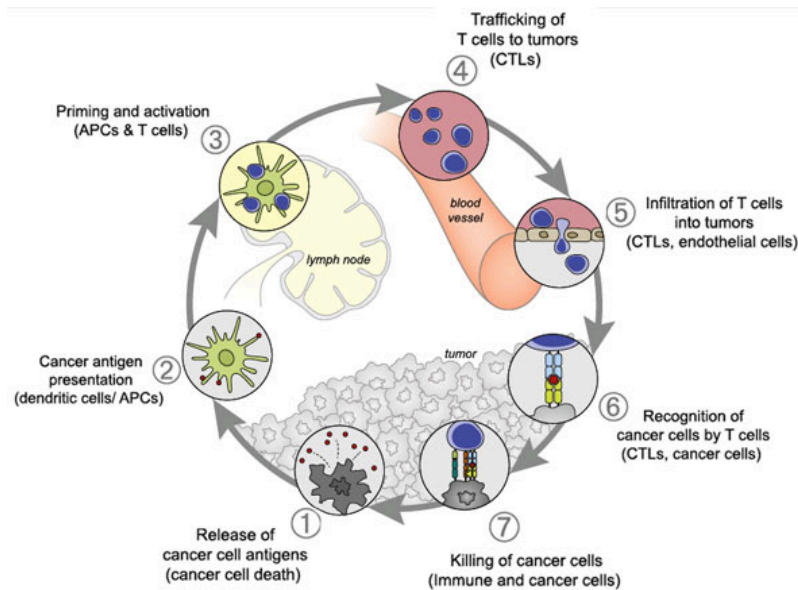


Figure I. Cancer immunity cycle detailing the seven-step process involved in the generation of an anti-tumor immune response. Individual steps are detailed in the text above. Adapted from *Chen et al, 2013 (7)*.

1.3 Cancer despite immunosurveillance: the 3E's of cancer immune-editing

Given that the immune system can recognize and eliminate malignant self-cells in a specific manner, early immunotherapists anticipated distinct clinical responses in tumor patients upon adoptive cellular transfer of high numbers of autologous, tumor-reactive T cells. However, early clinical studies involving adoptive immune cell-based therapies produced mediocre results at the very best, driving the clinicians back to bedside to look for the answers to explain the lackluster performance of T cell-based therapies (13). It soon became apparent that immune surveillance in patients runs in parallel with tumor-mediated immune evasion and that the relatively transient equilibrium between these two now forms the basis of the modified theory of 'immune-editing' (14). The principle of immune-editing recognizes the fact that tumor development and progression is a process guided and molded by the host immune system right from the early stage, involving the 3E-phases: elimination, equilibrium and escape. Nascent transformed cells are under attack by the host's innate defense mechanisms involving NK cells, macrophages and neutrophils; all of which are capable of recognizing and eliminating the transformed host cells to maintain cellular homeostasis. Following this, in the equilibrium stage the transformed cancerous cells recognize and adapt to the immune selection pressure leading to the loss of MHC molecules, downregulation of surface antigens, defects in the antigen-presentation machinery, all in order to avoid the

immune attack. If the tumor cells succeed in tilting the balance in their favour during this equilibrium stage, immune-escape variants of the tumor emerge that are further equipped to escape immune surveillance. Therefore, targeting these immune escape mechanisms in conjunction with conventional immunotherapeutic approaches to reactivate the immune system would be crucial for realizing the full potential of cancer immunotherapy in clinics. But in order to achieve that, elucidation of the tumor-mediated immune escape pathways is imperative.

1.4 Immune-escape pathways

Peripheral immune tolerance is an integral component of a healthy body's defense program against self-reactive immune cells. However, in diseased state, these pathways are hijacked by the cancer cells to thwart and escape the immune response. Basically, every step in the cancer immunity cycle, described above in Figure I, is susceptible to escape routes mediated by the tumor. The means of tumor-mediated immune escape are as varied and complex as the anti-tumor immunity itself and are described here in some detail.

1.4.1 Impairment of antigen-presentation by tumors

CD8 effector T cells recognize their tumor targets for clearance only in context of the peptide-bound MHC (pMHC) complex. This therefore requires the appropriate processing of the tumor antigens to relevant epitope-harboring peptides which can be presented on the cell surface in MHC-I grooves for recognition by CTLs. In this regard, tumors can escape recognition by CTLs via two possible routes (Figure II):

- Down-regulation or loss of antigen: Occurs via genetic deletions or frequent mutations to alter the immune-dominant epitopes on the antigen, leading to immune-escape tumor variants that can evade immune surveillance (15).
- Defects in the antigen-presentation machinery: Not only can tumor cells lose or mutate their immunogenic peptides, but they can also downregulate the MHC-I molecule, via deletion or frame-shift mutations in the beta 2-microglobulin gene ($\beta 2m$), so that the antigen is not even presented on the tumor cell surface for recognition by antigen-specific effector T cells (16). Loss of HLA alleles has also

been reported in multiple cancers, including colorectal carcinoma and melanoma, aiding in immune escape (17). Furthermore, cellular components of the antigen-processing machinery and of the immunoproteasome (such as transporter-associated with antigen processing: TAP or LMP2, LMP7) can be mutated leading to defective antigen presentation by the tumor cells (18).

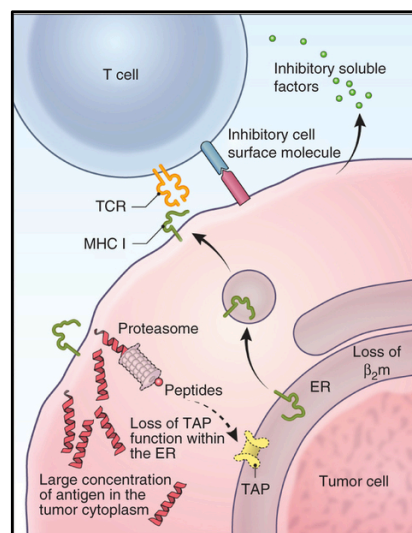


Figure II. Mutations in the cellular proteins responsible for antigen processing and presentation ($\beta 2m$, MHC, TAP) may result in the failure of target antigen's presentation by the tumor cells, thereby leading to an inhibition of T cell's reactivity against their tumor targets. Adapted from *Hinrichs et al, 2013* (19).

1.4.2 Elaboration of soluble immune-suppressive mediators

Tumor and the stromal cells in the tumor microenvironment secrete a plethora of immune-suppressive cytokines, growth factors and metabolites that are capable of actively silencing an effector anti-tumor T cell response, or creating an immune-suppressive environment around the tumor bed for maintaining immunological anergy against the developing tumor. These soluble mediators and their role in immune suppression are summarized below in Table I.

Agents	Role in immune suppression
TGF-β	Inhibits T-cell activation, proliferation and differentiation (20)
VEGF	Suppresses T-cell adhesion to tumor endothelium and prevents homing to tumors (21)
IL-10	Reduces antigen presentation by downregulating TAP1 and TAP2, reduces Th1 cytokine secretion, induces regulatory T cells (Treg) and impairs DC function (22)

Prostaglandin E2 (PGE2)	Impairs the ability of DCs to attract and activate naive T cells, induces accumulation and function of regulatory immune cells and impairs CTL activation (23)
Indoleamine 2,3-dioxygenase (IDO) and Arginase	Involved in the catabolic degradation of tryptophan and L-arginine respectively, depletion of which in the tumor surrounding leads to an inhibition of T cell proliferation (24, 25).

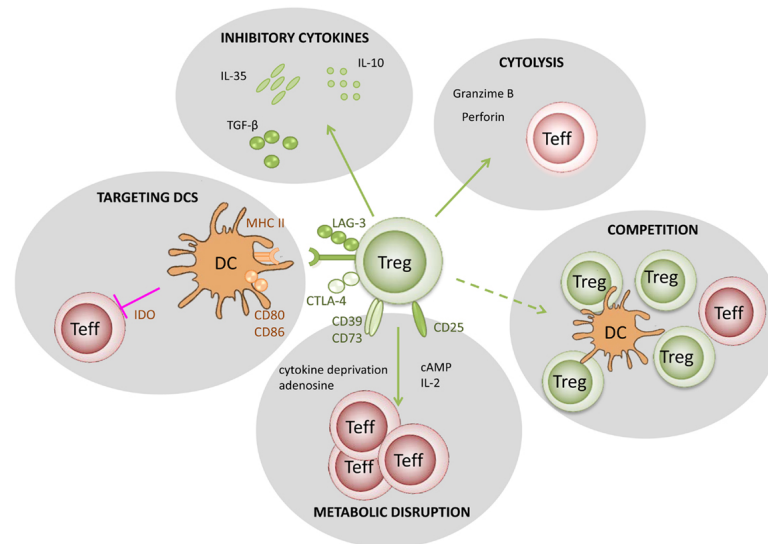
Table I. Soluble immunosuppressive mediators released by the tumor cells and their role in immune escape.

1.4.3 Specific recruitment of the immune-regulatory cell populations

Besides active subversion of the effector T cell responses via secretion of immunosuppressive mediators, tumors can also enrich their microenvironment by deploying cell populations to the tumor bed that promote tumor progression, along with maintaining immunogenic energy and suppression. Such cell populations mostly include regulatory T cells (Tregs), immature and plasmacytoid dendritic cells (iDCs, pDCs), myeloid-derived suppressor cells (MDSCs), mesenchymal stem cells (MSCs) and tumor-associated macrophages (TAMs).

- **Regulatory T cells (Tregs):** These subset of CD4 T lymphocytes are marked by CD25^{hi} FOXP3^{hi} expression and are typically involved in maintaining immune homeostasis and peripheral tolerance against self-antigens. However, in the case of tumor progression, they are preferentially recruited to the tumor microenvironment over effector T cells to suppress effector T cell function and maintain immune tolerance against the tumor antigens. Local accumulation of Tregs has been correlated to poor survival in many cancer types including gastric, esophagus, breast and ovarian cancer (26-29). They can suppress anti-tumor immunity through plethora of mechanisms (briefed in Figure III), for example via immune-inhibitory surface molecules like CTLA4, LAG3 (detailed in 1.4.4), or via soluble mediators such as TGF- β and adenosine (30).

Figure III. Potential modes of Treg-mediated immune suppression which includes: DC impairment via inhibitory receptor engagement, cytokine deprivation, competitive inhibition of the effector T cells, inhibitory cytokine and metabolite production (IL-10, IDO, adenosine) and direct cytolysis of the effector T cells. Adapted from *Caridade et al, 2013* (31).



- Immature and plasmacytoid dendritic cells (iDCs and pDCs): iDCs are those dendritic cells that leave the bone marrow and express very low levels of the co-stimulatory molecules CD80 or CD86 that results in poor maturation of the DCs and subsequent impairment of T cell activation. They produce little or no amount of IL-12 which is required to support T cell proliferation. As a result, accumulation of these immature DCs in the tumor microenvironment leads to immune escape (32, 33). Plasmacytoid DCs (pDCs) on the other hand are a small subset of dendritic cells that are believed to actively suppress T cell response in the tumor tissues (34). They induce the expression of the immunosuppressive mediators IL-10 and IDO that inhibits the clonal expansion of effector T cells and promotes T cell apoptosis. Besides, they also favor the growth and expansion of Tregs, adding to their immunosuppressive profile (35). Overall, the lack of proper costimulatory signal in these defective DCs induces tolerance towards the recognized tumor antigen, leading to T cell anergy rather than anti-tumor T cell response.
- Myeloid-derived suppressor cells (MDSCs): These are immature myeloid cells with a heterogeneous hierarchy and often found to be elevated in inflammation and cancer. Tumor associated growth factors and cytokines, such as CCL2, CXCL12, and CXCL5, support the recruitment and proliferation of MDSCs in the tumor bed, while in return MDSCs suppress the host immune system via production of arginase, inducible nitric oxide synthase (iNOS), IDO and immunosuppressive cytokines that negate CTL function (36). Elevated levels of MDSCs have been shown to correlate with poor survival in many tumor types (37).

- Mesenchymal stem cells (29): These are immuneprivileged, multipotent stem cells found in adult connective tissues and bone marrow with the capability of differentiating into any cell type of mesodermal lineage (38). Injection of human MSCs into the tumor-bearing BALB/c mice have shown that MSCs exert immune-protection by inhibiting DC maturation as well as T cell proliferation, promoting apoptosis of effector CTLs, secreting immunosuppressive factors like PGE₂, IDO and by increasing Treg proportion (39, 40).
- Tumor-associated macrophages (TAM): Macrophages are mononuclear phagocytic cells of the myeloid lineage which are characterized by their phenotypic plasticity depending on the microenvironment. Classically activated (M1) macrophages are anti-tumoral in nature, whereas alternatively activated (M2) macrophages support tumor growth and immune-suppression (41). TAMs are an integral cellular component of the inflamed, heterogeneous tumor microenvironment where they acquire an M2-like phenotype. Besides secreting tumor promoting growth factors, they also actively suppress anti-tumor immunity by secreting immunosuppressive mediators such as iNOS, arginase, IL-10, as well as by defective antigen presentation and inhibition of T cell proliferation (42).

1.4.4 Activation of negative co-stimulatory signals on the immune cells – the case of immune modulatory ligands

Tumors can engage the T cells directly via their immune-modulatory receptors and ligands on the cell surface, which provide negative co-stimulatory signal to the interacting T cells. This subsequently leads to the inhibition of TCR activation and downstream signaling and sometimes even apoptosis of the reactive T lymphocytes. In a healthy state, these immune-inhibitory switches serve as fail-safe mechanisms of immune-modulation that control over-activation of T cell responses and limit autoimmunity. However, in the diseased state of tumor progression, these immune-checkpoint nodes are exploited by the malignant cells to shut down and inactivate the anti-tumor immune response. Of such inhibitory pathways, CTLA4-CD80/CD86 and PD1-PDL1 axis have gained major prominence in the last decade for elucidating the immunosuppressive potential of such negative interactions. Therapeutic blocking of these immune-checkpoint entities now represents one of the most attractive paradigms of cancer immunotherapy (43).

1.4.4.1 CTLA4-CD80/CD86 axis

Biology and the functional role:

Cytotoxic T lymphocyte antigen 4 (CTLA4, also known as CD152), expressed on the activated T cells, is a cell surface receptor belonging to the immunoglobulin superfamily. Structurally, it is a homolog of the T cell co-activation receptor CD28, even binding to the same ligands - B7-1 (CD80) and B7-2 (CD86) which are expressed on the specialized APCs - but with higher affinity (44, 45). However, functionally it is an exact opposite. It possesses a cytoplasmic immunoreceptor tyrosine-based inhibitory motif (ITIM) domain which, upon successful engagement with its respective ligand on the APCs, recruits SHP family of phosphatases to reverse TCR activation-induced phosphorylation of signaling molecules and thereby serves to limit the T cell response. Role of CTLA4 in immune inhibition is further exemplified by *Ctla4*^{-/-} mice that develop fatal multi-organ destruction due to uncontrolled lymphocyte proliferation and infiltration (46, 47).

Role in tumor immune biology:

Even though tumours can present antigens in the context of MHC molecules, they still elicit insufficient immune response. One of the reasons for this was believed to be the lack of co-stimulatory signals provided by B7-CD28 interaction, as the expression of B7 ligands are restricted to specialized APCs. However, it is now known that even tumors that express B7 ligands elicit only partial immune response (48). Work from James P. Allison's group using B7+ve and B7-ve murine colon carcinoma cells has shown that the expression of immune inhibitory CTLA4 on tumors can explain the lack of immune reactivity against B7-positive tumors. Furthermore, inhibition of CTLA4-mediated negative stimulatory pathway could not only lead to tumor regression, but also result in immunological memory (49). Targeting CTLA4 therefore lowers the threshold of T cell activation and promotes expansion and maintenance of activated T cells. Moreover, Treg-specific CTLA4 deficiency leads to systemic lymphoproliferative disorder, indicating that CTLA4 is also crucial for the suppressive function of natural Tregs (50) and that targeting CTLA4 using antibody therapy might further aid in clinical immune response (Figure IV).

Blocking antibodies and clinical success:

Based on the above rationale, clinical trials have been conducted with ipilimumab, a human IgG₁ anti-CTLA4 blocking antibody, whereby an overall response rate of 10.9 % has been

noted in patients with advanced melanoma (51). It is the only treatment to date for advanced metastatic melanoma patients whereby 46% of the treated patients are disease-free after 1 year, as opposed to the 1-year survival rate of 25% with alternative treatment modalities (52). Encouraged by these durable responses, FDA approved ipilimumab in 2011 as a first-in-line treatment option for advanced melanoma (53). Notably, about 80% of the patients treated with ipilimumab presented adverse toxicity-related events which could be traced back to the serious autoimmune phenotype of *Ctla4*^{-/-} mice, highlighting the central role of CTLA4 in immune tolerance. Interestingly, treatment-related adverse events in some of these patients were found to be correlated with improved patient outcome, underscoring the need for modified treatment-evaluation parameters for immunotherapy trials (54, 55).

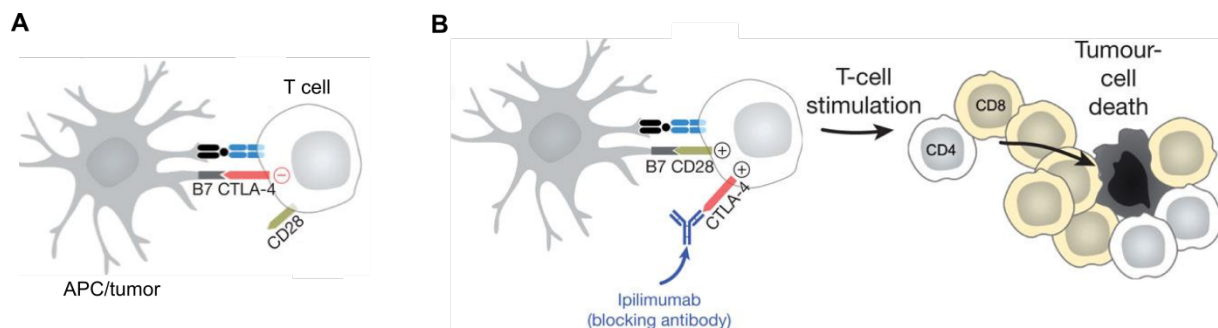


Figure IV. (A) The interaction between the B7 ligands, on the surface of APCs, and CTLA4, on the surface of T cells, leads to the inhibition of TCR signaling in activated T cells. (B) Blocking this interaction by using the anti-CTLA4 antibody (ipilimumab) allows for enhanced T cell stimulation and anti-tumor response. Adapted from Mellman *et al*, 2011 (56).

1.4.4.2 PD1-PDL1 axis

Biology and the functional role:

Programmed death receptor 1 (PD-1, also known as CD279) is an inhibitory co-signaling receptor which also belongs to the CD28-B7 family of proteins. It is induced only upon activation on the surface of T cells, B cells, natural killer T cells, monocytes and dendritic cells (57). It pre-dominantly binds to its ligands PD-L1 (also known as B7-H1 or CD274) and to some extent to PD-L2 (also known as B7-DC or CD273), both of which are cell surface proteins that are constitutively expressed on the APCs and inducible on epithelial and endothelial cells upon inflammation (58). Besides the ITIM motif, PD-1 also contains a cytoplasmic immunoreceptor tyrosine-based switch motif (ITSM) domain, which recruits the

SHP2 phosphatase to dephosphorylate the TCR-induced phosphorylation event. Ligation of PD-1 with PD-L1 (or PD-L2) therefore transmits an inhibitory signal into the T cell, which reduces cytokine production, T-cell proliferation and promotes apoptosis of effector T cells, ultimately leading to the T cell ‘exhaustion’ (59, 60).

Role in tumor immune biology:

Tumors exploit this immune-inhibitory capacity of the PD-1/PD-L1 signaling axis by upregulating PD-L1 expression via the loss of tumor suppressor protein PTEN (61). Additionally, IFN- γ released by the activated T cells could also upregulate the expression of PD-L1 on tumor cells (62). Overexpression of PD-L1 has been demonstrated in many different cancer types (eg, melanoma: 40%-100%, non-small cell lung cancer: 35%-95%, breast cancer: 30-50%, pancreatic cancer: 40% and multiple myeloma: 93%), and high levels of PD-L1 expression have been correlated to poor clinical outcomes (63-66). Besides active inhibition of the T cell response, PD1-PDL1 signaling between the T cells and DCs can also polarize the nature of the immune response to a Treg phenotype (67), thereby further suppressing the anti-tumor immune response (Figure V).

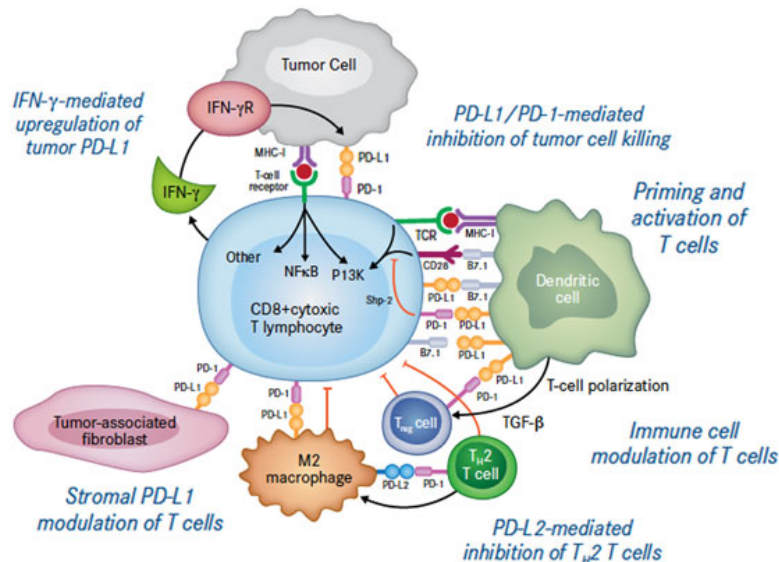


Figure V. PD-1 receptor, expressed on the activated T cells, binds to the ligands PD-L1 (or PD-L2) expressed on the tumor cells. PD-L1's expression is induced by IFN- γ secreted by the activated T cells. PD1-PDL1 ligation inhibits the TCR-induced downstream signaling events in effector T cells, creating a phenotype known as T-cell exhaustion. PD1-PDL1 signaling in other immune subsets could also lead to pro-tumor immune escape. Illustration by *Sznol et al. 2013* (66).

Blocking antibodies and clinical success:

Given its critical role in immune suppression, cancer immunotherapy based on the targeted inhibition of PD-1 or PD-L1 is currently being explored in the clinics. *In vitro* studies with blocking antibodies against PD-1 or PD-L1 demonstrated higher cytokine production by the effector T cells, prolonged survival and proliferation, as well as higher cytolytic activity (68). Nivolumab, a humanized IgG₄ monoclonal antibody against PD-1, was the first antibody to demonstrate broad and encouraging results in the phase I clinical trials with objective, and most importantly durable response rates, observed in 31% of metastatic melanoma patients, 16% of non small cell lung cancer patients and 29% of metastatic renal cell carcinoma patients (69). These impressive preliminary results in previously-treated, late-stage cancer patients have ushered the PD-1 and PD-L1 based therapeutics for a fast track FDA approval that is anticipated this year.

Combinatorial therapy:

Adverse events associated with the PD-1 antibody therapy were less severe than those observed with anti-CTLA4 therapy and this can be explained in view of the distinct roles that CTLA4 and PD-1 play in immune regulation. CTLA4 dampens the activation signal in T cells during the initial activation stage and fine-tunes the magnitude of early activation of naïve and memory T cells, while PD-1 functions to limit the activity of already activated T cells in the periphery in order to limit autoimmunity. Therefore, CTLA4 is more critical in establishing a central tolerance threshold for T cells activation, whereas PD-1 checks upon the activation status of already activated T cells (66). In light of these complementary pathways of immune regulation which are temporally and spatially distinct, combinatorial trials with nivolumab and ipilimumab are currently underway in advanced melanoma patients to exploit any potential synergistic effect that might result from co-inhibition of PD-1 and CTLA4. Early results report an objective response rate of 40% in these patients with rapid and deep tumor regression observed in many patients (70).

1.4.4.3 Other immune modulatory ligands

- **FasL:** Fas ligand (FasL or CD95L) is a type-II transmembrane protein belonging to the TNF family that interacts with its receptor Fas (CD95), triggering a cascade of subcellular events leading to the induction of apoptotic cell death of sensitive target cells (71). Fas/FasL interaction plays an important role in the activation-induced cell

death (AICD) of cytotoxic T cells. FasL-expressing tumors exploit this pathway for clearing effector T cells by inducing T cell apoptosis (72).

- **Galectins:** Galectins are evolutionarily conserved glycan-binding proteins that bind to N-acetyllactosamine sequences on both N- and O-glycans on the cell surface (73). Galectins are expressed by multiple tumor types as well as by tumor stromal cells (73). Few of the galectin members have exhibited immunosuppressive function. Galectin-1 has been shown to sensitize T cells towards FasL-induced apoptosis and suppression of Th1 responses (74). Tumor-associated galectin-3 has been shown to promote tumor growth and suppress tumor-reactive CD8⁺ T cells in mice receiving adoptive T cell transfer (75). Multimeric complexes of galectin-3 have also been shown to impose steric hindrance to TCR complex and restrain the TCR-induced activation signaling (76). Galectin-9, on the other hand, is believed to be the ligand for T cell immunoglobulin (Ig) domain and mucin domain 3 (Tim-3), a Th1-specific type 1 membrane protein expressed on the cell surface of fully differentiated CD4⁺ Th1 cells (77). Binding of galectin-9 to Tim-3 results in an inhibitory signaling cascade downstream of Tim-3 leading to apoptosis of Tim-3 expressing Th1 cells. Tim-3 expression on T cell surface has therefore been correlated with an exhausted immune status. Notably, recent evidences have emerged that suggest galectin-9 is not the ligand for Tim-3, leaving this field of investigation open for further in depth analysis (78).
- **LAG-3:** Lymphocyte activation gene-3 (LAG-3) is a cell surface molecule expressed on a subset of immune cells. It has been shown to be important for the immune-suppressive function of CD4⁺CD25⁺ Tregs (79). It has also been shown to be expressed on antigen-specific CD8⁺ T cells, restraining its accumulation and effector function at the tumor site. Antibody blockade of LAG-3 has been shown to alleviate the proliferative capacity and the effector function of antigen-specific CD8⁺ T cells, indicating its role in immune tolerance (80). Recently, it has been shown that LAG-3 and PD-1 pathway act synergistically in maintaining tolerance towards both self and tumor antigens, providing strong rationale for co-inhibition in clinical studies (81).
- **CEACAMs:** Carcinoembryonic antigen-related cell adhesion molecules (CEACAMs) are a part of the immunoglobulin superfamily which are characterized by their

involvement in cell-to-cell adhesion (82). Multiple members of the CEACAM family have been implicated in tumor progression and metastasis, including CEACAM-1 and CEACAM-6. CEACAM-1, which contains a cytoplasmic immunoreceptor tyrosine-based inhibitory motif (ITIM), is expressed on T cells upon activation and inhibits TCR signaling, thereby modulating immune response (83). Recently, the host laboratory has shown the novel involvement of CEACAM-6 expression on multiple myeloma in suppressing the anti-tumor function and reactivity of T cells. Inhibiting CEACAM-6 with blocking antibody could effectively rescue the anti-tumor reactivity of patient-derived T cells (84).

- **RCAS-1:** Breast cancer cells have been shown to express RCAS1 (receptor-binding cancer antigen expressed on Siso cells), which induces cell cycle arrest and apoptosis of activated T-cells via interaction through a putative RCAS1 receptor (85).

Nevertheless, the immune-inhibitory interactions presented above do not necessarily represent an exhaustive list of pathways that tumor cells exploit to antagonize the anti-tumor T cell response. Treatment unresponsiveness has been noted in a good proportion of patients undergoing PD-1/PD-L1 or CTLA4 blockade therapy (51, 68, 69, 86). For example, about 50% of the PD-L1-positive tumors failed to respond to treatment with MPDL3280A, an anti-PD-L1 blocking antibody, in Genentech's ongoing clinical study (87). Moreover, it has been shown that targeting PD1-PDL1 pathway alone does not always result in a complete restoration of T cell functionality (88), hinting at the involvement of other undefined immune regulators. Given that the tumors are inherently heterogeneous, probably even in their expression of immunosuppressive entities, there is a strong rationale to believe that other immune-checkpoint pathways may be active besides the ones that are being currently targeted in the clinics.

Therefore, successful cancer immunotherapy in the future would require a systematic dissection of the entire immune-modulatory circuitry that regulates the magnitude of anti-tumor immunity. However, such an approach towards a systematic and high-throughput delineation of novel immune regulators has been largely missing in the field.

1.5 High-throughput RNAi-based screen

Genetic screens based on the principle of RNA interference (RNAi) have become a standard practice to uncover modifiers of biological phenomena in a high-throughput and systematic fashion (89). RNAi is an intracellular defense mechanism whereby messenger RNA is targeted for destruction by double-stranded RNA (dsRNA) which contains sequence homology to the targeted gene, leading to a block in translation of the transcribed mRNA and thereby resulting in gene silencing (90). Since its discovery in nematode worms *Caenorhabditis elegans* in 1998, it has become a powerful tool for experimentally-induced gene silencing protocols with an extended use in therapeutics (91).

1.5.1 RNAi: principle and formats

Small interfering RNAs (siRNAs) are the main effector molecules of the RNAi pathway that bring about the sequence-specific gene silencing (Figure VI). These are 21-28 nucleotide long RNA duplexes with 2-nucleotide long 3'-overhangs which are generated upon the cleavage of long dsRNA by RNase-III-type enzyme termed Dicer. These siRNA duplexes are then recognized by the RNA-induced silencing complex (RISC) which incorporates the anti-sense strand of the duplex into the complex and guides it to the complementary sequence on the target mRNA. Perfect complementarity between the target mRNA and the antisense strand of siRNA duplex leads to the cleavage and degradation of the mRNA by the RISC complex. Imperfect complementarity however results in a steric inhibition of the RNA translation machinery. Ultimately, both lead to posttranscriptional gene silencing of the targeted gene (92). Cellular source of an siRNA can be endogenous (endo-siRNAs) or processed from long dsRNAs of viral origin or can be introduced synthetically in an experimental set-up. On the other hand, microRNAs (miRNAs) are endogenously synthesized double stranded RNA molecules that are transcribed as a RNA-hairpin loop structure (pri-miRNA) initially that gets processed into 22-nt long miRNA duplex to mediate gene silencing in a similar fashion as siRNA (92). Exogenously introduced short-hairpin RNAs (shRNAs) or dsRNAs undergo similar processing by cellular machinery to get converted into direct effectors of gene silencing.

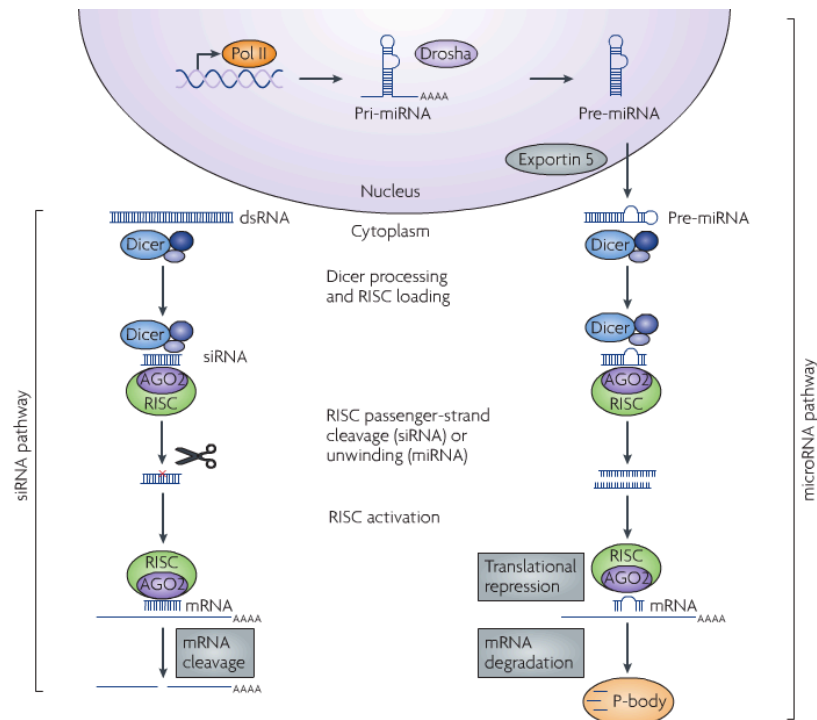


Figure VI. RNA interference (RNAi), mediated by siRNA or miRNA effector molecules, basically involves a RNA duplexes, one strand of which is complementary to the mRNA of the target gene (guide or antisense strand). The guide strand is imported into the RNAi-induced silencing complex (RISC) which consists of the Argonaute protein (AGO2). AGO2 cleaves the target mRNA upon perfect complementarity or inhibits the translation in case of partial complementarity. In both cases, expression of the target mRNA is inhibited leading to the gene knockdown phenotype. miRNAs differ from siRNAs in that they are produced endogenously as primary miRNAs (pri-miRNAs) which subsequently gets processed by cellular machinery into the mature miRNA duplex. Illustration by *Fougerolles et al, 2007 (93)*.

High-throughput RNAi-based genetic screens in mammalian cells have largely employed either synthetic siRNAs or vector-based expression of shRNAs to create gene knockdown phenotypes in target cells and assess their role in context of a particular biological process defined by the readout assay. RNAi screening based on siRNA library involves the delivery of artificially synthesized siRNA duplexes with desired sequence specificity to target cells, typically via liposomal transfection or electroporation, for transient knockdown of target gene. Whereas in shRNA-based RNAi screens, shRNA-expressing plasmids carried by lenti-, retro or adenoviral particles are used to transduce mammalian cells to mediate transient or stable gene knockdowns. Both these formats have their own set of salient features. Formats based on siRNA offer ease of production and transfection, generally high transfection efficiency as well as greater control over the amount of siRNAs transfected, which in turn means greater control over concentration-based non-specific side effects. In comparison, shRNA-based libraries are

advantageous for transducing non-transfectable cell types and for stable as well as inducible expression that could allow for long duration-based readout assays (91). Based on individual experimental needs, both these formats have been widely employed by the scientific community in cancer genetics to find modifiers of tumor growth, metastasis, drug susceptibility/resistance, synthetic lethality (94-96).

1.5.2 Cell-based assays and workflow for an RNAi screen

One of the key steps involved in a large scale RNAi screen is the design of an assay that is suited for reading out the exact biological question under investigation and its scale up to a high-throughput level. In addition, the screen would require the selection and optimization of a high-throughput-compatible gene knockdown strategy in the desired cell culture system, data acquisition, normalization and analysis to reveal the primary hit list. Once a primary hit list of candidate genes is generated, potential hits are re-validated in re-runs, creating a secondary hit list of reproducible hits that are then followed up in secondary and tertiary assays. These are designed independently of the primary assay used in the screening methodology to rule out false-positive hits. The basic workflow of an RNAi screen and the associated hit validation strategy is outlined in Figure VII.

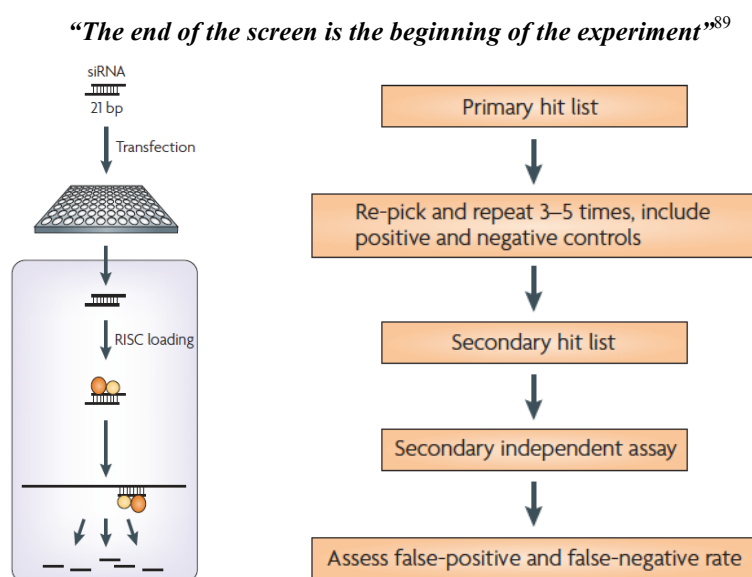


Figure VII. siRNA-based RNAi screen involves the transfection of double-stranded siRNAs, either in individual wells or delivered as pools, into cell cultures to induce gene silencing. Gene silencing-induced phenotype is then readout using the appropriate assay creating a primary hit-list of candidate genes which is subjected to further validations as outlined in the flow-chart on the right. Adapted from *Boutros et al. 2008* (89).

1.5.3 Data analysis from RNAi screen experiments

Depending on the complexity of the readout assay (image-based or value-based), large scale RNAi screens can be data intensive, requiring dedicated statistical analysis and computational resources. Software packages that integrate data analysis pipeline (such as cellHTS (97), RNAither (98), GUItars (99) among others) have been developed to streamline the data analysis part of RNAi screen approaches. Numerical datasets, such as luciferase intensity from the assay readout, could be imported into these software packages for normalization, quality metrics calculation and finally for setting filtering parameters for hit identification (100).

Normalization of the raw data is usually performed to account for and remove systematic technical errors that can vary from plate to plate, even within the same experimental setting, thereby allowing for data comparison and summation across the different plates in a screen. Various methods of data normalization, including control-based or sample-based normalization exist and are chosen depending on the data distribution parametric of the involved study. In the more commonly used plate-based median normalization method, signal intensity of each well in a plate is calculated relative to the plate's median intensity to scale plate-to-plate differences. The data is then deemed ready for further processing, but before that one must ensure the quality of the produced data meets the quality control requirements. Firstly, the performance of the replicates can be compared to each other to ensure reproducibility. Technical errors resulting from faulty pipetting or robotics, edge effects or spatial effects on plates could be further normalized to a certain extent at this stage using specialized normalization methods such as B-score or local regression (loess)-based normalization techniques (101). A clear dynamic range, defined as the degree and clarity of separation between the positive and negative controls, is desirable to ease the complexity of high-confidence hit calling and this can be mathematically deduced using the geometric means of the respective controls. For final generation of the hit-list, strength of individual siRNAs can be ranked based on their z-score, defined as the number of standard deviations from the mean of the sample distribution. User-defined threshold parameters, which can be control-based or quartile-based, are then employed to deduce meaningful hits from the ranked list. Nevertheless, it remains to be said that algorithms for hit identification are seldom absolute and are rather largely dependent on the biological significance of the gathered phenotypes compared to the relevant positive or negative controls (89).

In the field of cancer immunity, RNAi screens have been very recently employed to investigate genes that modify antigen-presentation by dendritic cells (102) or impair tumor susceptibility to NK cells (103). It is worthwhile to note that the success of any high-throughput screen largely depends on the careful design of the screening assay. Systematic discovery of tumor-associated immune-checkpoint molecules has proven to be challenging for the same reason, since a reliable high-throughput scale-compatible immune assay that measures the impact of tumor-specific gene expression on anti-tumor capacity of T cells has been largely lacking.

1.6 Aims and objectives of the thesis

Immunotherapy has emerged as a new pillar of cancer treatment over the last decade, but its clinical efficacy requires further optimization and tweaking. One of the major limitations to cancer immunotherapy is posed by the immunosuppressive ligands present on the tumor cell surface that inhibit an effector anti-tumor T cell response. Targeting these immune-checkpoint nodes is considered as the next paradigm shift in the realms of cancer immunotherapy. However, the current knowledge about the repertoire of such immunosuppressive ligands that are presented by the tumor is rather limited due to the lack of systematic, high-throughput studies that are devoted to the discovery of immune modulators.

Therefore, the major aim of this thesis was to establish and to functionally validate a high-throughput and robust screening assay which could uncover novel tumor-associated immune modulators. To achieve this aim, the following objectives were laid out:

- i. An immune assay will be established which combines gene knockdown via RNAi in tumor cells with the assessment of T cell-mediated tumor cell death in order to quantify the influence of individual cell surface-associated genes in cancer on the cytotoxic potential of effector T cells.
- ii. The above-mentioned immune-based screening assay will be employed at a high-throughput level to systematically screen for potential immune modulators expressed by the cancer cells. The robustness and the feasibility of such a screening strategy under various biological parameters would also be tested.
- iii. Validity of the screening approach to yield meaningful immunosuppressive candidates will be verified by functional characterization of the identified hits. For this, the effect of candidate gene knockdown on the function and anti-tumor reactivity of antigen-specific T cells in multiple tumor settings will be investigated. Potential route of mediating immune suppression by the candidate gene will be additionally explored.

2. Materials

2.1 Chemicals, reagents and consumables

Product	Supplier
1 kb DNA Ladder (GeneRuler)	Thermo Fisher Scientific
100 bp DNA Ladder (TrackIt)	Life Technologies
AB human serum	Valley
Agar	Fluka
Agarose	Life Technologies
AMP	Sigma-Aldrich
Ampicillin	Sigma-Aldrich
Aqua ad iniectabilia	B. Braun
ATP	Roche
Benzonase	Merck
Beta-mercaptoethanol	Gibco
Biocoll solution (density 1.077 g/ml)	Biochrom
Bovine serum albumin (BSA), fraction V	Sigma-Aldrich
Bromphenol blue	Merck
Cell culture dishes	TPP
Cell strainers (40 and 100 µm-pores)	Falcon, BD
Conical centrifuge tubes	TPP
Cryogenic vials (2 ml)	Corning
DharmaFECT1, 2 and 4 transfection reagents	Dharmacon, GE
Dimethyl sulphoxide (DMSO)	Sigma-Aldrich
Disposable needles (0.4 x 20 mm)	Henke Sass Wolf
Disposable syringes (1 ml)	Henke Sass Wolf
Disposable syringes (50 ml)	BD
Dithiothreitol (DTT)	Gerbu
D-luciferin (for Luc-CTL assay)	Biosynth
D-luciferin potassium salt (for <i>in vivo</i> injection)	Synchem
dNTP mix (10mM)	Invitrogen
Dulbecco's PBS powder without Ca ²⁺ , Mg ²⁺ (for 10 L)	Biochrom
Dulbecco's PBS without Ca ²⁺ , MgCl ₂ (1X)	Sigma-Aldrich
Dynabeads CD3/CD28 T cell expander, human	Dynal

Dynabeads Pan-Mouse IgG kit	Invitrogen
EDTA 1% (w/v) without Mg ²⁺	Biochrom
Enhanced chemiluminescence (ECL) detection reagents	GE Healthcare
Ethanol absolute	Sigma-Aldrich
Ethidium bromide	Sigma-Aldrich
Fetal bovine serum	Biochrom
Ficoll tubes - Leucosep (50 ml)	Greiner Bio-one
Flat-bottom plates (6, 12, 24, 48, 96 well)	TPP
Freezing container (Mr. Frosty)	Nalgene, Thermo Scientific
GeneJammer transfection reagent	Agilent Technologies
Geneticin sulfate (G418)	Gibco
Glycerol	Carl Roth
HEPES buffer (1 M)	Sigma-Aldrich
Hoechst dye	Invitrogen
IL-2 (human, recombinant)	Novartis
Isoflurane	Baxter
Isopropanol	Fluka
Library Efficiency DH5 α competent cells	Invitrogen
Lipofectamin LTX/ PLUS reagent	Life Technologies
Lipofectamin RNAiMAX	Life Technologies
Loading dye solution (6X)	Fermentas
LumaPlates	PerkinElmer
Luminometer plates (white, 96 well, flat)	PerkinElmer
Magnetic particle concentrator	Life Technologies
Matrigel basement membrane matrix	BD
MES SDS running buffer (20X)	Life Technologies
Methanol	VWR
Milk powder	Carl Roth
Multichannel pipette (50 μ l)	Thermo Scientific
MultiScreen-HA filter plates (0.45 μ m, clear, sterile)	Merck
Na ₂ ⁵¹ CrO ₄ (5 mCi, 185 MBq)	Perkin-Elmer
Negative control siRNA 1 and 2	Ambion
Non-essential amino acids (100X)	Sigma-Aldrich

Nuclease free water	Ambion
Oxalic acid	Sigma-Aldrich
PageRuler prestained protein ladder	Thermo Fisher Scientific
Pertussis toxin	Sigma Aldrich
Phenylacetic acid	Sigma-Aldrich
Pipette filter tips (10 µl -1000 µl)	Starlab
Plastic serum pipettes, sterile	Greiner bio-one
Polybrene (Hexadimethrine bromide)	Sigma-Aldrich
Polystyrene round bottom tubes with caps (5, 15 and 50 ml)	Falcon
Polyvinylidene difluoride (PVDF) membrane	Millipore
PowerPac Basic Power Supply	Bio-Rad
Protease Inhibitor tablets (complete)	Roche
Puromycin (10 mg/ml)	Gibco
Recombinant human CCL25/TECK protein	R&D Systems
Recombinant human PD-L1 protein	Life Technologies
Round-bottom plate (96 well)	TPP
Safe-lock tubes (0.5, 1.5, 2 ml)	Eppendorf
SDS polyacrylamid gels (4-12% Bis/Tris)	Life Technologies
Shaver for mice (Exacta)	Aesculap
siGENOME set of 4 upgrade siRNAs against CCR9, CCL25, CCRL1, PTGER3 and GHSR.	Dharmacon, GE
siGENOME SMARTpool siRNAs against PD-L1, CEACAM-6, RCAS-1, GAL-3, UBC, PLK-1, R-Luc, Chk 1, Elmo 2, FLuc and Control siRNA	Dharmacon, GE
Syringe filter units (0.22 and 0.45 µm-pores)	Millipore
<i>Taq</i> DNA polymerase, recombinant	Invitrogen
Tissue culture flask/filter cap (25, 75, 150 cm ²)	TPP
TransIT-LTI transfection reagent	MirusBio
Transwell inserts; thin-certs 8µm pore size	Greiner bio-one
Triton X-100	Fluka
Trypan blue solution (0.4%)	Fluka
Trypsin-EDTA (1X) (sterile filtered)	Sigma-Aldrich
TurboFectin	OriGene
Tween 20	Sigma-Aldrich
Whatman 3 mm gel blot paper	Sigma-Aldrich

2.2 Assay kits

Kits	Supplier
5-Plex STAT Phosphoprotein kit, Milliplex MAP	Millipore
7-plex T Cell Receptor Signaling phosphoprotein kit, Milliplex MAP	Millipore
9-Plex Multi-Pathway Cell Signaling kit, Milliplex MAP	Millipore
Bight-Glo luciferase assay system	Promega
Bio-Plex Pro Assay kit	Bio-Rad
CCL25/TECK ELISA kit	R&D systems
CellTiter-Glo Luminescent Cell Viability Assay kit	Promega
Compensation Beads set (anti-mouse)	BD
Dynabeads FlowComp Mouse CD8 Kit	Life Technologies
EndoFree Plasmid Maxi Kit	Qiagen
IFN- γ ELISA kit	BD
Live/Dead fixable yellow dead cell stain kit	Life Technologies
QIAprep Spin Miniprep Kit	Qiagen
QuantiTect reverse transcription kit	Qiagen
RNeasy Mini Kit	Qiagen

2.3 Buffers

- **ACK lysis buffer for red blood cell lysis**

NH ₄ Cl	8.3 g
KHCO ₃	1.0 g
EDTA	0.037 g
ddH ₂ O	1 L

- **Dulbecco's PBS without Ca²⁺, Mg²⁺ (10X)**

Dulbecco's PBS powder	95.5 g
ddH ₂ O	1 L

- **ELISpot washing solution**

PBS (Sigma-Aldrich)	500 ml
Tween-20	1.25 ml

- **ELISpot blocking solution**

RPMI (Sigma-Aldrich)	500 ml
AB serum	25 ml

- **FACS buffer**

PBS (Sigma-Aldrich)	49.5 ml
FCS	0.5 ml

- **MACS buffer**

EDTA	2.5 ml
Filtered AB serum	250 μ l
PBS (Sigma-Aldrich)	47.5 ml

- **BL buffer**

ddH ₂ O	84,8 ml
HEPES (50mM Stock)	5 ml
EDTA (0,5 mM Stock)	0,1 ml
Phenylacetic acid (0,33 mM)	0,033 ml
Oxalic acid (0,07 mM Stock)	0,07 ml

pH adjusted to 7,6 and stored at 4°C for up to 4 weeks

- **Lysis buffer for Luc-CTL assay**

BL buffer	48.5 mL
10% TritonX-100	1.5 mL

- **B2 Buffer**

ddH ₂ O	85 ml
DTT (415 mM stock)	6,4 g
ATP (33 mM stock)	1,82 g
AMP (0,996 mM source)	0,035 g

Aliquots were stored at -20°C.

- **F-Luc mix for Luc-CTL assay**

ddH ₂ O	8ml
D_luciferin (35,7 mM stock)	0,1 g

NaOH was added until the color changes. Aliquots were stored in dark eppendorf tubes at -20°C.

- **FLuc buffer for Luc-CTL assay**

BL buffer	44.35 mL
Buffer B2	5 mL
D-Luc (10mg/mL)	0.65 mL
1M MgSO ₄	751 uL

- **Hoechst dye staining solution**

PBS	10 ml
BSA	2.4 %
Hoechst stain	1.25 µg/ml

- **SDS-PAGE running buffer**

MES SDS running buffer (20X)	50 ml
ddH ₂ O	950 ml

- **Immunoblot transfer buffer (10X)**

Tris base	30.3 g
Glycine	144 g
ddH ₂ O	1 L

- **Immunoblot washing solution (PBS-T)**

PBS (10X)	100 ml
ddH ₂ O	900 ml
Tween-20	1 ml

- **Immunoblot blocking solution**

WB washing solution	50 ml
Milk powder	2.5 g

- **Whole cell protein extraction (WCE) buffer**

Tris-HCl (pH 7.4)	50 mM
-------------------	-------

NaCl	250 mM
NP-40	0.5%
Glycerol	10%
EDTA	1 mM
DTT	0.5 mM
Protease inhibitor (added fresh each time)	1X

- **Tris-acetate-EDTA (TAE) buffer (50X)**

Tris	242 g (2 M)
Glacial acetic acid	57.1 ml
0.5 M EDTA	100 ml
ddH ₂ O	1 L
pH	8.5

2.4 Media and supplements

Product	Supplier
AB serum, human	Pan Biotech
AIM-V with L-glutamine, streptomycin sulfate, gentamycin sulfate	Gibco
Cell dissociation Buffer; enzyme-free PBS-based (1X)	Gibco
DMEM; high glucose (4.5 g/l), L-glutamine, sodium pyruvate, NaHCO ₃	Sigma-Aldrich
Dulbecco-PBS without Ca ²⁺ , MgCl ₂ (1X)	Sigma-Aldrich
Fetal calf serum (FCS)	Biochrom
Ham's F12 Nutrient Mixture	Gibco
HEPES buffer (1M)	PAA
Human rIL-2 (for TIL expansion)	Novartis
Human rIL-2 (Proleukin; for T cell culture)	Chiron
LB broth	Carl Roth
LB-Agar	Carl Roth
L-Glutamine (200 mM)	BioWhittaker, Lonza

Non-essential amino acids (NEAA; 100X)	BioWhittaker, Lonza
OPTI-MEM (1X) with HEPES buffer, Lglutamine, NaHCO ₃	Gibco
Penicillin/Streptomycin (P/S; 100X)	PAA
RPMI 1640 with L-glutamine	Gibco
RPMI 1640 with L-glutamine, NaHCO ₃	Sigma-Aldrich
S.O.C. medium	Invitrogen
Trypsin/EDTA (1X)	Sigma-Aldrich
X-VIVO 20 (serum free)	Lonza

FCS and AB serum were heat-inactivated and filtered through 0.22 µm pore-sized filters before being used as media supplements. Penicillin/Streptomycin (P/S) mix was also filtered through 0.22 µm filters before use.

- **Complete melanoma medium (CMM)**

DMEM	300 ml
RPMI	100 ml
Ham's F12 Nutrient Mixture	100 ml
HEPES buffer	5 ml
FCS	50 ml
P/S	5 ml

- **Complete lymphocyte medium (CLM)**

RPMI	500 ml
AB serum	50 ml
HEPES	5 ml
P/S	5 ml
2-mercaptoethanol	50 µl

- **Freezing medium**

FCS	9 ml
DMSO	1 ml

- **LB-Amp medium**

LB broth	25g
dH ₂ O	1L
Ampicillin	100 µg/ml

- **LB agar medium**

LB-Agar	40g
dH ₂ O	1L

- **TIL expansion medium with feeder cells**

CLM	50%
AIM-V	50%
Feeder cells	1x10 ⁶ /ml
IL-2	6,000 U/ml
OKT-3	30 ng/ml

- **TIL expansion medium without feeder cells**

CLM	50%
AIM-V	50%
IL-2	6,000 U/ml

- **T cell medium (for short-term culture)**

X-VIVO 20	50 ml
Human rIL-2 (Proleukin)	100U/ml

2.5 Cell lines

All cell lines were of human origin:

Cell lines	Type (derived from)	Culture medium
HEK 293T	Embryonic kidney	DMEM, 10% FCS, 1% P/S
M579	Melanoma patient-derived primary cell culture	Complete melanoma medium
MCF7	Breast adenocarcinoma	DMEM, 10% FCS, 1% P/S
MCF7-luc	Breast adenocarcinoma	DMEM, 10% FCS, 1% P/S, 550 µg/ml G418
MDA-MB-231	Breast adenocarcinoma	DMEM, 10% FCS, 1% P/S
PANC-1	Pancreatic adenocarcinoma	DMEM, 10% FCS, 1% P/S
PANC-1-luc	Pancreatic adenocarcinoma	DMEM, 10% FCS, 1% P/S, 1 mg/ml G418
Phoenix ampho	Embryonic kidney	DMEM, 10% FCS, 1% P/S

Cells	Type (derived from)	Culture medium
Polyclonal CD8 ⁺ T cells	Leukocyte concentrates (Buffy coat) from healthy donors	X-VIVO 20
Survivin antigen-specific T cells	Peripheral blood of breast cancer patient	X-VIVO 20
SW480	Colorectal adenocarcinoma	RPMI, 10% FCS, 1% P/S
TIL 412	Melanoma patient-derived	Complete lymphocyte medium
TIL 53, and TIL 34	Pancreatic cancer patient-derived	Complete lymphocyte medium

2.6 Antibodies

All antibodies used were reactive against human epitopes, unless otherwise stated.

2.6.1 Flow cytometry

Specificity	Species	Isotype	Conjugate	Clone	Company	Application
CD69	mouse	IgG ₁	PE	FN50	BD	5 µl in 50µl volume
CD8	mouse	IgG _{2a}	FITC	G42-8	BD	5 µl in 50µl volume
CD4	mouse	IgG ₁	PerCP-Cy5.5	RPA-T4	BD	2.5 µl in 50µl volume
CD8	mouse	IgG ₁	V450	RPA-T8	BD	2.5 µl in 50µl volume
CD3	mouse	IgG _{2A}	APC	HIT3a	BD	2.5 µl in 50µl volume
CD45	mouse	IgG _{2A}	FITC	5B1	Miltenyi biotec	2.5 µl in 50µl volume
PD-1	mouse	IgG ₁	PE/Cy7	EH12.2H7	BioLegend	5µl in 100µl volume
TIM-3	rat	IgG _{2A}	PE	344823	R&D Systems	20µl in 100µl volume
CCR9	mouse	IgG _{2A}	Alexa-Fluor 647	112509	BD	5 µl in 50µl volume
Isotype control	mouse	IgG _{2A}	APC	S43.10	Miltenyi biotec	2.5 µl in 50µl volume
Isotype control	mouse	IgG _{2A,k}	Alexa-Fluor 647	G155-178	BD	5 µl in 50µl volume

2.6.2 Immunoblot

Specificity	Species	Isotype	Clone	Provider	Application
CCR9	rabbit	IgG	E99	Abgent	1:1000
CEACAM-6	mouse	IgG ₁	GM8G5	Axxora (Enzo)	1:1000
Beta-actin	mouse	IgG ₁	AC-15	Abcam	1:3000
PD-L1	mouse	IgG ₁	130021	R&D Systems	1:1000
Phospho-STAT1 (Tyr701)	rabbit	IgG	58D6	Cell Signaling	1:1000
Anti-mouse IgG- HRP	goat	IgG	sc2005	Santa Cruz	1:2000
Anti-rabbit IgG- HRP	goat	IgG	sc2004	Santa Cruz	1:2000

2.6.3 Cell-based assays

Specificity	Species	Isotype	Clone	Provider	Application and concentration
CCR9	mouse	IgG _{2A}	112509	R&D Systems	Blocking assays (BA): 30 or 60 µg/ml
CCR9	rabbit	IgG	ab38564	Abcam	BA: 30 µg/ml
CEACAM-6	mouse	IgG ₁	GM8G5	Axxora (Enzo)	BA: 30 µg/ml
Isotype	mouse	IgG ₁	MG1-45	BioLegend	BA: 30 µg/ml
Isotype	mouse	IgG _{2A}	20102	R&D Systems	BA: 30 or 60 µg/ml
PD-L1	mouse	IgG ₁	130021	R&D Systems	BA: 30 µg/ml
CCL25	mouse	IgG _{2B}	52513	R&D Systems	BA: 30 µg/ml
CD3	mouse	IgG _{2A}	OKT3	Dr. G. Moldenhauer	TC activation, as indicated in methods
CD28	mouse	IgG ₁	15E8	Dr. G. Moldenhauer	TC activation, as indicated in methods
CD3 x EpCAM bsAb	mouse		OKT3 x HEA125	Dr. G. Moldenhauer	Cytotoxicity assays: 5 µg/ml

2.7 Mice

Non-obese diabetic (NOD)-severe combined immunodeficient (SCID) $Il2rg^{-/-}$ gamma (NSG) mice were used in this study. Original mouse strain was obtained from the Jackson Laboratory (strain name: NOD.Cg-PrkdcscidIl2rgtm1Wjl/SzJ) and were bred in-house at the DKFZ Animal Facility. Animal experiments were approved by the regulatory authorities (Karlsruhe). Mice were housed in sterile, individually ventilated cages (IVC). Ethical guidelines were followed according to the local regulations.

2.8 Equipments

Instrument	Associated software (version) and developer	Manufacturer
Acumen Explorer eX3, fluorescence microplate reader		TTP LabTech
Axiovert 40 CFL microscope/AxioCam MRm	AxioVision LE (4.4)	Carl Zeiss
Caliper (digital)		Carl Roth
Casy cell counter		Innovatis
CTL ImmunoSpot S5 UV analyzer	ImmunoSpot (5.0 Pro DC)	CTL
FACS Canto II Flow cytometer	FACS Diva software (6)	BD
Gamma Counter (Cobra Packard)		PerkinElmer
Gammacell 1000		Best Theratronics
Infinite M200 plate reader	iControl (1.6)	Tecan
IVIS100 <i>in vivo</i> imaging system	Living Image (2.50), Igor Pro (4.09A)	Xenogen
Luminex100 Bio-Plex System	Bio-Plex Manager (4.1.1)	Bio-Rad
Mithras LB 940 microplate reader		Berthold
Molecular Imager (ChemiDoc XRS+)	ImageLab (5.0)	Bio-Rad
MultiDrop Combi I		Thermo Scientific

Instrument	Associated software (version) and developer	Manufacturer
NanoDrop 2000c	NanoDrop 2000c (1.3.1), Thermo	Peqlab
Thermal Cycler, Peltier PTC-200		MJ Research
UV gel documentation system		Konrad Benda
XCell SureLock Mini-Cell Electrophoresis System		Life Technologies

2.9 Additional software

Software (version)	Developer
Adobe Illustrator (CS5)	Adobe systems
cellHTS2	Boutros <i>et al</i> (101), Heidelberg
Clone Manager Professional (9)	Scientific and education software, Cary, NC, USA
EndNote (X4)	Adept Scientific
FlowJo (8.8)	Tree Star
GraphPad Prism (6)	GraphPad Software
ImageJ (1.44)	Wayne Rasband
Microsoft Office 2007	Microsoft, USA

3. Methods

3.1 Cell culture techniques

3.1.1 Tumor cell lines

MCF7, MDA-MB-231 (both breast cancer), HEK 293T (human embryonic kidney), PANC-1 (pancreatic cancer) and SW480 (colorectal cancer) cell lines were acquired from the American Type Cell Culture (Wesel, Germany). Cell lines were authenticated using multiplex PCR at the DKFZ Genomics and Proteomics Core Facility. MCF7luc cells were generated by electroporation with pEGFP-Luc plasmid (kindly provided by Dr. Rudolf Haase, LMU, Munich) and sorted GFP-positive clones were expanded in selection medium containing 550 µg/ml geneticin/G418 (Gibco, UK). M579-A2-luc melanoma culture, stably transfected with HLA-A2 expression construct and luciferase plasmid, was established from a patient as described before and were kindly provided by Dr. Michal Lotem, Hadassah Hebrew University Medical Center, Israel (104). PANC-1-luc cells were generated by Antonio Sorrentino in the laboratory via transfecting pEGFP-Luc plasmid using the TransIT transfection reagent (as described in section 3.2.6) and subsequently sorted for GFP expression using flow cytometry. After two rounds of sorting, more than 95% of the sorted PANC-1 cells maintained stable expression of GFP over time under the selection pressure of G418 (1 mg/ml). All cell lines were cultured in the described culture media (see section 2.5) and maintained at 37°C, 5% CO₂, except for melanoma cell culture which was maintained at 8% CO₂.

3.1.2 Generation of stable CCR9 knockdown cell lines

For stable knockdown of CCR9 in tumor cell lines, a lentiviral vector expressing shRNA targeting CCR9 mRNA was produced according to the manufacturer's instructions (Cellecta). Briefly, DNA sequence coding for shRNA hairpin loop structure targeting CCR9 were obtained from the DECIPHER module library database and corresponding oligonucleotides for the sense and antisense strand were synthesized (Sigma-Aldrich). Single stranded oligonucleotides were phosphorylated and annealed using a T4 polynucleotide kinase and ATP. Phosphorylated, double-stranded oligonucleotides were ligated into the linearized

backbone of the pRSI9-U6-sh-HTS3-UbiC-TagRFP-2APuro lentiviral shRNA expression vector (Cellecta). Successful ligation was confirmed using colony PCR and DNA sequencing. Plasmid containing non-targeting shRNA sequence (NTS) in place of CCR9-specific shRNA sequence was used as a control (Cellecta). Lentiviral particles bearing the shRNA-encoding plasmids were produced by Tobias Speck in the laboratory. For this, 1.2×10^6 of low-passage number HEK 293T cells were seeded in 75 cm^2 tissue culture flasks and co-transfected the following day with the second generation lentiviral packaging plasmid psPAX2 (coding for gag and pol), the VSV-G envelope protein expressing plasmid pMD2.G (encoding for env) and the pRSI9 transfer plasmids (encoding the NTS or CCR9 shRNAs), in a ratio of 2:1:2 (1 = 1.5 μg DNA) using Lipofectamine LTX with PLUS as transfection reagent. Afterwards, cells were incubated at 37°C and supernatants containing the lentiviral particles were harvested after 48 h and 72 h. Cellular debris were removed by passing through a $0.45 \mu\text{m}$ filter. The produced lentiviral particles were used for transduction of tumor cells by seeding 5×10^5 cells in 25 cm^2 flasks in growth media. On the following day, growth media was replaced by 2 ml of lentiviral particle-containing media (diluted 1:20) along with 4 $\mu\text{g}/\text{ml}$ polybrene. Cells were incubated at 37°C for 16 h and afterwards, lentiviral medium was removed and flasks were washed with PBS. Cells were incubated at 37°C for additional 48 h to allow stable integration and expression of plasmid encoded gene products. Cells were then transferred to 75 cm^2 culture dishes in the presence of 1 $\mu\text{g}/\text{ml}$ puromycin for positive selection of transduced cells.

3.2 Molecular biology techniques

3.2.1 RT-PCR

To evaluate the gene knockdown efficacy of siRNAs, mRNA transcript levels were measured using RT-PCR. Tumor cells were harvested after siRNA transfection (described below) and total RNA was extracted from the cell pellets using the RNeasy Micro kit (Qiagen). 1 μg RNA from each sample was reverse transcribed to cDNA using the QuantiTect reverse transcription kit (Qiagen) as instructed by the manufacturer. Water blank, instead of template RNA, was used as control for the reverse transcription reaction. Transcribed cDNA were amplified using PCR. PCR reaction was set up in a 25 μl volume using the recombinant Taq DNA polymerase (Invitrogen) as detailed in the manufacturer's protocol. Water blank, instead

of template cDNA, was used as control. Following primers were used for the detection and amplification of the respective target genes:

Gene	Primer sequences (5'- 3')
CCR9	Forward: CAGTGAACCCCTGGACAACT
	Reverse: TGCCACTCAACAGAACAAGC
PD-L1	Forward: GTACCTTGGCTTTGCCACAT
	Reverse: CCAACACCACAAGGAGGAGT
GAPDH	Forward: GAGTCAACGGATTTGGTTCGT
	Reverse: TTGATTTTGGAGGGATCTCG

The PCR reaction was carried out initially at 94°C for 2 min, followed by 35 cycles of 3-step process: denaturation (94°C for 30 s), annealing (55°C for 30 s) and extension (72°C for 30 s); and finally once at 72°C for 7 min using the PTC-200 Peltier Thermal Cycler (MJ Research). 5 µl of the PCR product was mixed with equal volume of the DNA loading dye and separated on a 1.8% agarose gel using the gel electrophoresis unit. Separated DNA bands were visualized using the UV gel documentation system (Konrad Benda).

3.2.2 Protein extraction

Tumor cells were harvested and pelleted via centrifugation at 1600 rpm for 5 min and washed once with PBS to remove any traces of media. Depending on the pellet size, cells were resuspended in 30-50 µl of whole cell extract buffer containing the protease inhibitor cocktail (diluted 1:20). Cell lysates were incubated for 20 min, followed by centrifugation at 13,000 rpm at 4°C for 20 min. Supernatants containing the protein lysates were transferred into fresh tubes and quantified using the NanoDrop analyzer (blanked with water). Protein lysates were stored at -80°C.

3.2.3 Immunoblotting

For immunoblotting analysis, 25 µg of protein lysates were separated on the 4-12% Bis/Tris SDS polyacrylamide gels (Invitrogen) under reduced condition. PAGE-separated protein bands were blotted onto the PVDF membrane using the 1X wet-transfer buffer at 400 mA for 45 min at 4°C. Membranes were blocked with 5% milk powder in PBS-Tween (PBS-T) at 4°C overnight to reduce unspecific binding of the antibody. On the following day, membranes were incubated with the primary and HRP-conjugated secondary antibody prepared in the blocking buffer at the dilutions indicated in section 2.6.2. Between incubation with each

antibody, the membranes were washed thrice with PBS-T for 10 min each. Protein bands were detected using the ECL developing solution containing luminol substrate which is catalyzed by the antibody-conjugated peroxidase (HRP) enzyme, resulting in the emission of low intensity light that can be detected at 428 nm. Chemiluminescent signal was acquired using the ChemiDoc XRS system.

3.2.4 Bacterial transformation and plasmid extraction

For plasmid DNA amplification, DH5 α (*E. coli*) competent cells (Invitrogen) were transformed with 2 ng of plasmid DNA by heat-shock method as detailed by the manufacturer. Next, competent cells were plated onto the LB plates containing 100 μ g/ml ampicillin and incubated at 37°C overnight to obtain successfully transformed antibiotic-resistant bacterial clones. Isolated colonies were picked up on the following day and used to inoculate 100 ml of LB culture containing 100 μ g/ml ampicillin for plasmid DNA isolation. Plasmid DNA from bacterial culture was isolated and purified using the EndoFree Plasmid Maxi Kit (Qiagen) as per the manufacturer's instruction. Integrity of the purified DNA was analyzed via gel electrophoresis after enzymatic digestion. For glycerol stock preparation of bacterial clones, 500 μ l of turbid bacterial culture was mixed with 500 μ l of 50% glycerol, vortexed, placed on ice for 30 mins and then stored at -80°C in cryotubes.

3.2.5 Reverse siRNA transfection

To induce gene knockdown in tumor cells, 6-well plates were coated with 250 μ l of 500 nM siRNA stock solution per well for 10 min at room temperature. 4 μ l of RNAiMAX (Invitrogen) transfection reagent was diluted in 200 μ l final volume of OPTI-MEM and incubated for 10 min at RT. 400 μ l of additional OPTI-MEM was then added and overlaid onto the siRNA coated wells for 30 min. 3×10^5 tumor cells were resuspended in 1,200 μ l of antibiotic-free culture medium supplemented with 10% FCS and seeded onto the siRNA-RNAiMAX wells for reverse transfection with the siRNAs and incubated for 72-96 h at 37°C, depending on the experimental requirements. For transfection in 96- or 384-well plate formats, the above protocol was proportionally scaled down keeping the final siRNA concentration to 50 nM. For testing the siRNA transfection efficacy, cells were reverse transfected with lethal or control siRNAs in 384-well plates and cell viability was determined after 72 h as described in section 3.2.8.

3.2.6 Plasmid Transfection

For overexpression, codon-optimized CCR9 ORF encoded in the backbone of the pCMV6-AC-His vector, which contains a C-terminal histidine tag, was obtained from Origene. For plasmid transfection, 3×10^5 HEK2393 or MCF7 cells were seeded in a 6-well plate and incubated in 37°C cell culture incubator overnight. On the following day, 6 µl of TransIT-LT1 transfection reagent (Mirus Bio) was added in 200 µl final volume of OPTI-MEM solution, mixed gently and incubated for 10 min at room temperature. Simultaneously, 3 µg of pCMV6-AC-His-CCR9 encoding vector or pCMV6-AC-His control vector was diluted in 600 µl OPTI-MEM and mixed gently. After 10 min incubation, 200 µl of OPTI-MEM/TransIT-LT1 mix was added to the 600 µl of plasmid/OPTI-MEM mix and incubated for 30 min at room temperature. Normal growth media on the seeded cells was replaced with antibiotic-free media in the meanwhile and to this plasmid/TransIT mix was added. Cells were incubated at 37°C for 48 h before use in other assays. For transient transfection of the pEGFP-Luc plasmid into the MCF7 and SW480 cell lines in 384-well plates, the above protocol was proportionately scaled down with 50 ng of plasmid DNA and 0.2 µl of individual transfection reagents used accordingly per well.

3.2.7 Fluorescent microscopy

GFP and phase contrast images of the MCF7luc cells were acquired using the inverted Axiovert 40 CFL microscope and analysed using the Axiovision 4.4 software.

3.2.8 Cell viability assays

To assess cell viability after siRNA transfection, growth media was removed from wells and cells were fixed in 50 µl of fixation buffer (PBS, 4% PFA) for 30 min at room temperature. Buffer was removed and 20 µl of the DNA-binding Hoechst dye staining solution was added per well and incubated for 1 h at room temperature. Following this, the staining solution was removed and wells were washed twice with 80 µl PBS to remove any unbound dye. Plates were read using the Acumen Reader at 460 nm.

For screening viability-related genes, CellTiter-Glo (CTG) assay (Promega) was employed. It quantifies the level of ATP present in the culture based on the luminescence signal generated by oxidative catalysis of luciferin to oxyluciferin by recombinant luciferase already present in the reagent mix. Therefore, it is important to note that CTG assay can only be performed with

luciferase negative cell lines. For CTG assay, siRNA transfected 384-well plates were soaked off media and incubated with 20 μ l of CTG solution per well which was pre-diluted 1:4 in media and kept for 15 min in the dark. Luminescence was measured with the Mithras reader using 0.1 sec as the acquisition time with no filter setting.

3.2.9 Transwell migration assay

To evaluate the migration of CCR9⁺ve cells towards the chemotactic stimulus of CCL25 and to assess the capacity of pertussis toxin in inhibiting this migration, transwell migration assay was performed in 24-well plates with 8 μ m transwell inserts. The receiver well was cultivated with 500 μ l of medium alone or medium supplemented with 3 μ g/ml of rhCCL25 protein (R&D systems). Transwell inserts (Greiner bio-one) containing 1×10^5 MDA-MB-231 cells in 200 μ l DMEM medium, supplemented with or without pertussis toxin (2 μ g/ml), were overlaid onto the receiver wells and incubated for 24 h. Cells that migrated into the lower chamber were carefully harvested after 24 h and quantified using the CTG assay, as described in section 3.2.8. Experiment was performed in triplicates per sample group.

3.2.10 Global gene expression analysis

For transcriptomic analysis, 2.5×10^5 MCF7 cells per group were reverse transfected with control or CCR9 s1 siRNA in 6-well plates as detailed in section 3.2.5. Transfection was set up in triplicates per knockdown. After 72 h, 5×10^6 survivin T cells were added to each well of siRNA-transfected MCF7 cells and co-incubated for 12 h in 37°C incubator. Following co-incubation, supernatant from each well were harvested and wells were additionally rinsed with 1 ml of culture media and pooled with the remaining supernatant. Survivin TCs in the supernatant were separated from the MCF7 tumor cells using anti-EpCAM antibody-coated magnetic beads as detailed in section 3.4.7. Total RNA was isolated from the purified T cells using the RNeasy Mini kit (Qiagen) as instructed by the manufacturer and diluted to 40 ng/ml final concentration using the RNase free water. RNA hybridization onto the GeneChip Human Genome U133 Plus 2.0 Array (Affymetrix) was performed by the Genomics and Proteomics Core Facility (DKFZ, Heidelberg). Gene expression intensity was quantile normalized and significant differences in the log fold-change of gene expression between the CCR9^{hi} versus the CCR9^{lo} treated TCs was evaluated using the Welch's *t*-test. Gene expression comparison between the two groups was represented using the volcano plot distribution and the top

differentially up and down regulated genes were plotted as heatmaps using heatmap.2 function. Gene enrichment analysis based on the GO molecular functions terms was performed for the top differentially expressed genes using DAVID. The obtained gene expression profile was compared with a publically available gene expression dataset from a previous study (105), which compared CD8⁺ T cells from the peripheral blood of healthy donors before and after 24 h of activation with anti-CD3/CD28 antibody plus IL-2. The published dataset was retrieved from the Gene Expression Omnibus using the accession code GSE7572 and analyzed using standard methods in R. Data analysis was kindly performed by Ashwini Kumar Sharma (DKFZ, Heidelberg).

3.3 Immune-RNAi screen

3.3.1 Screen layout and the Luc-CTL assay

GPCR-targeting sub-library of the genome-wide siRNA library siGENOME (Dharmacon, Thermo) containing 516 siRNA pools, each pool consisting of four synthetic siRNA duplexes, was prepared as described (106). Four RNAi screens were performed in duplicate wells. Positive and negative siRNA controls were distributed into empty wells prior to the screening. Reverse siRNA transfection was performed by delivering 0.05 μ l of RNAiMAX in 15 μ l RPMI (Invitrogen). After 30 min, 3000 MCF7 cells (screen 1 and 3: MCF7luc, screen 2 and 4: MCF7) in 30 μ l DMEM medium (Invitrogen) supplemented with 10% FBS (Invitrogen) were added. Plates were incubated at 37°C for 24 h and for screens 2 cells were transiently transfected with a luciferase expression plasmid using the TransIT-LT1 transfection reagent (Mirus Bio). 72 h post siRNA transfection cancer cells were either challenged with CTLs and anti-CD3 x anti-EpCAM bi-specific antibody (0.2 μ g/well; screen 1 and 2) or survivin-specific CTLs (screen 3) or left untreated (condition without addition of CTLs and screen 4). T cells were isolated and activated as described in section 3.4.1 for use in the screen. Screen 1 contained CTLs from one single donor and screen 2 CTLs from two different donors; one for each technical replicate within the screen. Tumor lysis was quantified 18 h later by analysis of residual luciferase expression in tumor cells (107). For screen 1-3, supernatant was removed using a 24-channel suction comb and cells were lysed by adding 20 μ l of the Luc-CTL lysis buffer per well for 10 min at room temperature. After this, 30 μ l of FLuc buffer was added per well and plates were read after 1 min using the Mithras reader with 0.1 sec counting time.

Viability measurements were performed for screen 4 using the CellTiter-Glo assay as described in section 3.2.8.

3.3.2 Data analysis

Plate reader data from RNAi screens were analyzed using the cellHTS2 package in R/Bioconductor (101). Scores from both conditions, i.e. addition of CTLs and without addition of CTLs, were quantile normalized against each other using the aroma.light package in R. Differential scores were calculated using a loess regression fitting. Given the biologically mixed setup used for the three different screens, unsupervised hierarchical clustering of differential score of all genes from all screens was performed using the loess score to assess inter-screen heterogeneity on a per gene basis. To derive the candidate hit list, firstly, preliminary thresholds for the toxicity and the viability scores were determined for each screen based on the quartile distribution of z-scores of the samples. For identifying negative immune modulators, genes in the 75% to 100% quartile of the toxicity score (representing elevated CTL-mediated lysis) and below 75% quartile for the viability scores (representing negligible impact on cell viability) were chosen as hits in each screen. For identifying positive immune modulators, range of the toxicity score was chosen as 0% to 25% (representing lowered CTL-mediated lysis) and viability score of 15% to 75% (corresponding to the normalized score of -1.5 to +1.5). Next, these statistical thresholds based on sample distribution parameters were individually adjusted for each screen based on the biological performance of the relevant controls within the individual screens with PD-L1, GAL-3, RCAS-1 used to determine the toxicity threshold; PLK-1, UBC used for viability thresholds and control siRNA 1 and 2 used for both the scores. Genes satisfying the above threshold criteria were identified individually for each screen and those which popped up in at least two screens were selected. Top positive and negative immune regulators (ordered by highest and lowest summed loess scores across screens) were plotted as heatmaps using value imputation for highlighting their relative immunomodulatory strength across the individual screen setups. Finally, genes scoring in a CellTiterGlo-based viability screen were filtered out from the candidate list (score <-1.5 and >1.5) to exclude any additional siRNAs affecting cell viability. Data analysis was kindly performed by Dr. Marco Breinig and Ashwini Kumar Sharma (DKFZ).

3.4 Immunological techniques

3.4.1 T cell isolation and activation

For RNAi screens, CD8⁺ T cells were isolated from leukocyte cell concentrates (buffy coat) obtained from IKTZ Blood Bank (Heidelberg). Ficoll density gradient centrifugation was performed to isolate peripheral blood mononuclear cells (PBMCs) from buffy coats of healthy donors. CD8 Flow Comp kit (Invitrogen; Karlsruhe, Germany) was used to isolate CD8⁺ T cells from the isolated PBMCs as detailed by the manufacturer. 1×10^6 CD8⁺ T cells/ml of X-VIVO 20 medium (Lonza) were activated for 3 days using the Human T-Activator CD3/CD28 activation beads (Dyna, Invitrogen; bead:cell = 1:3) and 100 U/ml IL-2. On the day of the co-culture, activated T cells were magnetically separated from activation beads, washed twice in X-VIVO 20 and then used directly for the experiment. For alternate T cell activation protocols (section 4.3), purified 6×10^7 CD8⁺ T cells from PBMCs were cultured in 30 ml complete RPMI media in 75 cm² tissue culture flask which was pre-coated for 2 h at 37°C with 100 µg of anti-CD3 antibody (OKT3 clone from G. Moldenhauer). To this, either 150 µg anti-CD28 antibody (15E8 clone from G. Moldenhauer) was added or left alone in the presence 100 U/ml IL-2. T cells were used after 3 days for Cr-release assay and FACS staining. HLA-A0201 restricted survivin₉₅₋₁₀₄ (clone SK-1) specific CTL clones were generated from the PBMC of healthy donors as described (108). Tumor-infiltrating lymphocyte 412 microculture (provided by Dr. Michal Lotem, Hadassah Hebrew University Medical Center, Israel) was expanded from an inguinal lymph node of a melanoma patient as described before (109). Similarly, TIL 34 and TIL 53 microcultures (provided by Dr. Isabel Poschke and Dr. Rienk Offringa, DKFZ) were established from two different male patients with poorly differentiated pancreatic adenocarcinoma (PDAC). Both melanoma and pancreatic TIL cultures were expanded using the Rapid Expansion Protocol described in section 3.4.2.

3.4.2 Rapid expansion protocol (REP) for TILs

Isolated TILs were *ex vivo* expanded using the modified Rosenberg's REP protocol (110). Thawed TILs were treated with benzonase (500 U/ml) to avoid cell clumps and were diluted to 6×10^5 cells/ml in CLM supplemented with 6000 U/ml rhuIL-2. Cells were incubated for 48 h at 37°C and 5% CO₂. PBMCs from 3 different buffy coats (1:1:1) were irradiated with 60

Gray (Gammacell 1000) and used as feeder cells to support TIL expansion. 1×10^6 TILs were co-incubated with 1×10^6 feeder cells/ml in 150 ml of TIL expansion medium and incubated for 5 days without any disturbance. Afterwards, media was replenished with fresh TIL media containing IL-2. Henceforth, TILs were counted every second day and cell concentration was set to 6×10^5 TILs/ml. On 14th day of the expansion, TILs were counted and frozen in aliquots of 10×10^6 cells/ml or depleted of IL-2 overnight and used fresh for experiments the next day.

3.4.3 ⁵¹Chromium-release Assay

Tumor cells were transfected with described siRNAs or expression plasmids as detailed (section 3.2.5 and 3.2.6) and used for Cr-release assay after 72 h. For antibody-mediated inhibition of target protein, 10^6 tumor cells were harvested and incubated with 3 μ g of blocking mAb or isotype control antibody (unless otherwise stated) for 30 min on ice before being used as target cells. For CCR9 blockade using pertussis toxin (PTX), 10^6 tumor cells were incubated with 250 ng/ml of PTX (Sigma Aldrich) for 1 h at 37°C. In either case, treated target cells were washed and labeled with 200 μ L ⁵¹Cr/ 10^6 target cells (Perkins-Elmer, Germany) for 45 mins at 37°C. After labeling, the cells were carefully washed thrice to remove cell-free chromium and 3000 target cells /well were co-cultured with survivin-specific T cells in 96 well plates at a T cell to target cell ratio of 1:1 to 100:1 for 4 h at 37°C. In experiments where polyclonal T cells were used, 5 μ g/ml of anti-CD3 x anti-EpCAM bi-specific antibody was added to each well of the cytotoxicity assay to induce tumor lysis. Non-specific anti-CD3 x anti-CD19 bi-specific antibody was used at the same concentration as control. After 4 h of tumor and T cell co-incubation, plates were spun down and the supernatant was harvested for measuring the radioactivity released by dead cells using the Gamma counter (Cobra counter Packard, Perkin Elmer). As a control for spontaneous release, the labeled cells were co-incubated with media alone; and for maximum release, cells were incubated with 10% Triton X-100 instead of T cells. % specific lysis was then calculated using the formula given below:

$$\% \text{ specific lysis} = \frac{(\text{experimental release} - \text{spontaneous release})}{(\text{maximum release} - \text{spontaneous release})} \times 100$$

3.4.4 ELISpot Assays

IFN- γ or granzyme B secretion from T lymphocytes was determined using the enzyme-linked immunosorbent spot (ELISpot) assay, as detailed by the manufacturer (Mabtech, Nacka Strand, Sweden). Briefly, CCR9 expression was inhibited in the tumor cell lines using specific siRNAs or antibodies, along with the necessary controls. siRNA transfected cells were harvested after 48 h, washed and then added to the IFN- γ or granzyme B antibody coated ELISpot wells (1 μ g/well). For antibody blockade, 5×10^5 WT cells were pre-treated with 3 μ g of anti-CCR9 antibody (R&D systems or Abcam) for 1 h on ice, washed and then co-incubated with T cells in the ELISpot wells. For co-culture, either survivin-specific T cells (5000 cells) or polyclonal CD8⁺ T cells (10,000 cells) along with anti-CD3 x anti-EpCAM bsAb were used in a ratio of 5:1 (T cell to tumor cell) for 24 h at 37°C. After this, plates were washed and incubated with the respective biotinylated antibodies (0.1 μ g/well), followed by the addition of streptavidin-alkaline phosphatase conjugate. Secreted cytokines by T cells which are locally captured by the coated antibodies were developed as spots using the Mabtech kit and analysed using the ELISPOT software (CTL Europe). Experiment was performed in triplicate wells for statistical comparison using the two-sided student's *t*-test.

3.4.5 ELISA

To measure the production of CCL25 in different tumor cell lines, sandwich ELISA was performed using the commercial CCL25 ELISA kit (R&D systems). Briefly 96-well microplate were coated with 100 μ l of the anti-human CCL25 antibody (0.5 μ g/ml) and incubated overnight at room temperature. Plates were carefully washed thrice and blocked for 1 h at room temperature using the blocking buffer provided in the kit. CCL25 protein standards were used as positive control and rhPD-L1 protein (BioLegend) was used as a negative control to check for the unspecific binding of anti-CCL25 antibody coated plates. 25 μ g of protein lysates from the respective tumor cell lines were prepared in 100 μ l of the PBS-T and added to the washed wells for 2 h at room temperature. Afterwards, plates were washed, incubated with the detection antibody, followed by incubation with streptavidin-HRP solution, as indicated in the manufacturer's protocol. Finally, plates were developed using the provided substrate solution (containing H₂O₂ and tetramethylbenzidine) for 20 min in dark at room temperature after which reaction was stopped using 2 N H₂SO₄ solution. Absorbance or optical density was measured at 450 nm using the Infinite M200 plate reader (Tecan).

Similarly, IFN- γ ELISA was performed using the IFN- γ ELISA kit as detailed in the manufacturer's protocol (BD Biosciences). Experiments were performed in triplicate wells for statistical comparison.

3.4.6 Cytokine measurements using luminex

For simultaneous quantification of multiple analytes in the same sample, luminex xMAP technology was used (Bio-Rad). This utilizes distinctly colored microsphere beads that can be coated with specific antibody to capture the analyte of choice in the sample mix, which can then be quantified by excitation and subsequent emission of light from the colored beads. For luminex assay, MCF7 cells were transfected with CCR9-specific or control siRNA for 48 h and then harvested and cocultured with 10^4 survivin-specific T cells at 1:5 ratio in 96-well plate for additional 24 h at 37°C. After incubation, the plates were spun down and 100 μ l of the culture supernatant was collected from each test well and centrifuged at 1000 g for 15 min at 4°C. The clear supernatant was collected and used directly for cytokine measurement using the Luminex100 Bio-Plex System and the Bio-Plex Pro Assay kit, as described by the manufacturer (Bio-Rad). Data was analyzed using the Bio-Plex Manager software version 6.0. Individual measurements were acquired from three test wells per group.

3.4.7 Phosphoprotein analysis

MCF7 cells were transfected with either control or CCR9-specific siRNAs as described before. After 72 h, the cells were harvested and 8×10^4 cells in 100 μ l of cytokine free X-VIVO 20 medium were plated per well of a 96-well plate. To this 2×10^6 survivin-specific T cells, suspended in 100 μ l of X-VIVO 20 medium, were added. Tumor and T cells were cocultured for 1 min, 5 min and 20 min for T cell receptor complex analysis and for 20 min, 1 h and 2 h for phospho-STAT analysis. After respective co-incubation time points, each cell group was added to 100 μ l of pan mouse IgG beads (Invitrogen) that were coated with 4 μ g of anti-EpCAM antibody (clone HEA125, provided by G. Moldenhauer, DKFZ) for 30 min at 4°C to separate EpCAM+ve MCF7 tumor cells from EpCAM-ve T cells. Bead-separated TCs were then lysed and total protein concentration was measured using the BSA Protein Assay kit (Thermo scientific) as detailed in the product manual. Protein concentration was normalized across all samples before phosphoprotein detection using the 7-plex T cell receptor signaling phosphoprotein kit or phospho-STAT 5-plex kit (Millipore, Billerica, U.S.),

as instructed by the manufacturer. For phospho-transcription factor analysis (section 4.19), 5×10^5 MCF7 cells were transfected with control or CCR9 s1 siRNA for 72 h and protein lysates were used for phosphoprotein detection as above using the Multi-Pathway Cell Signaling kit (Millipore). Measurements were performed using the Luminex100 Bio-Plex System (Luminex) and all the data were analysed using the Bio-Rad Bio-Plex Manager software version 4.1.1 (Bio-Rad).

3.4.8 Imprinting T cells with immunosuppressive tumor supernatants

To assess whether CCR9 mediates suppression on T cells via soluble mediators, MCF7 tumor cells were reverse transfected with control or CCR9 s1 siRNA in 6-well plates as detailed in section 3.2.5. After 60 h, cell culture supernatants were harvested from both the knockdown conditions and used to culture 1×10^7 fresh survivin T cells, each with the respective supernatants overnight. On the following day, knocked down MCF7 tumor cells (CCR9^{hi} and CCR9^{lo}) were harvested and used as target cells, along with wild type MCF7 cells, and the respective supernatant treated T cells (CCR9^{hi} and CCR9^{lo} SSN treated TCs) were used as effector cells in the classical Cr-release assay.

3.4.9 Flow cytometry

For flow cytometric analysis of surface proteins, cells were harvested and washed in FACS buffer and set to 3×10^5 cells per sample. For harvesting adherent cells from tissue culture dishes, enzyme-free PBS-based Cell Dissociation Buffer (Gibco, Paisley, UK) was used instead of trypsin-EDTA, especially for CCR9 surface staining, as trypsinization resulted in the loss of surface expression when detected by flow cytometry. Fc receptors of the washed cells (human) were blocked with 166 μg of Kiovig (Baxter), a human immunoglobulin concentrate, in 100 μl FACS buffer for 20 min on ice to reduce unspecific antibody binding. For mouse samples, BD Fc Block (BD Biosciences) was used at 5% concentration in 50 μl FACS buffer for 20 min on ice. After blocking, cells were washed once in FACS buffer and then incubated with fluorophore-conjugated target-specific or isotype antibody at the concentrations indicated in section 2.6.1 for 20 min in dark on ice. After this, cells were thoroughly washed twice in FACS buffer to remove any unbound antibody. For human samples, 5 μl of 10 $\mu\text{g}/\text{ml}$ propidium iodide (PI) solution was added to each sample just before acquiring as a dead cell marker. For mouse samples, cells were stained with Pacific

Orange viability dye (1:1000 in 50 µl FACS buffer) for 15 min on ice before Fc blocking. All samples were acquired with the FACS Canto II Cell analyzer machine (BD Biosciences) and data was analyzed using FlowJo software (Tree Star).

3.5 Mouse work

Approval for the animal work was obtained from the relevant regulatory authorities (Regierungspräsidium, Karlsruhe). Experiments were performed by Tobias Speck as a part of his M.Sc. thesis under my guidance. For assessing the *in vivo* effect of tumor-specific CCR9 upon the anti-tumor cytotoxicity of T cells, xenograft mouse model based on immunodeficient NOD/SCID gamma (NSG) mice was used. Four-six weeks old female NSG mice were ordered from the Animal Core Facility at DKFZ, Heidelberg. CCR9-ve PANC-1-luc cells (transduced with the CCR9-specific shRNA plasmid) and CCR9+ve PANC-1-luc cells (transduced with the non-targeting shRNA control plasmid) were generated as described in section 3.1.2. Mice were shaved at the flank regions and subcutaneously injected with 4×10^5 CCR9+ve tumor cells in the left flank and 4×10^5 CCR9-ve tumor cells in the right flank at day 0. Cells were prepared in 100 µl of matrigel/injection and injected using the 0.4 mm x 20 mm needles. Following this, at d2 and d9, 5 out of the 8 tumor-bearing mice received adoptive transfer of expanded TIL 53 cells (described in section 3.4.2) intravenously into the tail vein (1×10^7 cells/100 µl PBS/mouse). The remaining three mice were left untreated. *In vivo* bioluminescent imaging using the IVIS1000 imaging system was used to monitor tumor growth. For this, mice were intraperitoneally injected with 100 µl of 30 mg/ml D-luciferin substrate and anaesthetized via inhalation of the isoflurane-O₂ mixture (5 L/min). Mice were then placed onto the imaging platform of the IVIS system to acquire the emitted bioluminescence signal using the CCD camera. Signal intensity was quantified in photons/second/cm²/steradian. Mice were imaged twice a week with an exposure duration of 10 sec.

For the flow cytometric analysis, mice were sacrificed via cervical dislocation at the end of the experiment and spleens and tumors were removed and placed in ice-cold PBS. To obtain single cell suspension from spleens, they were pushed through 100 µm-pore strainers. For tumors, they were cut into small pieces and pushed through 100 µm-pore strainers. Cell suspensions were washed with ice cold PBS and centrifuged at 1700 rpm for 5 min at 4°C.

For spleens, cells were briefly resuspended in 2.5 ml of ACK buffer to lyse the erythrocytes. Following this, the cells were washed, centrifuged again and resuspended in 1 ml of FACS buffer. They were then filtered using a 40 μ m-pore strainer and used for staining as described in section 3.4.9.

3.6 Statistical evaluation

Statistical differences between the test and the control groups were analyzed by the two-sided student's *t*-test, unless indicated otherwise. In all statistical tests, a *p*-value ≤ 0.05 was considered significant with * = $p < 0.05$, ** = $p < 0.01$, *** = $p < 0.005$. Pearson correlation test was used to ascertain the correlation between the replicates in the screen and for inter-screen comparisons of the overall cytotoxicity scores. Statistical analysis for the RNAi screen and gene expression datasets are detailed in the respective sections of the methods.

4. Results

4.1 Establishment of the Luc-CTL cytotoxicity assay for immune-RNAi screen

The primary aim of this thesis was to establish a large-scale-compatible, RNAi-based immunological assay which quantifies the effect of individual tumor genes on the cytotoxic ability of T cells. One of the attractive high-throughput approaches to quantify cell death in response to a treatment is the colorimetric measurement of release of either an exogenously introduced reporter enzyme or an endogenous enzyme released by the dying cells. In a tumor cell-T cell co-culture system, measurement of endogenous cellular metabolites as an indicator of tumor-specific cell death is invalid given the cross-contamination from metabolites released by the T cells themselves. Therefore, reporter enzymes, such as luciferase, could be employed to tag the tumor cells before the co-culture, making its detection in the co-culture supernatant a direct indicative of the T cell-mediated cytotoxicity. A typical immune-based kill assay requires the co-incubation of T cells and tumor cells for a minimum of 4 hours, but the half-life of the released luciferase enzyme from dying cells in the supernatant is approximately 20 minutes (111). Thus, rather than measuring the activity of the released enzyme, we aimed to measure the luciferase activity of the remaining live tumor cells that are left attached to the plate after treatment with T cells (112). Therefore, in this assay, termed as the Luc-CTL assay henceforth, lower the luciferase activity associated with the leftover tumor cells, higher is the T cell mediated cytotoxicity.

To employ the Luc-CTL assay for immune-checkpoint discovery RNAi was performed in luciferase-tagged tumor cells and the CTL-mediated lysis of RNAi-transfected tumor cells was measured based on the luciferase signal (Figure 1A). In order to exclude genes whose knockdown in itself impacts on cell viability and hence luciferase activity, the Luc-CTL assay included a viability control per gene knockdown, to which no CTLs were added (Figure 1A). The difference in luciferase activity between the toxicity wells (containing CTLs) and the viability wells (without CTLs) was then calculated per gene to ascertain the immune-modulatory hits (detailed in methods section 3.3.2). Importantly, the extent of tumor cell killing detected by the Luc-CTL assay was comparable to that obtained with a common test of T cell mediated cytotoxicity, the ⁵¹chromium-release assay (113), establishing the robustness and the reliability of the Luc-CTL assay (Fig. 1B).

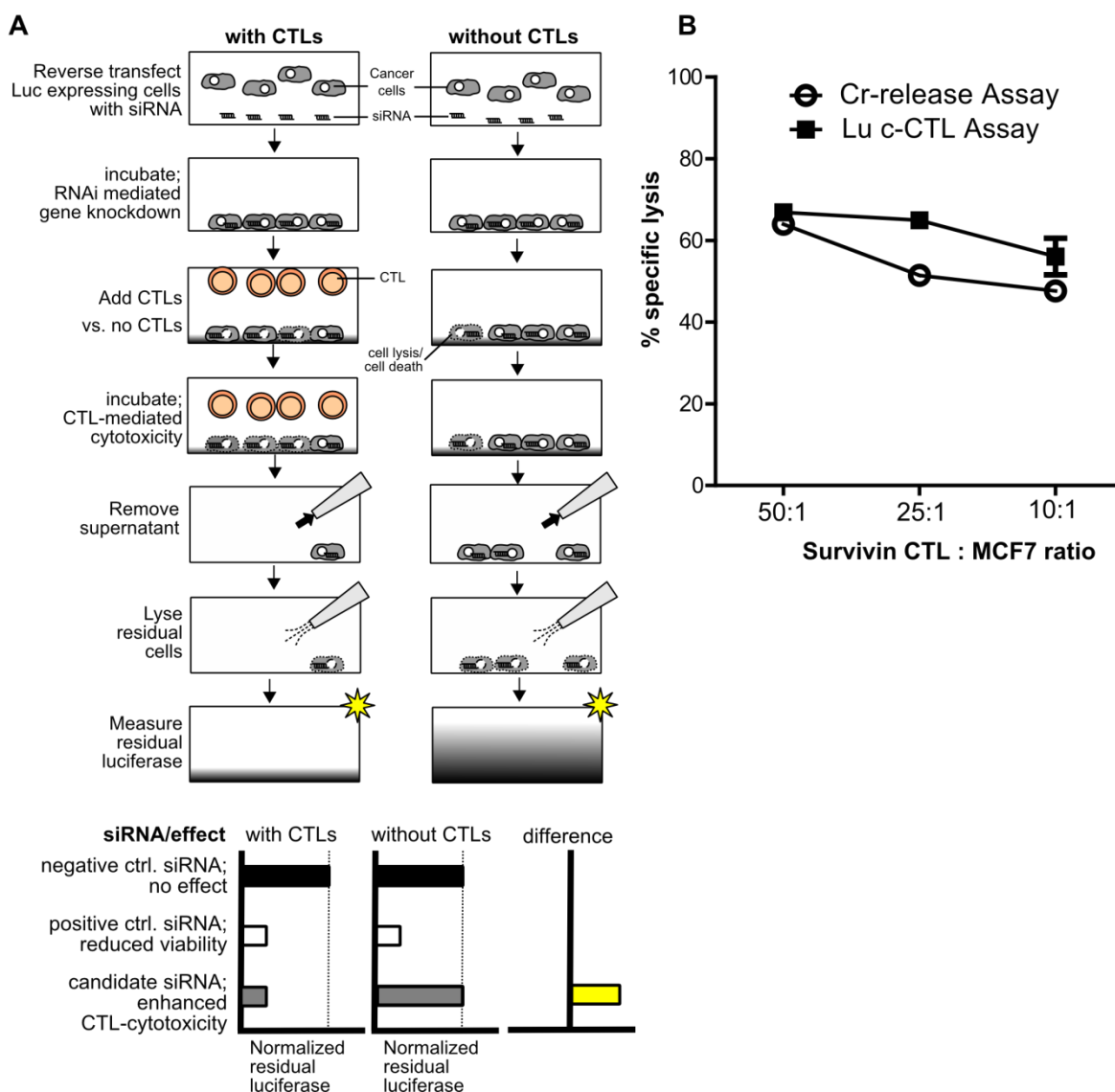


Figure 1. Principle and performance of the Luc-CTL assay. (A) RNAi is performed with luciferase expressing cells that are challenged with or without CTLs. Before readout, cell supernatant is removed and the remaining intact cells are lysed to measure the residual cell-associated luciferase. To identify immune-checkpoint regulators, the difference between normalized luciferase measurements for conditions with CTLs and without CTLs is calculated. siRNA enhancing CTL cytotoxicity will only reduce normalized luciferase levels under conditions with CTLs, hence the difference between luciferase measurements will be > 0 . **(B)** Comparison between the Luc-CTL assay (■) and the classical chromium release assay (○) with MCF7 breast cancer cells as target cells and survivin-specific T cells as effector cells at varying effector to target (E:T) ratios. Error bars denote \pm SEM; $n=3$.

4.2 Optimization of RNAi screen parameters: cell line, cell density, siRNA transfection and luciferase expression

Breast cancer was chosen as the model tumor type to implement the Luc-CTL assay-based screen for the discovery of novel immune modulators. This was not only because of its abundant prevalence, but also because its progression is marked with decreased immunocompetence, hinting at the involvement of putative immunosuppressive entities (114). To induce gene knockdown tumor cells were reverse transfected with siRNA pools, whereby four different siRNAs per target gene in a single pool were arrayed and coated onto the bottom of 384-well plates and overlaid with the transfection reagent and tumor cells. Since different cell lines exhibit different levels of susceptibility towards siRNA-based transfection, two different breast cancer cell lines, namely MCF7 and KS, were tested for their transfectibility with siRNAs. In parallel, different siRNA transfection reagents were tested to establish the most effective reagent that delivered the siRNAs to the cells. To achieve this, different lethal siRNAs targeting genes that are vital for cell growth and viability (described in Supplementary Table 1), such as ubiquitin C (UBC) or polo-like kinase 1 (PLK1), were used. Successful transfection of these siRNAs would lead to the loss of cell viability that can be read out via live/dead staining using the Hoechst dye. As shown in Figure 2A, MCF7 cells were found to be best transfectable with RNAiMAX and DharmaFECT2 in comparison to the other transfection reagents. However, DharmaFECT2 showed a mild cytotoxic impact on cells in comparison to RNAiMAX and therefore RNAiMAX was chosen as the desired transfection reagent for MCF7 cells for the high-throughput screen (Figure 2B). On the other hand, KS cells showed a strong resistance to siRNA-based transfection using the tested reagents (Figure 2A).

For the luciferase-based readout, MCF7 cells were tested for both transient and stable luciferase expression using a plasmid encoding a fusion protein of GFP and firefly luciferase (pEGFP-Luc). For stable cell line generation, MCF7 cells were electroporated with the GFP-Luc plasmid, selected under antibiotic selection pressure and subsequently FACS sorted twice based on GFP expression to select cell populations stably expressing GFP-luc. The selected clones (MCF7luc) maintained high levels of GFP expression over time, monitored via fluorescent microscopy (Figure 2C), as well as exhibited high luciferase signal that could be silenced using firefly luciferase (FLuc)-targeting siRNA (Figure 2D). Moreover, a linear relationship was observed between the seeded MCF7luc cell numbers and the associated

luciferase activity ($r^2 = 0.99$), whereby as low as 250 luc+ cells could be detected above the background (Figure 2E). Correlation between cell density and luciferase intensity was also used to determine the appropriate cell number for seeding in order to avoid overcrowding of the tumor cells in the small 384 wells which may lead to saturation of the luciferase signal. Since the generation of stable luciferase expressing clones can be tedious and time-intensive, transient luc expression in MCF7 cells for the Luc-CTL assay was next tested. Co-transfection of wild-type MCF7 cells with siRNAs and the GFP-Luc plasmid was found to be efficient, with GFP expression being noted in more than 85% of control siRNA-treated cells compared to negligible signal in the UBC siRNA-treated cells (data not shown). This indicated that transient transfection of luciferase plasmid could be exploited for rapid screening in wild type tumor cells without creating stable clones.

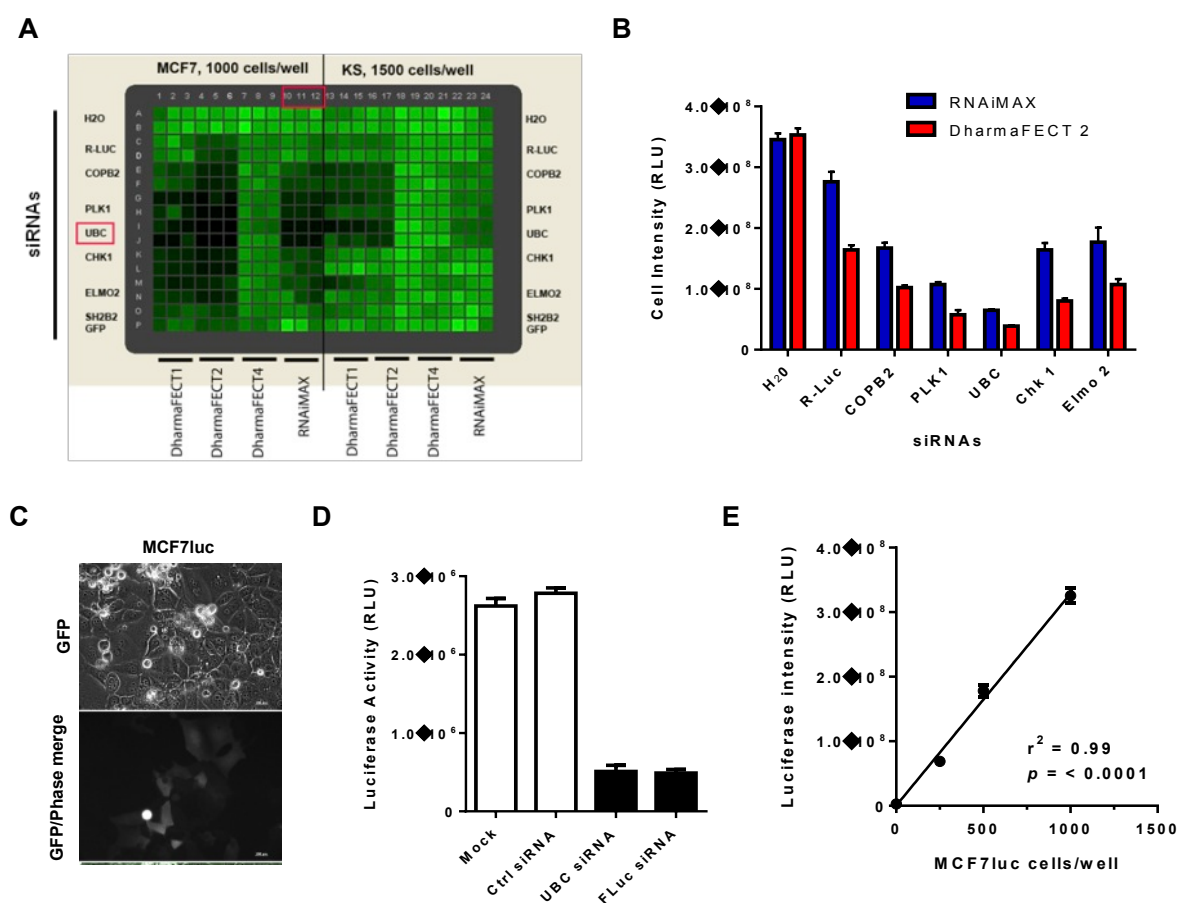


Figure 2. Optimization of RNAi screen parameters. (A) MCF7 and KS breast cancer cells were reverse transfected with the described control (H2O blank, RLuc) or lethal (UBC, PLK1, COPB2) siRNAs in 384 well plates using different transfection reagents (DharmaFECT1,-2,-4 and RNAiMAX). Loss in cell viability was readout after 72 h using Hoechst staining with light green representing viable cells and dark green indicating loss in viability. Mean cell intensities + SEM are quantified for MCF7 cells with DharmaFect2 (red bars) and

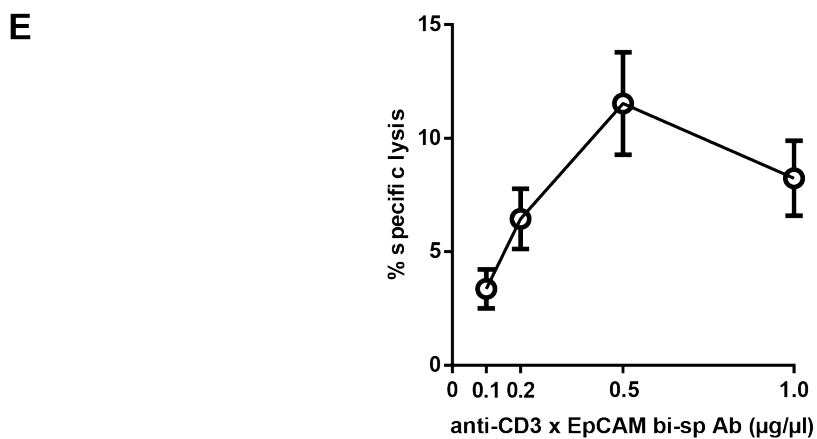
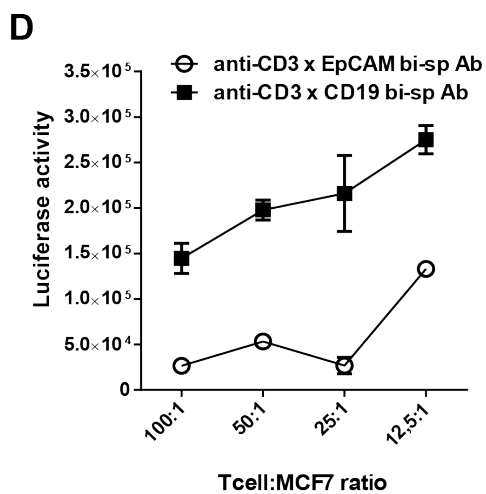
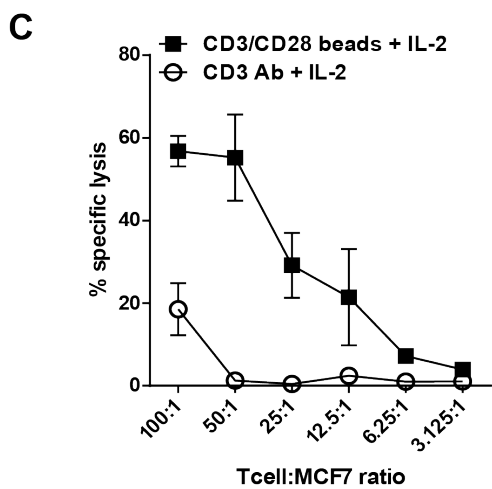
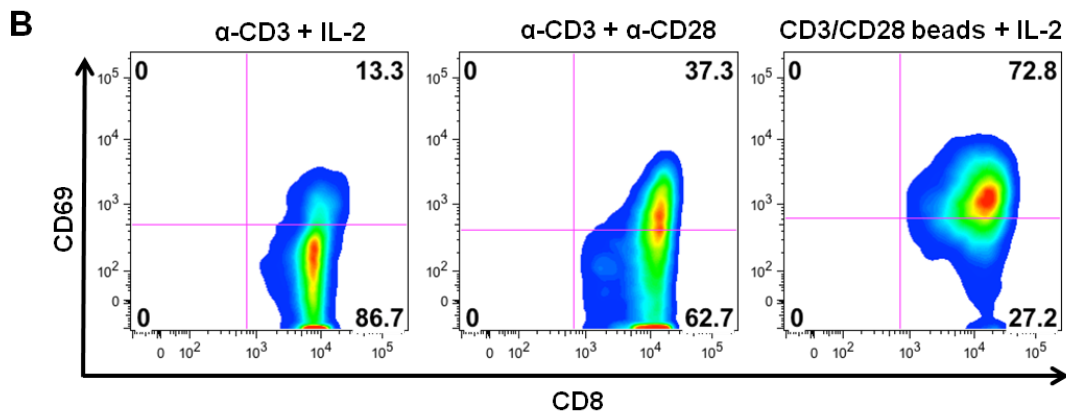
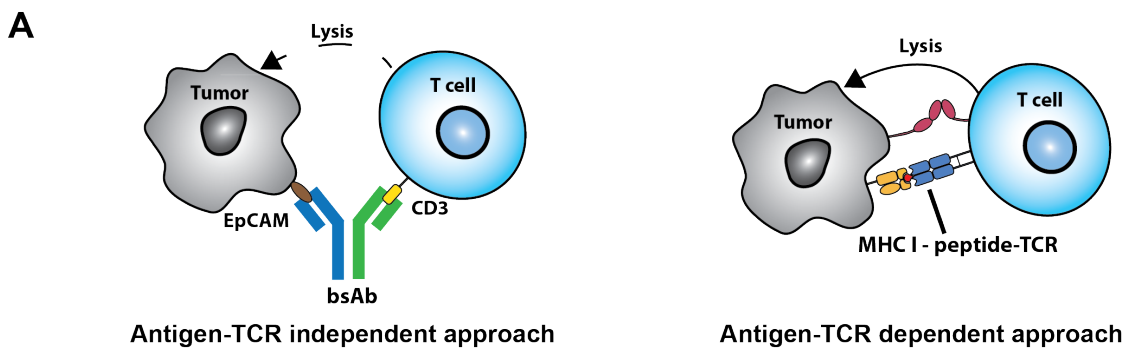
RNAiMAX (blue bars) in **B**. $n=6$. **(C)** Fluorescent microscopy showing GFP expression in MCF7luc stable cell line. Scale bar = 100 μ m. **(D)** Luciferase activity of the MCF7luc cell line upon transfection with mock, control siRNA, luciferase (FLuc)-targeting siRNA or UBC-specific siRNA using Trans-IT as the transfection reagent; $n=4$. **(E)** Linear relationship plotted between luciferase intensity versus cell number for MCF7luc cells seeded in 384-well plate ($r^2=0.9907$; $p<0.0001$). Error bars denote \pm SEM.

4.3 Antigen-restricted and antigen-unrestricted T cells for the high-throughput screen

As effector T cells for the high-throughput screen, both options of using an antigen-unrestricted as well as an antigen-restricted system were explored (Figure 3A). For the antigen-unrestricted system, polyclonal CD8⁺ T cells were purified from the peripheral blood lymphocytes of healthy donors and pre-activated in culture via triggering of the CD3-based primary and/or CD28-based co-stimulatory signals in the presence of interleukin 2 (IL-2). Degree of T cell activation using the three different activation protocols: anti-CD3 antibody + IL-2; soluble anti-CD3 and anti-CD28 antibody; or anti-CD3/CD28 antibody coated beads + IL-2, was compared using CD69 as an early T cell activation marker in flow cytometry based staining (115). As shown in Figure 3B, anti-CD3/CD28 antibody coated beads induced the highest level of activation of CD8⁺ T cells (72%) compared to the other activation protocols tested. Accordingly, it also induced a higher tumor lysis of MCF7 cells in comparison to the activation protocol using anti-CD3 antibody alone (Figure 3C) and was therefore chosen as the method of choice for polyclonal T cell activation. Tumor recognition and lysis by these pre-activated polyclonal T cells was induced by using anti-CD3 x anti-EpCAM bispecific antibody (bsAb). As shown in Figure 3A, one arm of this bsAb recognizes and binds to the EpCAM epithelial antigen, present on the MCF7 breast cancer cells, and the other arm binds to the CD3 receptor on the T cells, creating an artificial immune synapse which facilitates the lysis of target tumor cells in the proximity by pre-activated T cells (116). The specificity and effectiveness of the bsAb approach in mediating tumor lysis is shown in Figure 3D, whereby polyclonal T cells could induce tumor lysis in the Luc-CTL assay in the presence of anti-CD3 x anti-EpCAM bsAb, but not in the presence of anti-CD3 x anti-CD19 bsAb, which binds to an unrelated B-cell antigen CD19 that is absent on the MCF7s. Bi-specific antibody-induced tumor lysis was also found to be dose dependent as shown in Figure 3E. For the antigen-restricted system, survivin-specific CTLs (clone SK-1) were employed that recognize the HLA-A0201 restricted survivin₍₉₅₋₁₀₄₎ epitope expressed by the breast cancer cells, but fail to

recognize the T2 cells loaded with an unrelated HIV peptide (108). As shown in Figure 1B, survivin-specific CTLs recognize and lyse the MCF7 breast cancer cells in a dose-dependent manner. Both these systems have their own merits and limitations which are discussed in detail in section 5.1.3. Given that robust immune modifiers that extend beyond a single donor or setup were sought, the RNAi screen was performed in parallel under both the settings.

Figure 3. Effector T cells for immune RNAi screen. (A) Scheme showing the antigen-unrestricted approach whereby pre-activated, polyclonal T cells are cross-linked to tumor cells using bi-specific antibody and the antigen-restricted approach, whereby antigen-specific CTL clones recognize tumor targets in context of peptide-MHC I complex. (B) CD69 surface staining showing the activation of CD8⁺ T cells after 72h of stimulation with anti-CD3 antibody and IL-2, or with anti-CD3 and anti-CD28 soluble antibody, or with anti-CD3/CD28 antibody coated beads and IL-2. Gates were set based on the isotype control antibody. (C) Cr-release assay showing the cytotoxic capacity of polyclonal CD8⁺ T cells upon stimulation with either anti-CD3 antibody + IL-2 (○) or with anti-CD3/CD28 antibody coated beads (■) against MCF7 target cells. Lysis in both cases was induced by the addition of anti-CD3xEpCAM bi-specific antibody; n=3. (D) Luc-CTL assay performed at different T cell to MCF7 cell ratio with PBMC-derived CD8⁺ T cells and anti-CD3 x anti-EpCAM bi-specific antibody (○). Anti-CD3 x anti-CD19 bi-specific Ab (■) was used as a specificity control since CD19 is a B-lymphocyte-specific antigen and therefore this bsAb fails to crosslink tumor to T cells. Lower luciferase intensity indicates higher lysis; n=8. (E) Cr-release assay showing % specific lysis of MCF7 tumor cells by polyclonal pre-activated CD8⁺ T cells at E:T of 50:1 in the presence of the indicated doses (x-axis) of bi-specific antibody. Error bars denote SEM. Experiments are representative of at least three independent repeats.



4.4 Immunosuppressive positive controls for the screen

For a high-confidence hit calling from a data intensive RNAi screen, it is essential to have a clear distinction between the expected positive and negative phenotype. Therefore, as positive controls for the Luc-CTL assay, the reported immunosuppressive effects of PD-L1 (60), RCAS-1 (85) and CEACAM-6 (117) were validated in MCF7 cells. Knockdown of these immune-checkpoint molecules in MCF7 cells (Figure 4A) led to a varied but strong decrease in the luciferase activity of the remaining tumor cells upon co-culture with the pre-activated TCs and bsAb, indicating elevated immune-mediated tumor lysis under the knockdown conditions (Figure 4B). Downregulation of the respective immune-checkpoint molecules had no major impact on tumor cell viability *per se*, as determined in the CTG cell viability assay (Figure 4C). These were therefore chosen as the reference immunosuppressive controls for evaluating the screen efficacy, along with the scrambled control siRNA as the negative control.

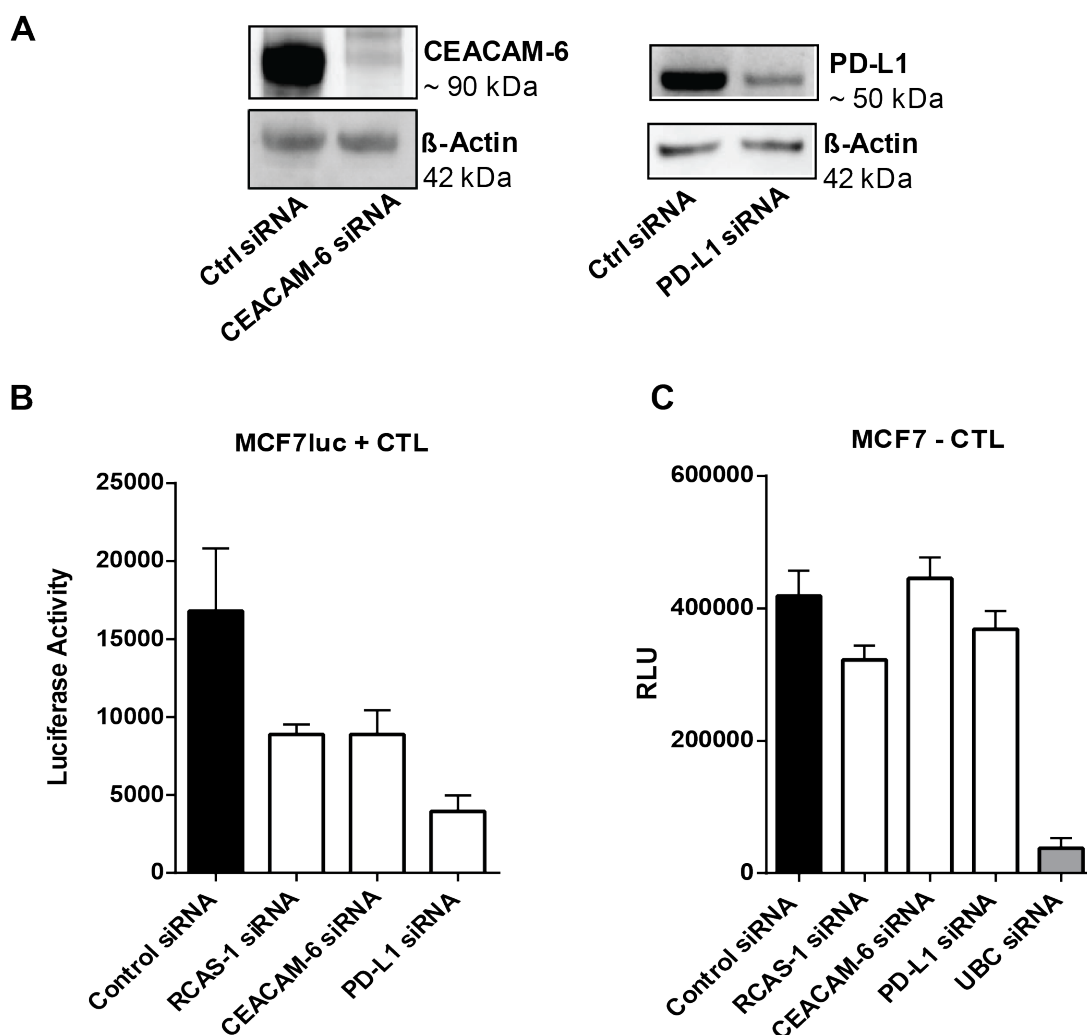


Figure 4. Positive immunosuppressive controls for the RNAi screen. (A) MCF7 cells were reverse transfected with scrambled control, CEACAM-6 or PD-L1 specific siRNAs and harvested after 72 h for determining protein knockdown efficacy using western blot analysis. Immunoblots were probed with anti-beta-actin antibody to verify equal protein loading. (B) Luc-CTL assay showing lysis of MCF7luc cells upon siRNA-mediated knockdown of indicated immune-checkpoint molecules by polyclonal pre-activated CD8⁺ T cells and CD3xEpCAM bi-specific antibody. (C) CellTiter-Glo (CTG) cell viability assay showing the impact of immune-checkpoint knockdown on the viability of MCF7 cells. siRNA against UBC, which is vital for cell viability, was used as a positive control. Error bars denote SEM. Experiments are representative of at least three independent repeats; n = 6.

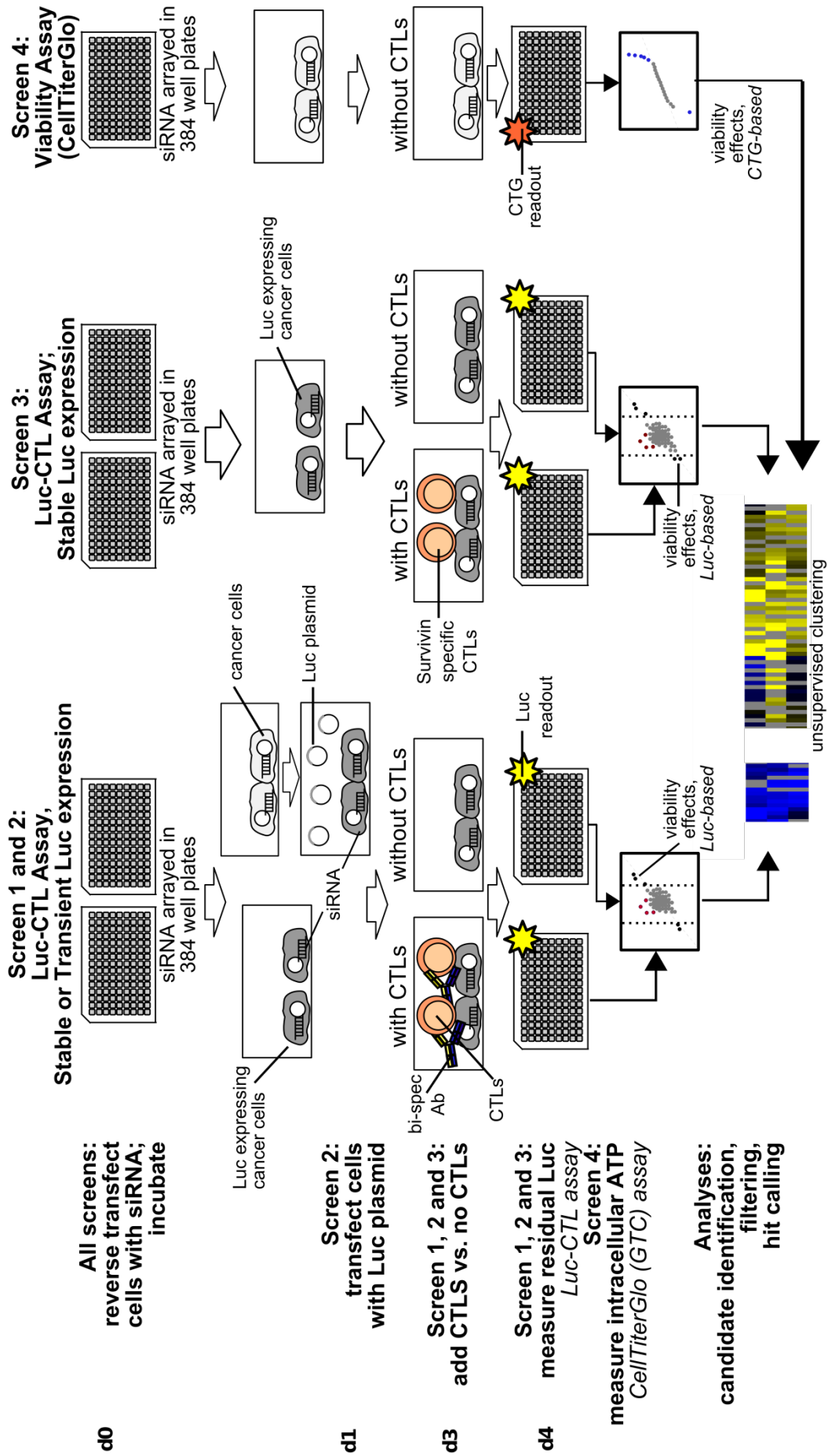
4.5 Workflow and performance of the high-throughput RNAi screen

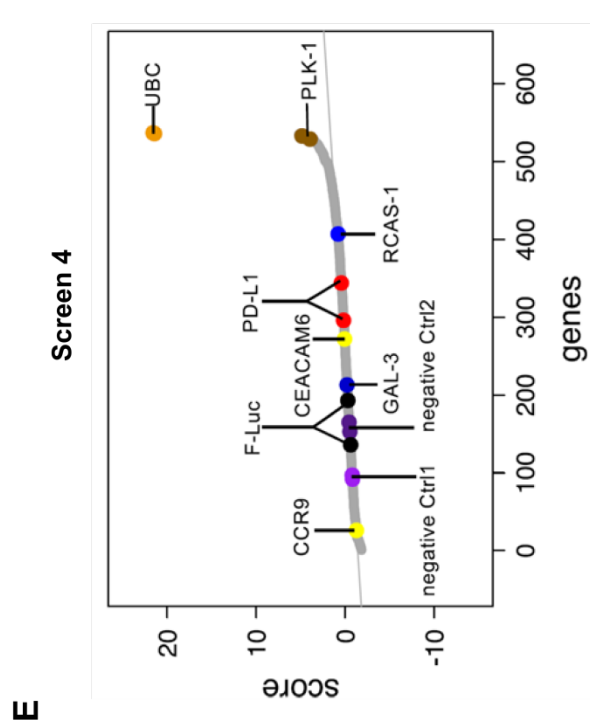
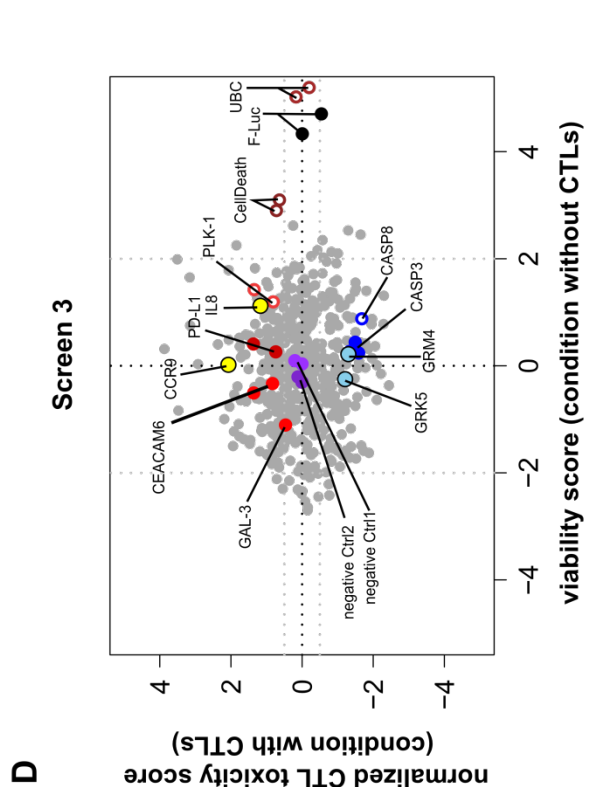
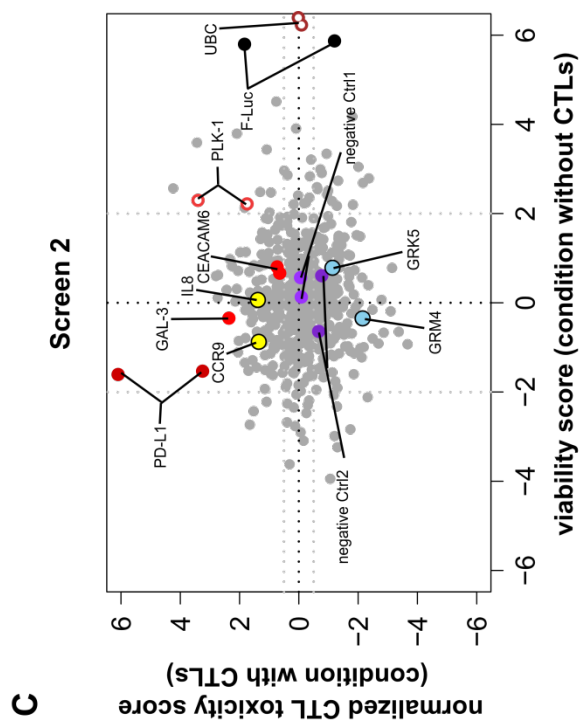
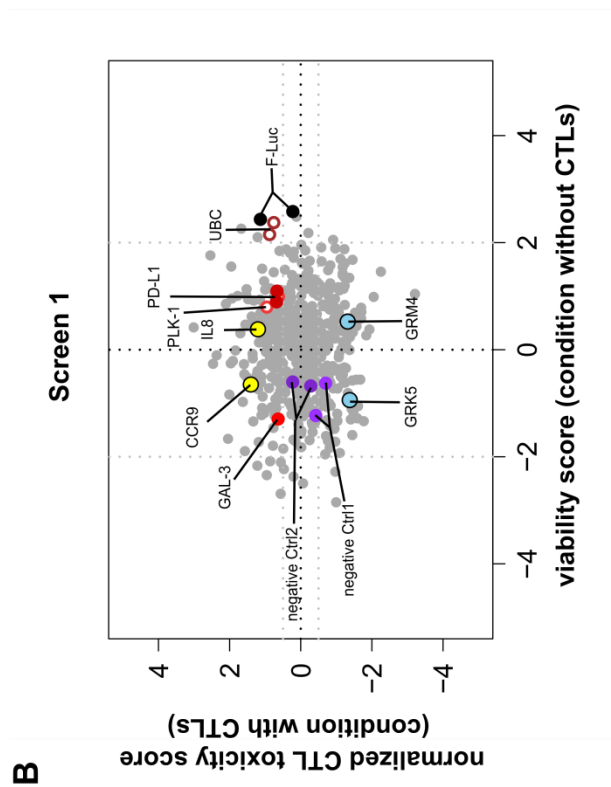
To translate the Luc-CTL assay to a high-throughput screening approach, a library of 516 genes coding for transmembrane and cell surface proteins, involving many G-protein coupled receptors (GPCRs), was chosen as these are suitable targets for therapeutic function-blocking antibodies. The entire RNAi screen workflow and candidate identification procedure is outlined in Figure 5A. In brief, screen 1 and 2 were conducted with polyclonally-activated PBMC-derived CD8⁺ T cells in the presence of the bispecific antibody, whereas screen 3 was conducted with survivin-specific CTLs. T cells derived from a single donor were used for screen 1 and two different donors were used for each technical replicate in screen 2. Additionally, the screens were conducted with not only stably transfected MCF7luc cells (screen 1 and 3), but also with wild type MCF7 cells that were transiently transfected with the luciferase plasmid (screen 2). The latter approach can be easily and rapidly employed for screening of various tumor cell lines without the time-intensive generation of stable luciferase-positive clones. Finally, data from an additional screen (based on the CTG assay) in which cell viability was determined independent of the luciferase activity by measuring intracellular ATP levels (screen 4) was employed to exclude genes that impacted cell viability. Each screen (screen 1-3) was performed a set of 4 replicates, two of which were exposed to CTLs (toxicity set) and two were incubated without CTLs (viability set). The reproducibility of the replicates within each individual screen was satisfactory for both the toxicity set and the viability set. For example, the Pearson's correlation coefficient for the replicates in the toxicity set in screen 2, which had two different donor-derived T cells per replicate, was 0.73 and for the viability set it was 0.94.

An overview of the results from the individual screens is depicted in Figure 5B-D, whereby each gene is plotted for its impact on cell viability (x-axis) and immune-susceptibility (y-axis). Knockdown using the FLuc siRNA expectedly abrogated the luciferase signal under both conditions and served as an internal control for the luciferase-based readout. siRNAs targeting genes indispensable for cell survival (UBC, PLK-1) resulted in a clear loss of cell viability, thereby yielding high scores under non-treated condition (without CTLs; x-axis). In contrast, the negative control siRNAs (Ctrl1 and Ctrl 2) impacted neither the cell viability nor the immune susceptibility of tumor cells and therefore showed no effect on the luciferase intensity under both conditions (Figure 5B-D). In accordance with their reported immune regulatory function, silencing of PD-L1, GAL-3 and CEACAM-6 resulted in higher cytotoxicity scores, whereby PD-L1 showed a higher impact on tumor lysis. On the other hand, knockdown of caspase 3 (CASP3) and caspase 8 (CASP8), which are required for the T cell-mediated apoptosis of target cell (118, 119), resulted in decreased cytotoxicity score (Figure 5D). Independent assessment of all genes for their impact on cell viability was achieved using the CTG assay as shown in Figure 5E.

Figure 5. Layout and analysis of the RNAi screen used to identify immune-modulatory tumor genes. (A) Workflow: RNAi screen was performed thrice, each time in duplicates, along with an additional CTG-based viability screen. Screen 1 and 2 were performed with polyclonal CD8⁺ T cells derived from three different donors along with bsAb, whereas screen 3 was performed with survivin-specific CTLs. MCF7luc stable cells were used for RNAi in screen 1 and 3, while transient transfection of the luciferase plasmid was employed 24 h after siRNA transfection in screen 2. Luciferase intensity after CTL challenge was acquired and data was normalized and analyzed using the cellHTS2 package. **(B-D)** Graphical summary of gene function related to modification of T cell mediated tumor lysis and cell viability for screen 1, 2 and 3 respectively. Positive score = reduced cancer cell viability, negative score = increased viability. X axis: Influence on cell viability without addition of T cells. Y axis: Influence on cell viability with addition of T cells. Appropriate immune-modulatory (PD-L1, CEACAM-6, GAL-3 and CASP3) and lethality (UBC, PLK-1) controls and few positive and negative immune modulatory hits (CCR9, GRM4) are highlighted herein. **(E)** Normalized score for all the tested genes depicted for the CellTiter Glo (CTG) assay used for determining lethal genes that directly affect MCF7 cell viability upon knockdown.

A





4.6 Data analysis and hit-calling parameters

For hit identification, loess-normalized differential score between the viability and toxicity values for all genes was calculated for each screen. As explained earlier in Figure 1A, a candidate immunosuppressive hit would reveal a positive differential score and a candidate immune-activating hit would exhibit a negative differential score. This is shown exemplarily for PD-L1 and CASP8 in Figure 6A, whereby the difference between without CTL and with CTL condition is positive for immunosuppressive control PD-L1, negative for immune-activating control CASP3 and no difference is observed for the control siRNA. Based on these differential scores, unsupervised hierarchical clustering was performed for all genes across the three screens to identify robust immune modulators that regulated anti-tumor immune response in all the three screening formats (Figure 6B). Clustering analysis revealed heterogeneity in the immunomodulatory performance of certain genes across the three screens, which is represented by the overall correlations between the three screens (Figure 6C). The observed heterogeneity was expected given the intentional assorted biological set-up used for the three different screens, including not only the source and format of effector T cells, but also the nature of tumor cell modification with regard to luciferase expression. Therefore, to identify only robust immune-regulatory genes that modified anti-tumor immune response irrespective of the T cell source or tumor modification, candidates were considered as hits if they popped up in at least two of the three screens. Notably, the loess differential score between the viability and cytotoxicity value can be high for even a non-immunosuppressive candidate if its viability score is too low while the cytotoxicity score is minimal. To account for this bias, clustered hits were filtered based on threshold values for both toxicity and viability scores that were set based on the performance of the controls and sample's quartile distribution (detailed in the methods section). Filtered genes were then ranked based on the sum of their loess differential scores from all three screens, resulting in top immunomodulatory candidates that are represented in Supplementary Figure 1. Filtering based on the CTG screen data was additionally employed as a second layer to exclude hits that revealed viability effects. Taken together, the presented screening methodology could reliably confirm the already established immune modulatory ligands in breast cancer cells, thereby proving its efficacy to identify novel immune modulatory ligands on tumor cells.

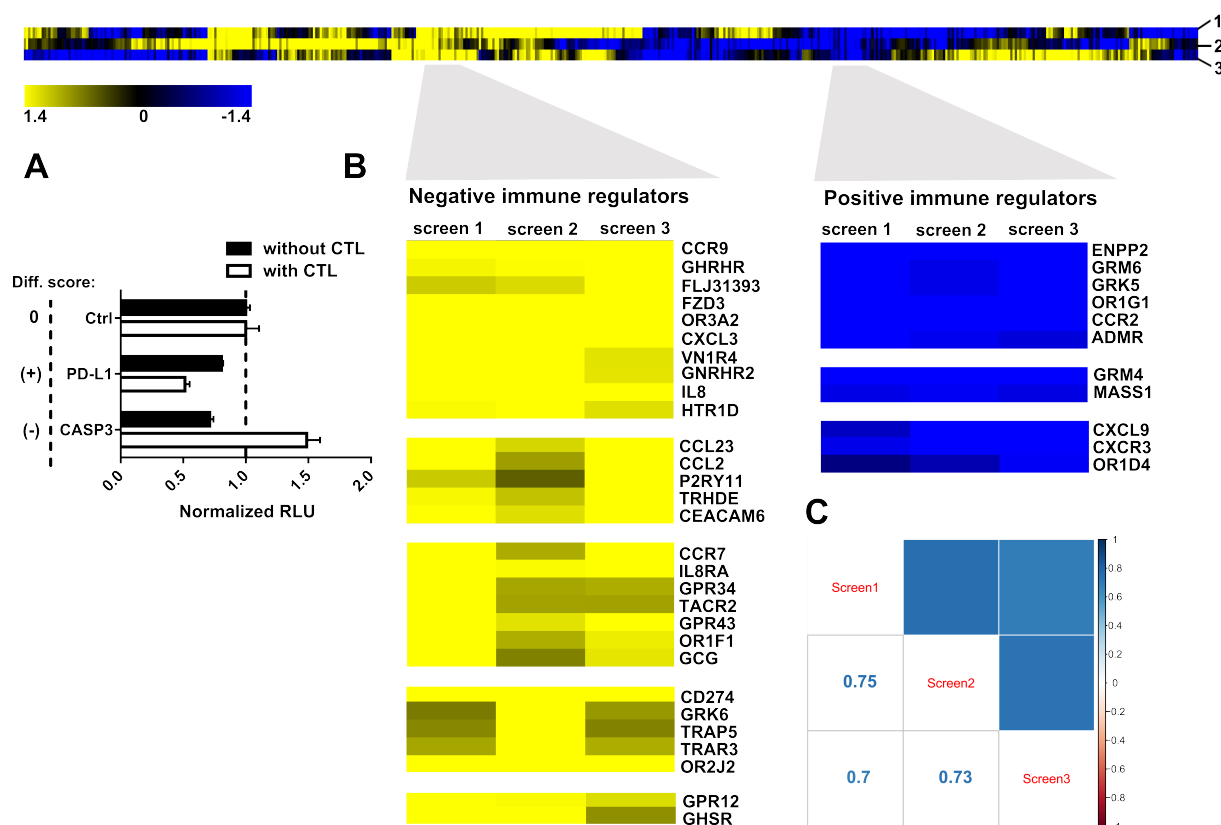


Figure 6. Identification of immune-modulatory tumor genes. (A) Principle behind hit identification using differential score calculation between without CTL and with CTL condition (black bar and white bar, respectively). MCF7 cells were transfected with siRNAs against immune-suppressive PD-L1 and immune-activating CASP3 and challenged with or without CTLs and bsAb in Luc-CTL assay. For each condition, the luciferase activity was normalized to that of the control treatment and is shown here. (B) Heat map representation of differential scores used to identify positive immune modulators (yellow), i.e. the knockdown of which enhance CTL mediated cell killing and negative immune modulators (blue), i.e. the knockdown of which reduce CTL mediated cell killing are depicted for all genes tested in the 3 different screens. Differential scores prior to filtering are shown (see methods). Selected representative clusters of high-confidence hits are displayed herein. (C) Correlation between the toxicity scores across the three screens as evaluated using the Pearson's correlation test.

4.7 Validating potential immunosuppressors in the re-run of the primary assay

Next, based on the overlap between the three screens and the exhibited immunosuppressive strength (Figure 6B, Supplementary Figure 1), selected hits (CCR9, GHSR and CCRL1) were repeated in the Luc-CTL assay for first round of validation. This was performed at least thrice with individual deconvoluted as well as the pooled siRNAs to reproduce the results obtained from the primary screens and to refine the candidate hit-list for further validation studies. As

shown in Figure 7A, the identified gene hits were compared for their impact on CTL-mediated tumor lysis based on the range set by control siRNA on one hand and the PD-L1 siRNA on the other hand. As a control for the selectivity of the RNAi screen, PTGER3 which was not identified as an immunosuppressive hit was also included in the assay re-run. Cell viability assay was performed to rule out the siRNA sequences that impacted cell viability (Figure 7B). Both GHSR and CCR9 exhibited a strong suppression on the CTL-mediated tumor lysis, comparable to that observed with PD-L1, without affecting cell viability *per se*. For CCRL1, s2 and s3 siRNA sequences resulted in an increase in tumor lysis, however they also showed a commensurate impact on cell viability. Based on the strength of immunosuppression observed in the screens as well as in the re-run assays, CCR9 was chosen for further validation studies. Interestingly, its role in immune modulation has never been reported before.

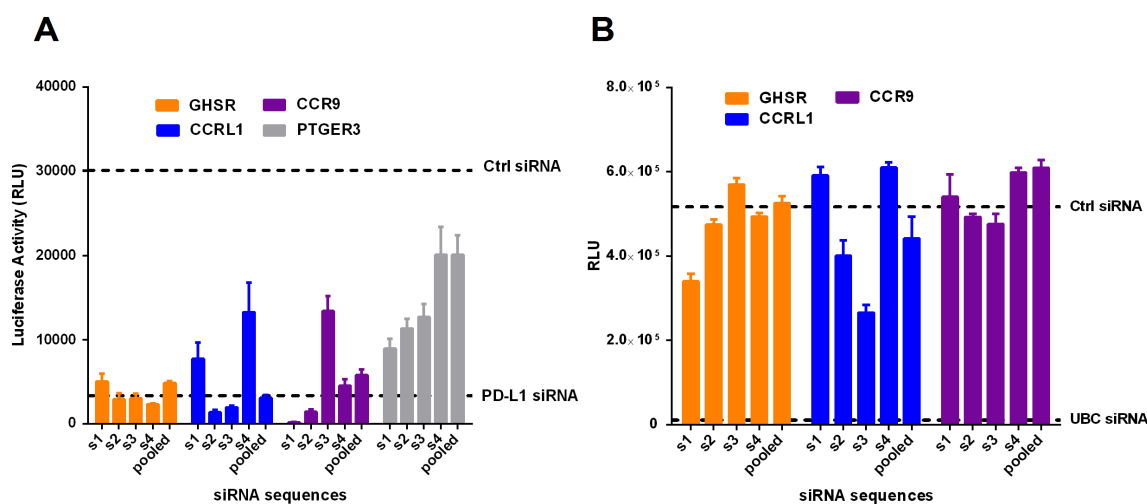


Figure 7. Pre-validation of the identified hits using primary assay re-runs. (A) Luc-CTL assay was performed with the deconvoluted siRNAs against the indicated target genes in MCF7luc cells using the PBMC-derived, pre-activated CTLs and bsAb at 10:1 (E:T) ratio. PD-L1 was used as the positive immunosuppressive control along with the negative control siRNA. (B) CTG cell viability assay was performed with the individual siRNAs transfected in MCF7luc cells. Mean +SEM are plotted herein; n=4. Data presented here is representative of at least three independent experiments.

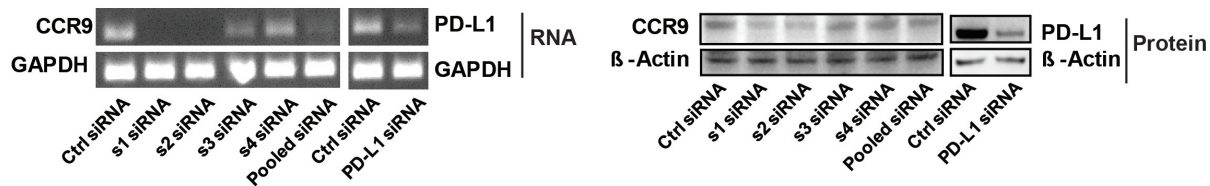
4.8 Knockdown of CCR9 sensitizes the breast cancer cells towards immune lysis

C-C chemokine receptor 9 (CCR9) is a surface bound receptor which binds to the chemotactic ligand CCL25 and is involved in the trafficking of a subset of immune cells to the intestinal

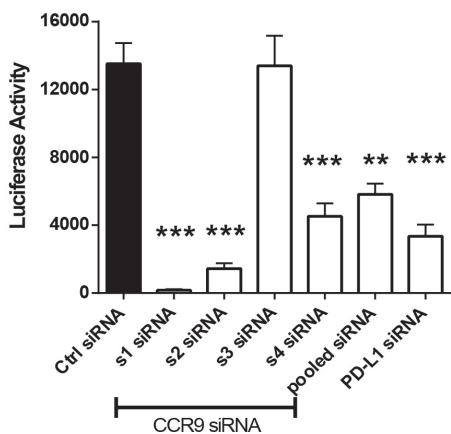
mucosa and thymus (120). To validate the role of CCR9 in suppression of anti-tumor immune response, correlation between the knockdown efficiency and the immunosuppressive phenotype of the individual siRNAs from the CCR9-targeting siRNA pool was first evaluated. CCR9's mRNA and protein estimation in the MCF7 cells after knockdown with individual siRNAs revealed s1 and s2 siRNA sequences to induce the strongest knockdown, which correlated well with their functional effect on the CTL-mediated cytotoxicity (Figure 8A, B). Since at least two different CCR9 siRNA sequences, amongst four, exhibited both knockdown as well as functional phenotype on CTL-mediated lysis, with CCR9 s1 siRNA being the strongest, it was reasonable to assume the direct involvement of CCR9 in immune-suppression rather than an off-target effect. None of the siRNAs by themselves impacted on cell viability as determined in the CTG assay (Figure 8C). Furthermore, CCR9 s1 siRNA was also found to reduce the surface expression of CCR9 receptor on MCF7 cells in the flow cytometry staining (Figure 8D). Therefore, s1 siRNA sequence was chosen as the model siRNA for further studies. Knockdown of CCR9 using the s1 siRNA sequence markedly increased the tumor lysis of breast cancer cell lines MCF7 and MDA-MB-231 by survivin-specific CTLs in the secondary independent chromium-release assays (Figure 8E, F), validating its role in tumor-mediated immune-inhibition. Impact of CCR9 knockdown on CTL-mediated cytotoxicity was found to be comparable to or even better than PD-L1 knockdown (Figure 8B and E).

Figure 8. CCR9 knockdown sensitizes breast tumor cells to immune attack. (A) MCF7 cells were transfected with the described siRNA sequences for estimating the mRNA and protein levels using RT-PCR (left) and western blot (right) analysis respectively. GAPDH and beta-actin were used as controls for RNA and protein normalization respectively. (B) Luc-CTL cytotoxicity assay with PBMC-derived CTLs as effector population and MCF7 as target cells, which were transfected with individual (s1-s4) or pooled CCR9 siRNA sequences. PD-L1 and non-specific control siRNAs were used as positive and negative controls respectively for CTL-mediated cytotoxicity. (C) CTG viability assay with MCF7 cells upon CCR9 knockdown using the described siRNAs, along with lethality control (UBC) and negative non-specific control siRNA. (D) Flow cytometry staining for CCR9 surface expression on MCF7 cells after 72h of knockdown with control or CCR9 s1 siRNA. Shift in the CCR9⁺ population can be seen in CCR9 siRNA treated samples. Gates were set based on the isotype antibody control. (E, F) Cr-release assay showing % specific lysis of MCF7 (E) or MDA-MB-231 (F) breast cancer cells by survivin-specific T cells at different ratios upon CCR9 knockdown and in comparison to the positive control PD-L1 (□) or non-specific control siRNA (■).

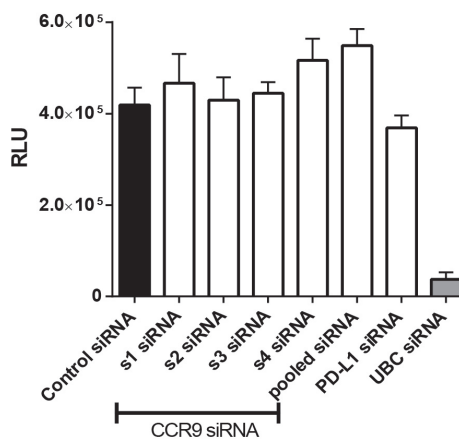
A



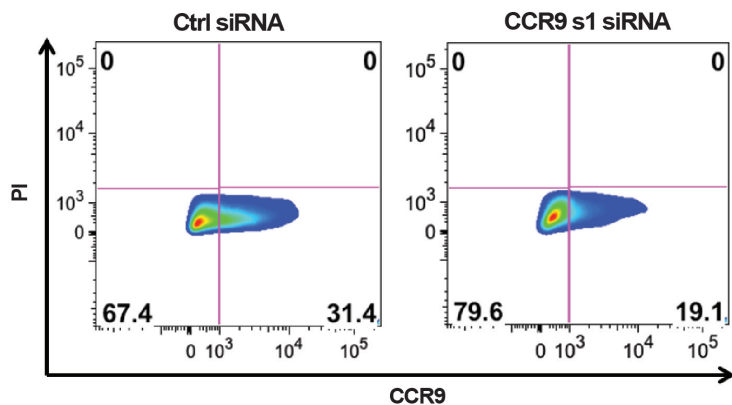
B



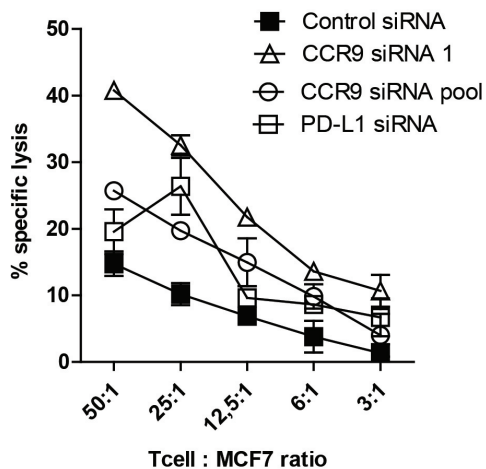
C



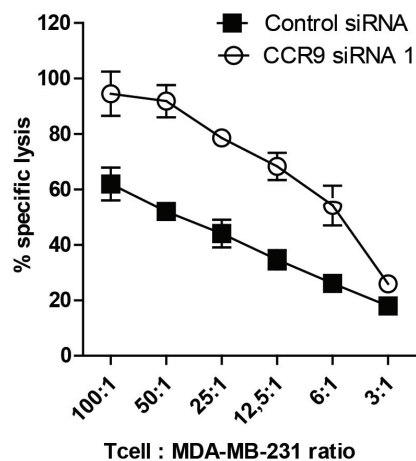
D



E



F



4.9 Overexpression of CCR9 on breast cancer cells inhibits immune lysis

Next, to investigate whether overexpression of CCR9, which is observed in many tumor entities, correlated with poor immune response, breast cancer cells were transfected with histidine-tagged CCR9 expression plasmid. Since CCR9 is a 7-transmembrane receptor, the efficacy of the exogenously introduced CCR9 to be expressed and targeted to the cell surface was first assessed. Easily transfectable HEK 293T cells showed a marked upregulation of CCR9 expression on the cell surface upon transfection with the CCR9 vector compared to the control vector in the flow cytometry staining (Figure 9A). Similar increase in cell surface expression of CCR9 was also noted in MCF7 cells transfected with the overexpression construct. Importantly, overexpression of CCR9 resulted in a clear decrease in antigen-specific lysis of MCF7 cells by the survivin-specific CTLs (Figure 9B), indicating that cell-surface bound CCR9 inhibits immune-recognition and lysis of the protected tumor cells.

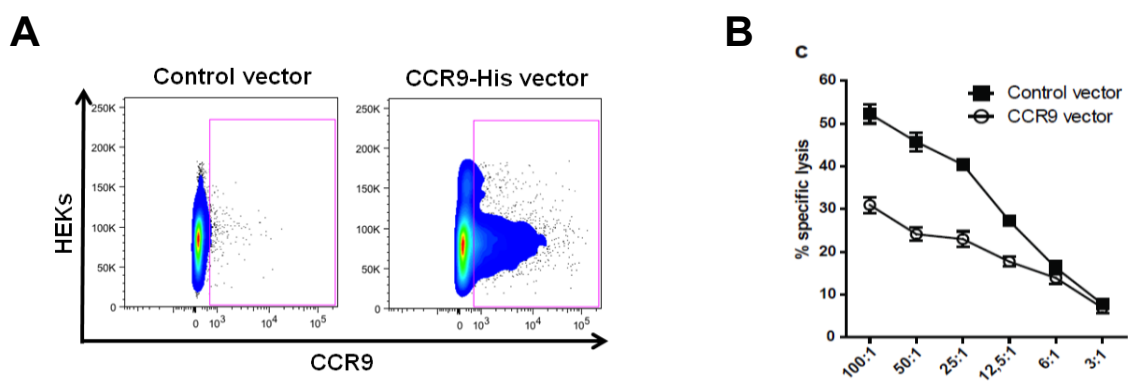


Figure 9. CCR9 overexpression inhibits immune lysis of tumor cells. (A) Flow cytometry staining for CCR9 surface expression in HEK 293 cells transfected with control or histidine-tagged CCR9 (CCR9-His) overexpression vector. Gates were set based on isotype control. **(B)** Cr-release assay showing % specific lysis of MCF7 cells by survivin-specific T cells. MCF7 cells were transfected with control vector (■) or CCR9-His expression vector (○) 72h prior to the assay.

4.10 CCR9 inhibits the secretion of cytolytic enzymes and Th1 cytokines

Cytotoxic T cells upon antigen encounter and engagement secrete effector cytokines such as interferon-gamma (IFN- γ), interleukin-2 (IL-2) and cytolytic enzymes such as perforin and granzyme B that bring about tumor lysis (121). Tumor-specific CCR9 inhibits this anti-tumor immune response by inhibiting the secretion of these immune mediators as seen in the IFN- γ

and granzyme B ELISpot assays. siRNA-mediated knockdown of CCR9 in MCF7 cells significantly increased the secretion of IFN- γ and granzyme B by survivin-specific T cells as shown in Figure 10A and B. Furthermore, luminex analysis of the tumor/TC co-culture supernatant revealed that CCR9 also selectively inhibited the secretion of T-helper-1 (Th1) cytokines, such as IL-2 and tumor necrosis factor-alpha (TNF- α), as well as IL-17, but increased the secretion of the immunosuppressive cytokine IL-10 (Figure 10C). Together, these data indicate that tumor-associated CCR9 impedes the anti-tumor, Th1 cytokine-based immune response.

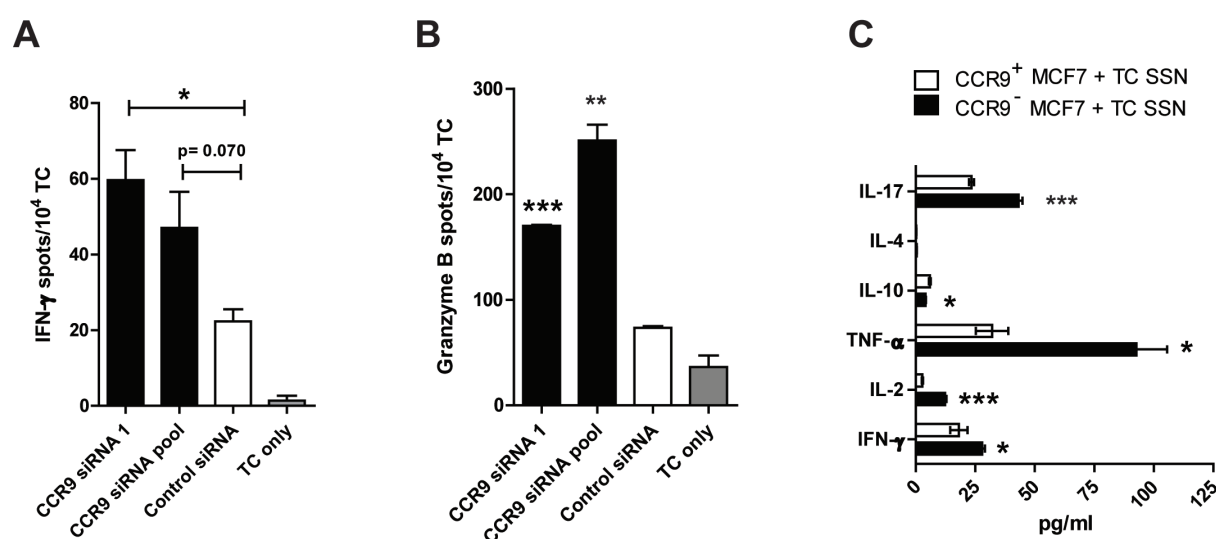


Figure 10. Tumor-specific CCR9 impedes Th1-type immune response. (A, B) ELISpot assay showing IFN- γ (A) and granzyme B (B) secretion by survivin-specific CTLs, as spot numbers, upon CCR9 knockdown (black bars) in MCF7 cells compared to the control knockdown (white bars). T cells (TC) only group was used to account for the background noise. Triplicate wells were used per sample group. (C) Luminex assay showing cytokine levels in the supernatant from the co-culture of survivin-specific T cells (TC) with either CCR9⁻ MCF7 (transfected with CCR9-specific siRNA) or CCR9⁺ MCF7 (transfected with control siRNA) cells. Error bars denote SEM. Statistical differences between the control siRNA and CCR9 siRNA treated groups were calculated using two-sided student's t-test: * = $p < 0.05$, ** = $p < 0.01$, *** = $p < 0.001$.

4.11 CCR9 expression in melanoma inhibits the anti-tumor reactivity of TILs

After validating the immunosuppressive role of CCR9 in breast cancer setting, its influence on anti-tumor immunity in other tumor entities was investigated next. For this, primary melanoma cells (termed as M579 cells) isolated from a metastatic melanoma patient were used. M579 cells were additionally stably co-transfected with an HLA-A2 expression

construct and luciferase-expressing plasmid (M579-A2-luc). At the same time, tumor infiltrating lymphocytes (termed as TIL 412) were isolated from a syngeneic metastatic melanoma patient and expanded *in vitro* using the modified Rosenberg's rapid expansion protocol. TIL 412 consists of CD8 (43%) as well as CD4 (55%) T cells as shown in the flow cytometry staining of Figure 11A. Amongst the CD8+ T cell compartment, almost half express PD-1, around 34% express TIM-3 and ~17% express both the exhaustion markers, underscoring the exhausted state of the tumor infiltrating T cells in this melanoma patient (122, 123) (Figure 11A). Since M579-A2 cells were also found to express CCR9, the next question therefore was whether CCR9 inhibition could alleviate the anti-tumor immune reactivity of the exhausted TIL 412 cells as well. Indeed, knockdown of CCR9 in M579 cells resulted in a marked increase in tumor lysis by TIL 412 cells in both Luc-CTL and Cr-release cytotoxicity assays, performing even better than PD-L1 inhibition (Figure 11B, C).

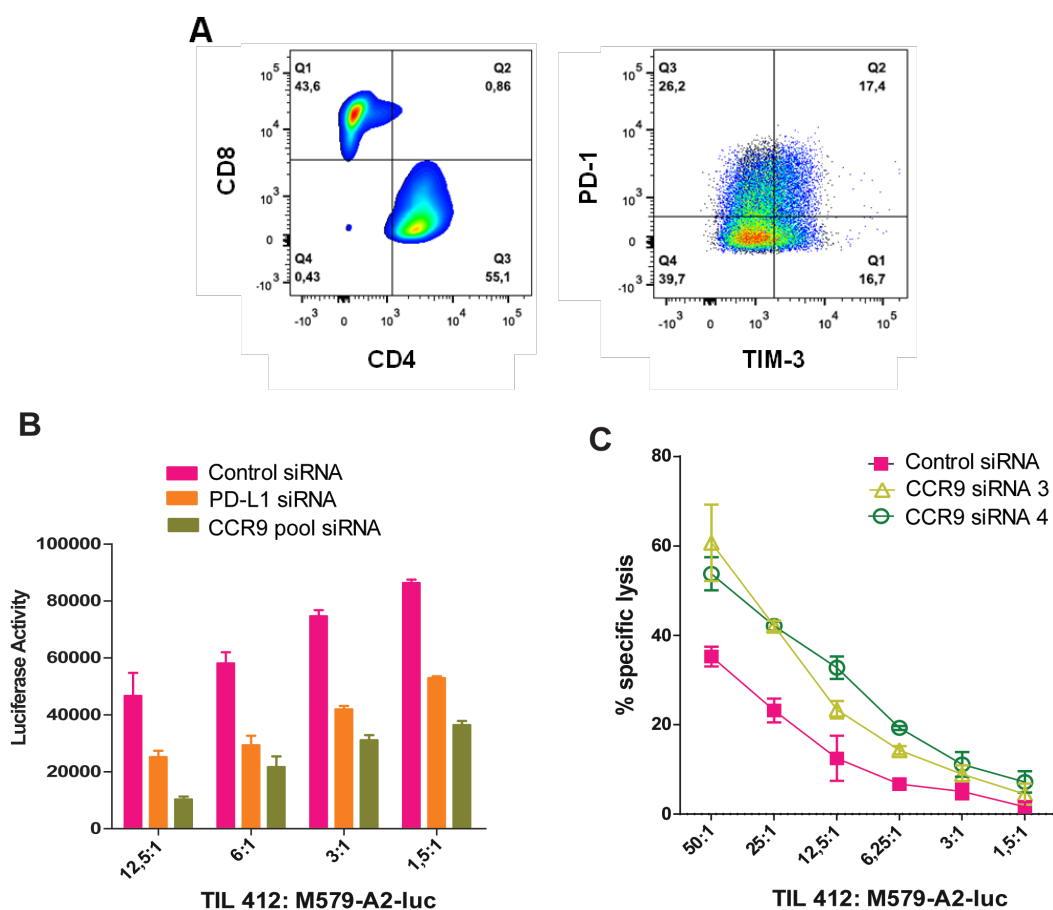


Figure 11. CCR9 inhibition induces anti-tumor reactivity of melanoma patient-derived exhausted TILs. (A) Flow cytometry staining showing the percentage of CD8 and CD4 T cells amongst CD3 T cells (left) and the percentage of PD-1 and TIM-3 positive T cells amongst CD8 T cells (right) in the melanoma patient-derived TIL

412 T cell culture. Gates were set based on the isotype controls. Stainings were performed by Tillmann Michels. (B, C) Luc-CTL (B) and Cr-release (C) cytotoxicity assays showing lysis of M579-A2-luc cells upon siRNA-mediated CCR9 knockdown by TIL 412 cells. Error bars denote +/- SEM.

4.12 CCR9 suppresses the tumor lysis potential of TILs in pancreatic adenocarcinoma

Next, the influence of CCR9 expression upon anti-tumor immune response in pancreatic adenocarcinoma (PDAC) was assessed. PDAC results from the malignant neoplasm arising in the exocrine component of the pancreas and has an extremely poor prognosis with the 5-year survival rate as low as 6% (124). Tumor infiltrating lymphocytes, although present in PDAC patients, are known to be subjected to systemic and local immune suppression (125). Accordingly, an exhausted immune phenotype, based on the PD-1 and TIM-3 surface staining, was noted in TIL 34 and TIL 53 T cell cultures which were isolated and established from two poorly differentiated PDAC male patients (Figure 12A). TIL 34 is a CD8/CD4 mixed T cell culture, whereas TIL 53 consists primarily of the CD8⁺ T cells (Figure 12A). Upon siRNA-mediated knockdown of CCR9 in PANC-1 pancreatic tumor cell line, a remarkable two-six fold increase in the tumor lysis capacity of both these exhausted TILs was noted in the Luc-CTL and Cr-release cytotoxicity assays (Figures 12B, C). Additionally, polyclonal CD8⁺ T cells derived from the peripheral blood of healthy donors also showed an enhanced IFN- γ secretion when co-cultured with CCR9 knocked down PANC-1 cells compared to the control knockdown cells (Figure 12D).

Taken together these data indicate that CCR9 mediates immunosuppressive effect in a broad variety of tumors with a clear clinical impact on the tumor lysis capacity of the infiltrating lymphocytes.

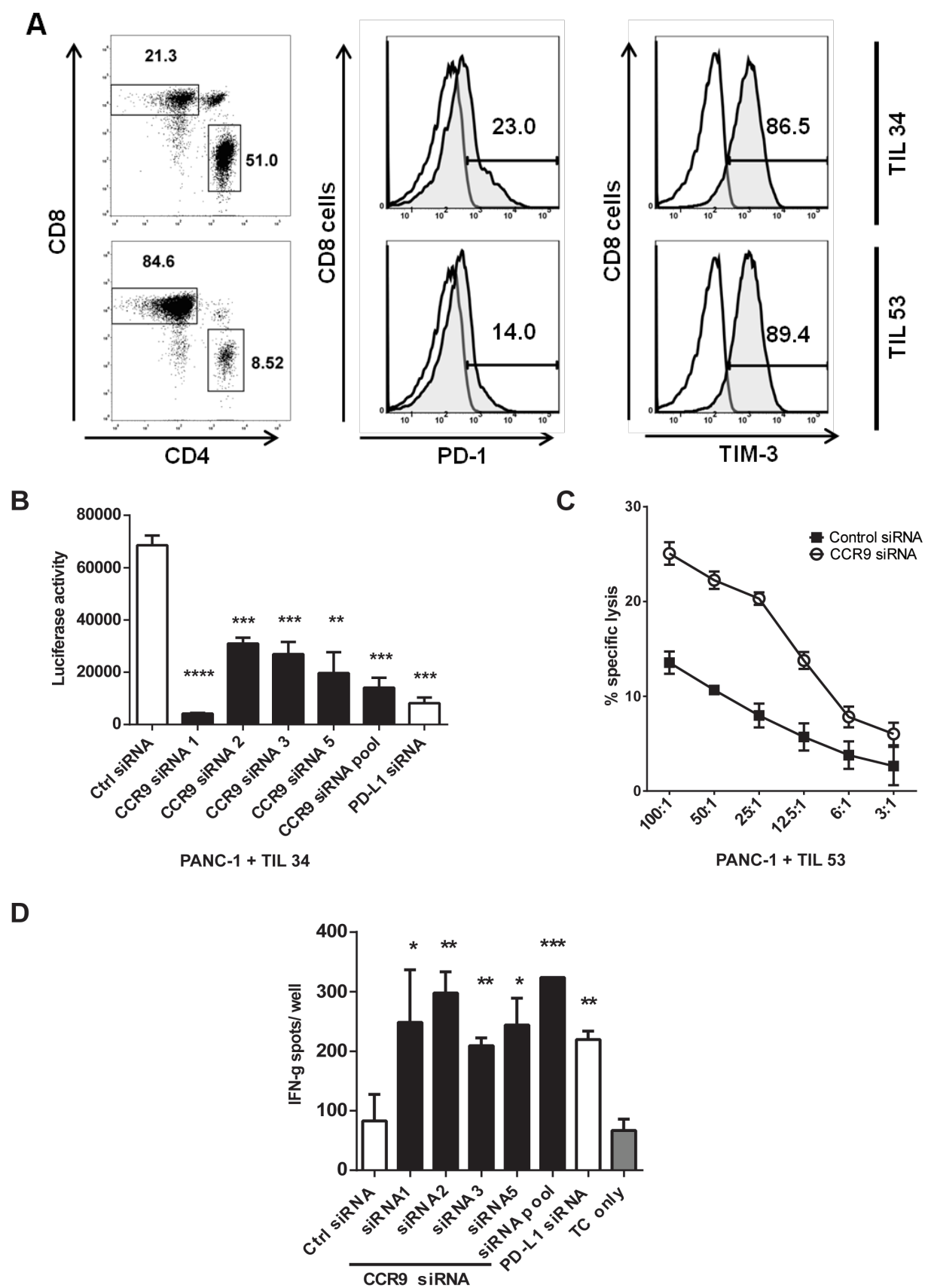


Figure 12. CCR9 mediates immune suppression in pancreatic cancer. (A) (left) CD8 and CD4 T cell population distribution amongst the TIL 34 and TIL 53 lymphocyte culture as determined by flow cytometry;

(right) PD-1 and TIM-3 expression on CD8⁺ T cells of TIL 34 and TIL 53 culture as analysed by flow cytometry (grey histogram: anti-PD-1 or anti-TIM-3 staining, white histogram: isotype Ab). Stainings were performed by Antonio Sorrentino. **(B, C)** Increase in TIL 34 (B) or TIL 53 (C) mediated lysis of PANC-1 cells upon CCR9 knockdown as determined by the Luc-CTL (B) or the Cr- release assay (C). **(D)** ELISpot assay showing IFN- γ secretion by polyclonal CD8 T cells upon co-culture with control or CCR9 knocked down PANC-1 tumor cells in the presence of anti-CD3 x EpCAM bi-specific antibody. Only T cells or PANC-1 cells were used as controls to account for the background signal. Error bars denote +/- SEM; statistical difference between control siRNA and tested siRNA groups are highlighted herein whereby * = $p < 0.05$, ** = $p < 0.01$, *** = $p < 0.001$.

4.13 Tumor-specific CCR9 does not impair the activation of the T cell receptor signaling complex

To explore whether the immunosuppressive effect of CCR9 on T cells is mediated by the impairment of the T-cell-receptor (TCR)-based signaling events, survivin-specific CTLs were co-cultured with either control siRNA-transfected (denoted as CCR9^{hi}) or CCR9 siRNA-transfected (CCR9^{lo}) MCF7 cells. The activation status of the TCR-associated signaling complex in these CCR9^{hi} or CCR9^{lo} treated TCs was then assessed at different time-points using the phospho-plex assay. Early TCR signaling events, upon antigen recognition and binding, involve the tyrosine phosphorylation of the cytosolic tyrosine kinase Lck, which phosphorylates ITAM (immunoreceptor-tyrosine based activation motifs) on the CD3 subunits. This leads to the phosphorylation of ZAP-70 and subsequently of the transmembrane adaptor protein LAT, which in turn recruits a broad range of signaling molecules in the T cell. As shown in Figure 13A and B, tumor-specific CCR9 did not alter the magnitude or the kinetics of the TCR activation and associated downstream signaling in the survivin-specific T cells upon antigen encounter. This indicates that CCR9-mediated immune suppression occurs via an alternate pathway in T cells that makes them unresponsive to tumor targets despite the presence of a sound and effective TCR signaling complex.

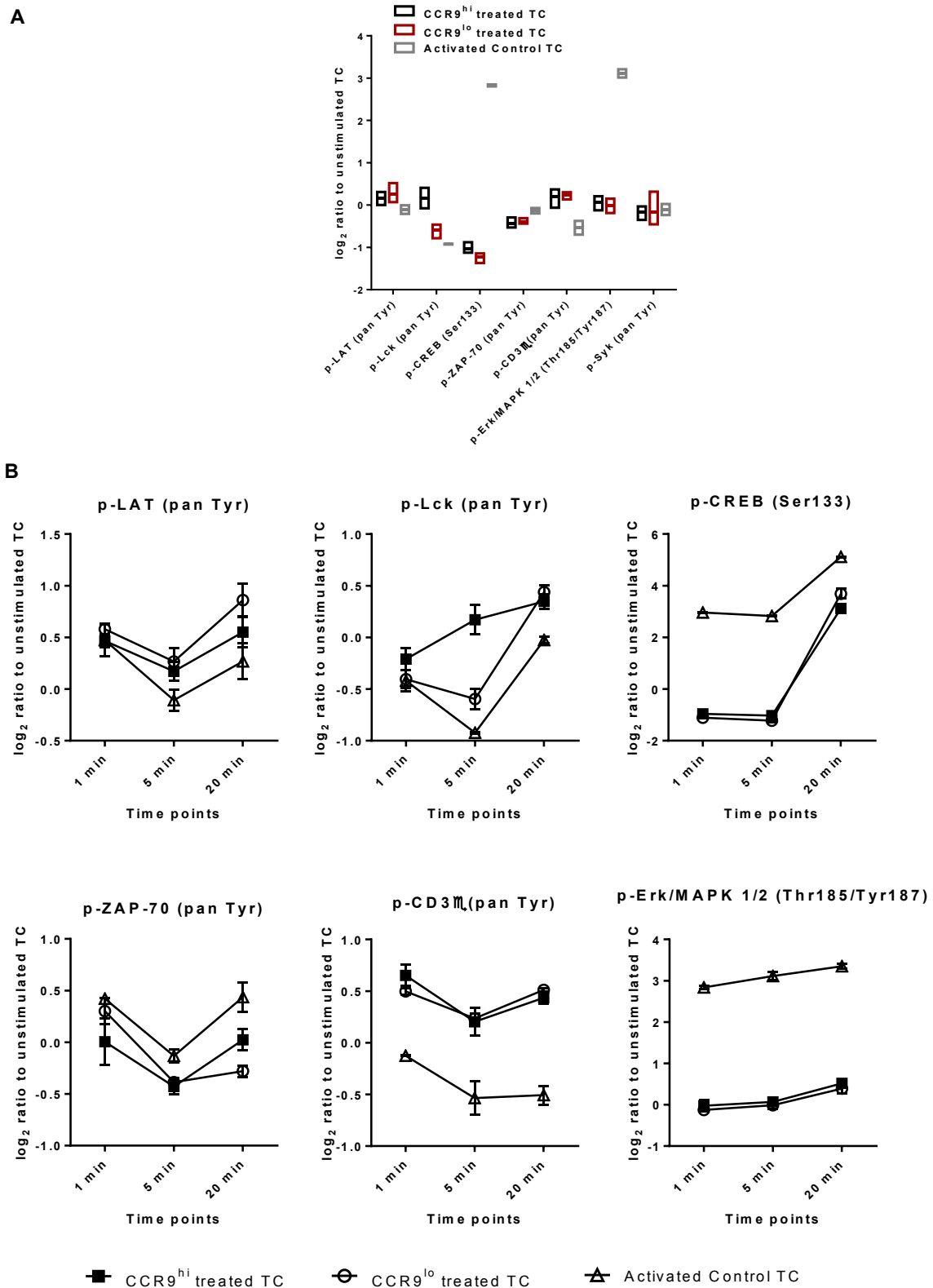


Figure 13. CCR9 does not impair TCR activation and signaling. (A-B) Phospho-plex analysis of the activated T cell receptor signaling complex in survivin-specific T cells (TC) that were co-cultured with MCF7 cells transfected with control (CCR9^{lo}) or CCR9-specific siRNA (CCR9^{hi}). Log₂ ratio of mean fluorescent

intensity (MFI) of specified phospho-proteins to the unstimulated survivin-specific TCs are depicted for all the studied analytes after 5 mins of co-incubation (A) or individually for all the analytes after 1 min, 5 min and 20 mins of co-culture (B). TCs stimulated with PMA and ionomycin were used as positive control. Experiments were performed in triplicates and are representative of at least three independent repeats. Mean \pm SEM are plotted herein.

4.14 CCR9 impedes STAT signaling in antigen-specific T cells

An alternative route of T cell activation is the STAT (signal transducer and activator of transcription) family of transcription factors which regulate the expression of cytokines in T cells (126). Since an impediment in Th1 cytokine production by T cells in response to CCR9+ tumor targets was already observed (Figure 10C), it was next sought to assess the impact of CCR9 on the activation status of STAT signaling in the encountered TCs. To analyze STAT signaling exclusively in the T cells after co-culture with the tumor cells, we exploited the preferential expression of EpCAM antigen on the surface of epithelial MCF7 tumor cells, and its lack thereof on the endothelial T cells, for separating the two cell populations (Figure 14A). Using anti-EpCAM antibody-coated magnetic beads, which effectively bound only EpCAM+ve MCF7 tumor cells, EpCAM-ve T cells were separated from the co-culture with more than 95% purity as assessed by the CD3 surface staining on the purified TCs (Figure 14B). Time-course based analysis of STAT activation in CCR9^{hi} and CCR9^{lo} treated TCs revealed a significant decrease in STAT1 signaling, along with decrease in STAT2 and STAT5a/b signaling, in survivin-specific T cells mediated by CCR9 (Figure 14C, D). This impairment in STAT1 signaling could also be verified on western blot using phospho-specific STAT1 antibody, indicating that tumor-derived CCR9 impairs STAT signaling, especially STAT1, in the encountering TCs (Figure 14E). Taking together the observations from the cytokine and phospho-STAT analysis, it can be concluded that tumor-specific CCR9 impedes Th1-type immune response via differential regulation of the STAT pathway.

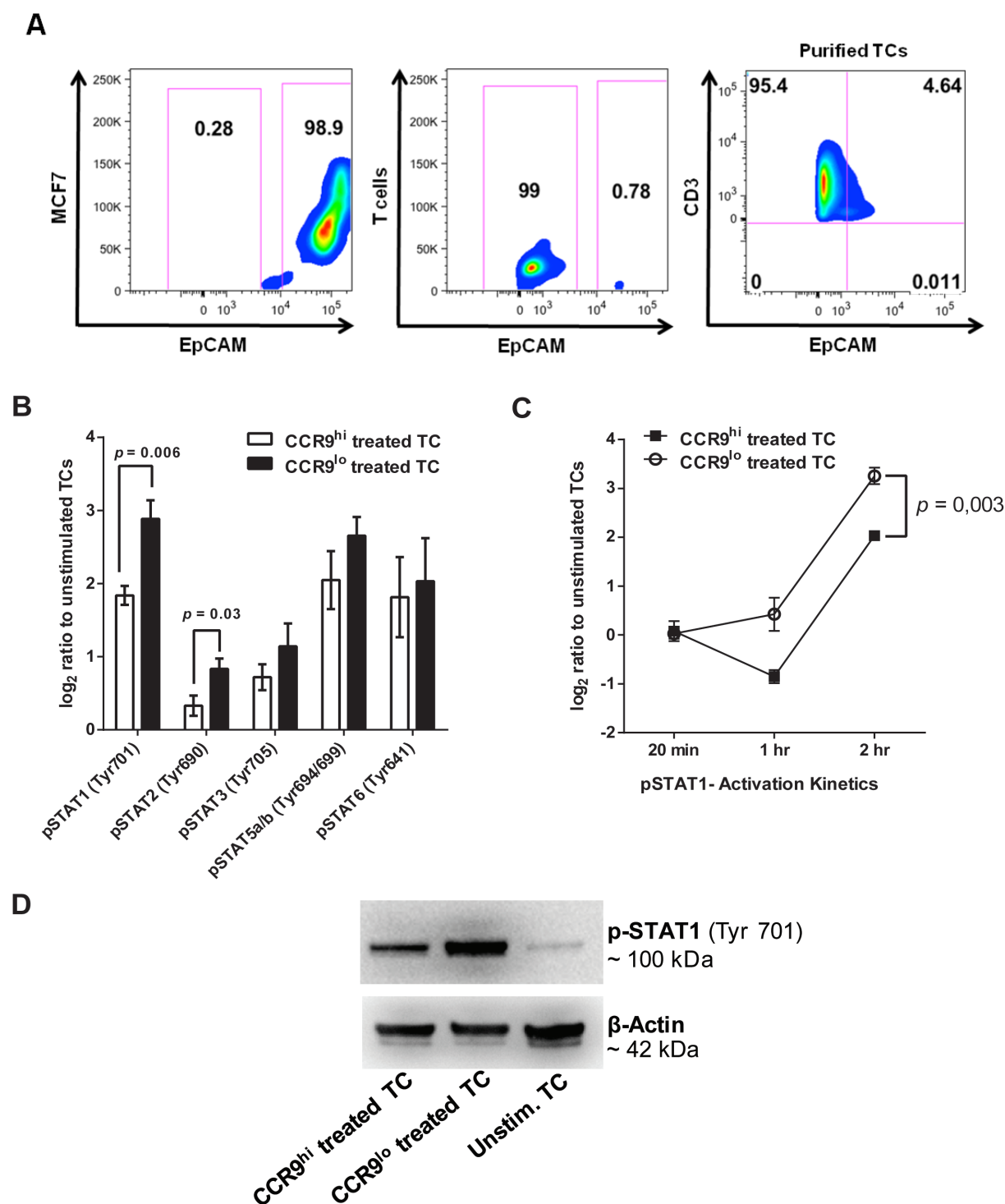


Figure 14. CCR9 impairs STAT activation in T cells. (A) Flow cytometry staining showing EpCAM expression on MCF7 and survivin T cells before co-culture. After 2h of co-culture they were separated using EpCAM-Ab-coated magnetic beads. EpCAM and CD3 staining on the bead-free cell suspension is shown at the extreme right. Cells were gated based on the isotype control. (B) Phospho-plex analysis showing the activation of STAT signaling in survivin-specific TC upon encountering CCR9^{lo} MCF7 cells (CCR9-siRNA transfected) compared to CCR9^{hi} MCF7 cells (control siRNA transfected). (C) Time-course based phosphorylation of STAT1 in survivin-specific T cells (TC) that were co-cultured with CCR9^{hi} or CCR9^{lo} MCF7 cells for the

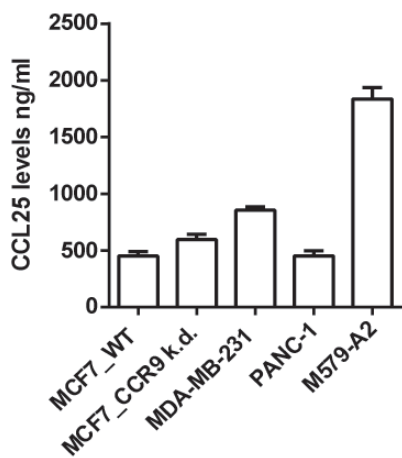
indicated time points. Log₂ ratio of mean fluorescent intensity (MFI) to the unstimulated TCs are plotted in B and C. **(D)** Western blot analysis of phospho-STAT1 protein levels in the respective TC samples. Beta-actin was used as the loading control. All experiments were performed in triplicates. Error bars denote +/- SEM. * = p<0.05, ** = p<0.01, *** = p<0.001, as calculated by two-sided student's *t*-test.

4.15 Role of CCL25 in CCR9-mediated immune-suppression

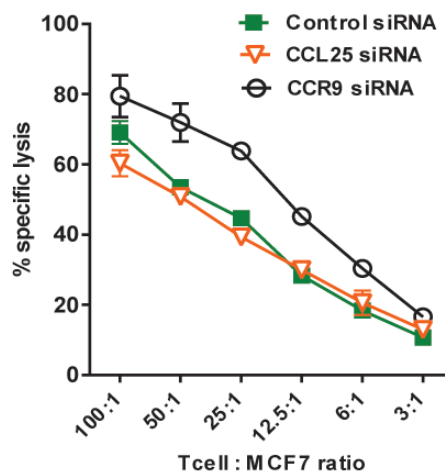
CCL25 is the only known interacting partner and ligand for CCR9 and was also found to be a weak immune-inhibitory hit in the first two screens (Supplementary Figure 1). Therefore, CCL25's involvement in tumor immune-suppression and its role in defining CCR9's tolerogenic phenotype were characterized next. Firstly, CCL25 was found to be produced by all the studied tumor cell lines, although at varied levels, as determined by ELISA (Figure 15A). Interestingly, shRNA-mediated stable knockdown of CCR9 did not affect CCL25 production by MCF7 breast cancer cells (Figure 15A). Next, inhibition of CCL25 using siRNAs or blocking antibody showed no effect on antigen-specific lysis of MCF7 or PANC-1 cells by the respective antigen-specific T cells, *au contraire* to the CCR9 knockdown (Figure 15B-D). Although, stronger responses were observed in IFN- γ and granzyme B secretion by T cells upon CCL25 knockdown in MCF7 cells (data not shown). In case of M579 melanoma cells, which secreted higher levels of CCL25 (Figure 15A), knockdown of CCL25 resulted in a significant increase in tumor lysis by TIL 412 (Figure 15E). Conversely, the addition of recombinant CCL25 protein to the tumor/TC co-culture led to a slight decrease in IFN- γ production as measured by ELISA (Figure 15F), which was not noted for the other cell lines. Thus, based on the current data, CCL25 does not seem to play a driving role in immune suppression of breast or pancreatic tumors, but might be crucial for melanoma cells. Further investigations would be required to clarify CCL25 as an immunosuppressive entity.

Figure 15. Role of CCL25 on immune-suppression of antigen-specific T cells. **(A)** ELISA showing CCL25 expression in cell lysates from indicated cancer cell lines. rhuCCL25 and rhuPD-L1 were used as positive and negative controls respectively for CCL25 detection by anti-CCL25 antibody coated ELISA plates. **(B-E)** Cr-release assay showing % specific lysis of MCF7 (B, C), PANC-1 (D) or M579-A2 (E) cells by survivin TC (B-C), TIL 53 (D) or TIL 412 (E) upon CCL25 inhibition using either specific siRNAs (B, D, E) or blocking antibody (C). Unspecific siRNAs or isotype antibodies were used as controls in the respective experiments. **(F)** ELISA showing HLA-A2-restricted IFN- γ production by TIL 412 cells in response to HLA-A2 positive M579-A2 cells or HLA-A2 negative MaMel 33 melanoma cells upon addition of rhuCCL25 protein to the co-culture. Error bars denote SEM; n=3. Parts of the experiments were performed by Tobias Speck and Tillmann Michels.

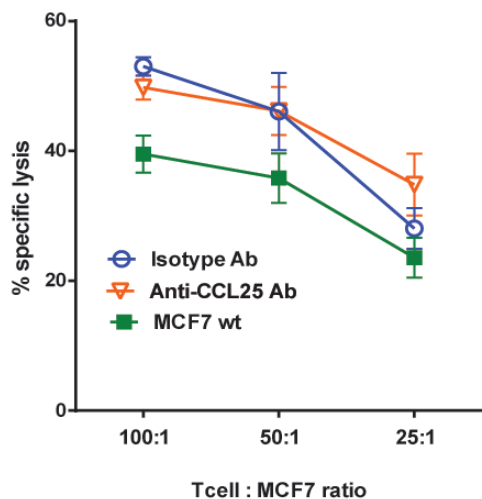
A



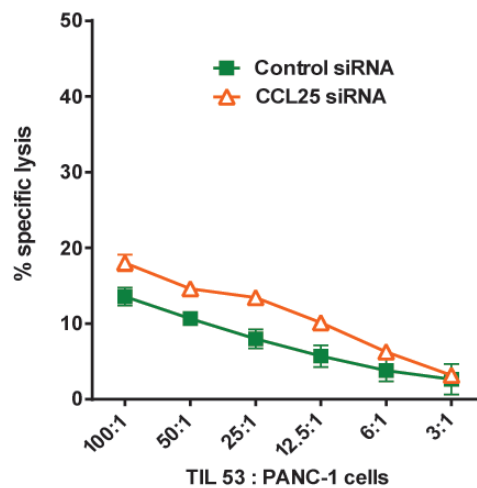
B



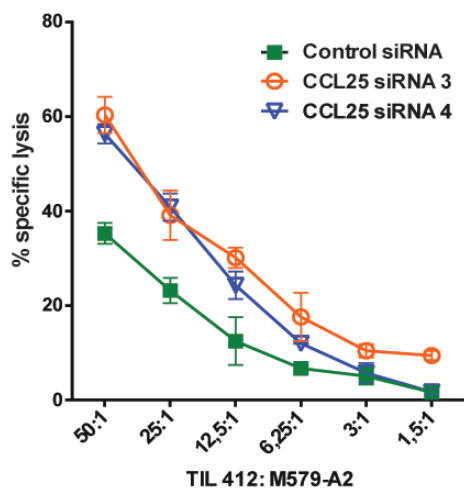
C



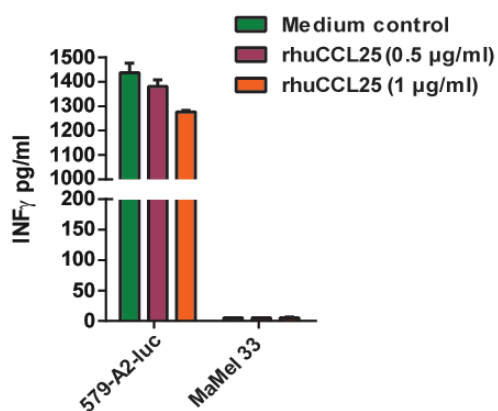
D



E



F



4.16 CCR9-mediated immune suppression requires direct cellular contact with T cells

It is possible that CCR9 mediates its immune-suppressive effect via other soluble ligands or mediators. To examine this possibility, survivin-specific T cells were treated with the cell culture supernatants from either the knocked down ($CCR9^{lo}$) or control ($CCR9^{hi}$) MCF7 tumor cells overnight and then challenged against $CCR9^{hi}$ or $CCR9^{lo}$ MCF7 cells in the cytotoxicity assay. Against the same tumor target, neither of the supernatant treated T cells showed any difference in their recognition and lytic capacity. The difference in lysis between the different groups depended entirely upon CCR9's expression on the tumor targets rather than on the TC treatment (Figure 16A). This clearly indicated that soluble mediators released by the tumor cells, including CCL25, are not involved in defining CCR9's immunosuppressive capacity. Rather direct cellular contact between the CCR9-bearing tumor cells and the T cells is essential for the observed immunosuppressive effect. To further assess whether cytoplasmic signaling mediated by the surface-bound CCR9 in tumor cells plays any role in immunosuppression, pertussis toxin (PTX) was used. PTX irreversibly inhibits and uncouples the $G_{\alpha i}$ family of proteins from binding to the GPCRs and thereby blocks the downstream GPCR signaling. Treatment of $CCR9^{+ve}$ MDA-MB-231 tumor cells with PTX inhibited its migration towards the chemotactic stimuli of CCL25 in a transwell migration assay, proving the effectiveness of pertussis toxin in blocking CCR9's downstream signaling that is responsible for its chemotaxis (Figure 16B). However, inhibition of intracellular CCR9 signaling by PTX failed to elicit elevated tumor lysis by antigen-specific T cells, when compared to the CCR9 gene knockdown, indicating that CCR9-mediated immune suppression on T cells is independent of its intracellular signaling in the tumor cells (Figure 16C).

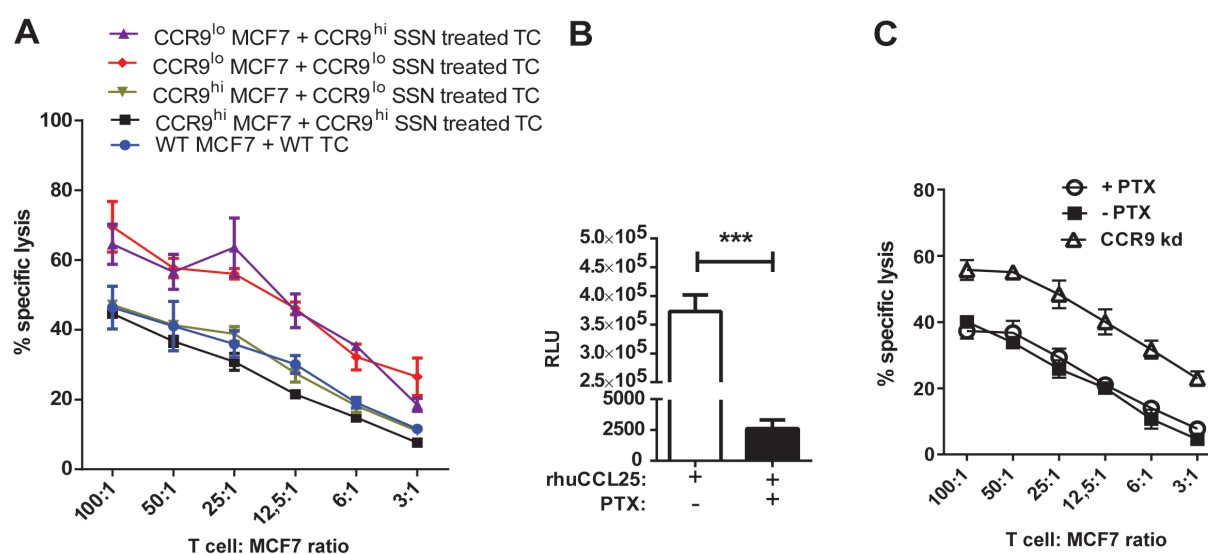
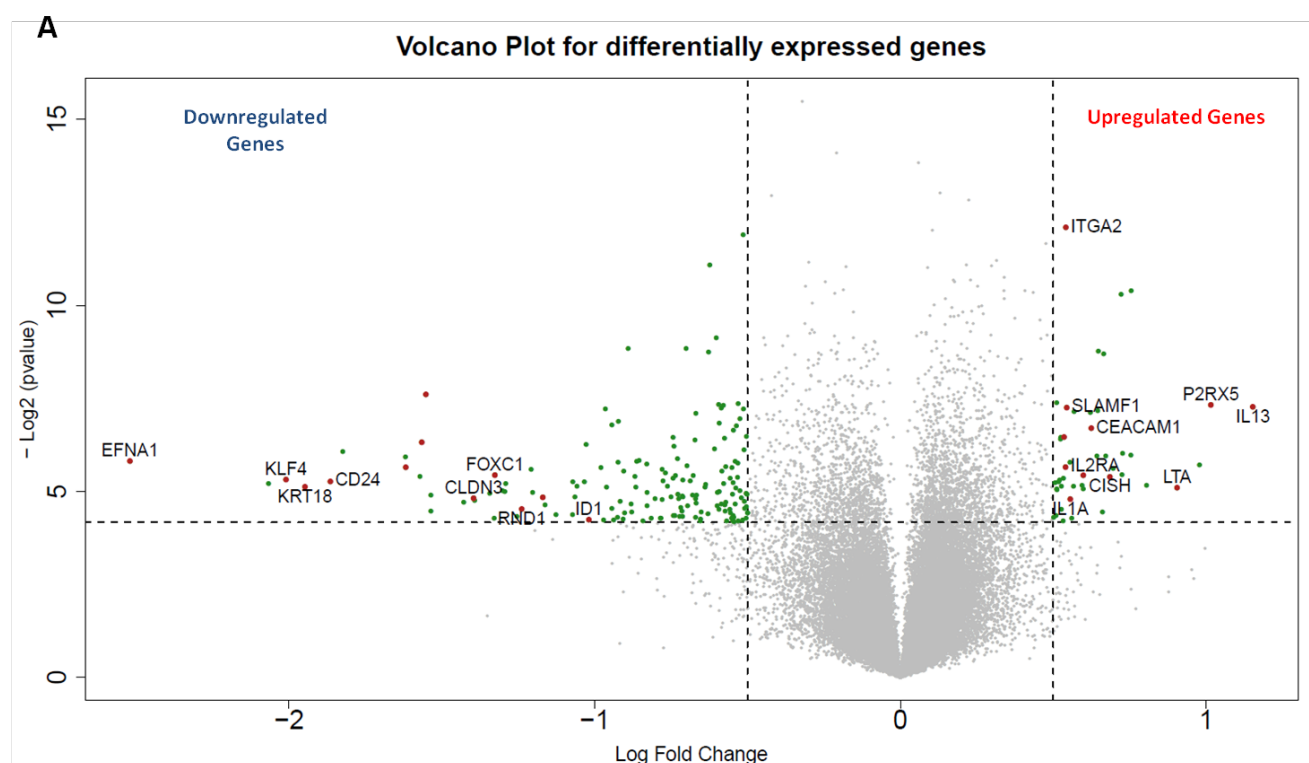


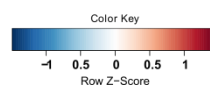
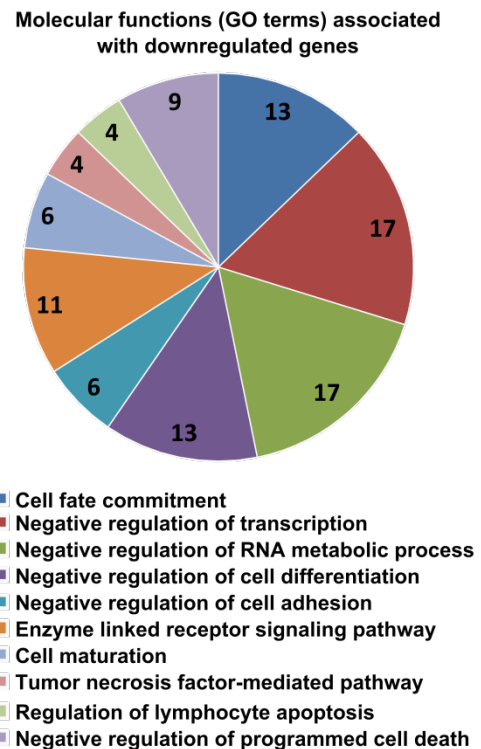
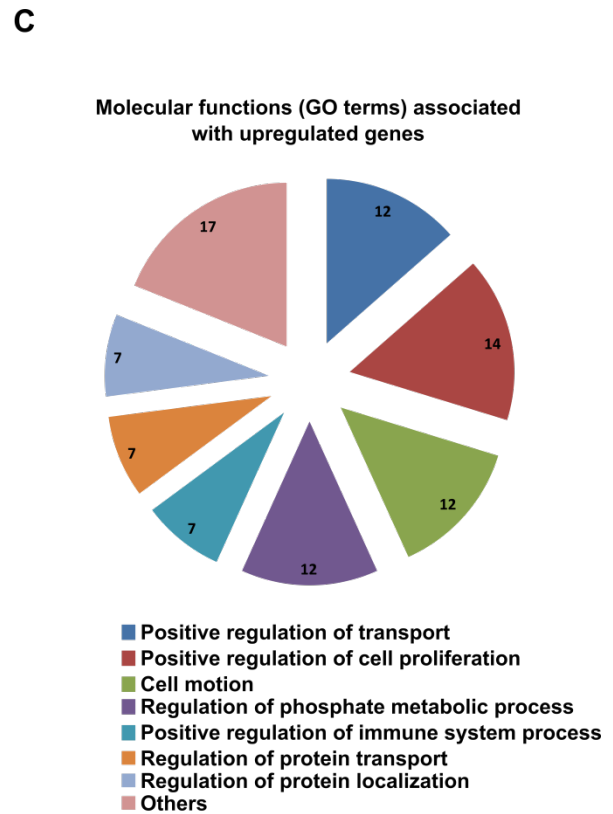
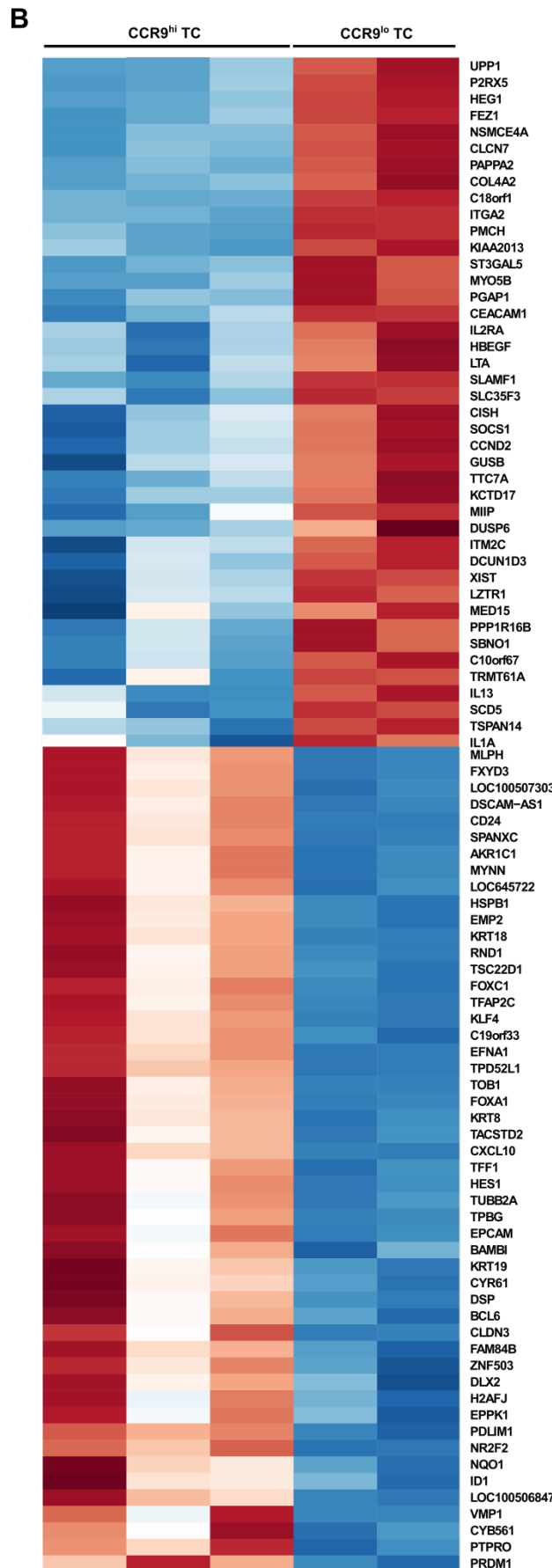
Figure 16. Direct cellular contact is essential for CCR9-mediated immunosuppression. (A) MCF7 cells were transfected with control or CCR9-specific siRNAs and 48h later the respective supernatants (CCR9^{lo} or CCR9^{hi} SSN) were used to culture survivin TCs overnight. Supernatant treated TCs were then used as effector cells against CCR9^{lo} or CCR9^{hi} MCF7 tumor cells in the Cr-release assay along with wild type MCF7 cells. (B) Migration of MDA-MB-231 tumor cells in response to rhCCL25 protein with or without pertussis toxin (PTX) in 24-well transwell migration assay. Migrated cells were fixed and stained with CTG dye and luminescence was used to score the migration capacity. ***= $p < 0.001$ (C) Cr-release assay showing % specific lysis of MCF7 cells pre-treated with or without pertussis toxin, along with CCR9 knockdown MCF7 cells as positive control. Error bars denote SEM.

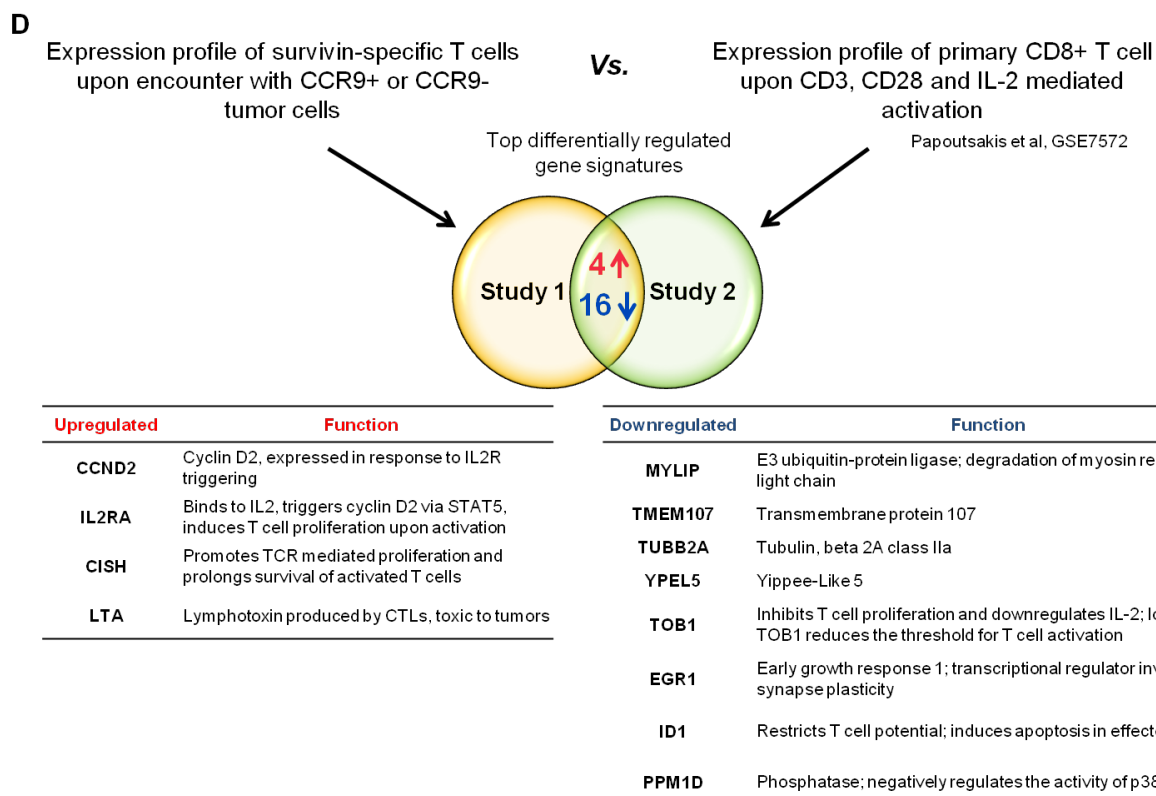
4.17 CCR9 induces immune-suppressive gene signatures in encountered T cells

To better understand the mode of CCR9-mediated immunosuppression in T cells, global gene expression study was performed to compare the changes in the transcriptome of the T cells that encounter CCR9^{hi} versus CCR9^{lo} MCF7 tumor cells. Microarray analysis comparing these two populations revealed a list of differentially up and down regulated genes in the CCR9^{lo} treated T cells compared to the CCR9^{hi} treated T cells which is represented in the volcano plot of Figure 17A and listed in the associated heatmap of Figure 17B. Immune response-related genes such as LTA, IL2RA, CISH were found to be upregulated; whereas genes that inhibit T cell maturation and effector function such as CD24, EFNA1, ID1, TOB1 were downregulated in the CCR9^{lo} treated T cells, which was found to be in accordance with the increased cytotoxicity observed before. Gene-annotation/ontology (GO) analysis of the top up-regulated genes revealed a significant enrichment of genes involved in the positive regulation of immune response, while genes involved in lymphocyte maturation and apoptosis were found to be significantly enriched in the downregulated list (Figure 17C). Next we wondered if these gene signatures associated with the re-activated T cells upon tumor-specific CCR9 knockdown overlap with the gene signatures generally associated with an activated T cell population. Using a publically available gene expression study comparing the unstimulated CD8⁺ T cells to activated T cells (105), overlapping gene signatures in the upper quartile could be identified that were present in both the studies (Figure 17D). Taken together, these data underscore CCR9's role in keeping the anti-tumor T cells in a suppressed and relatively immature phase, which can be reprogrammed to an effector phenotype upon successful inhibition of tumor-specific CCR9.

Figure 17. CCR9 knockdown on tumor cells reprograms the T cells towards an immune effector phenotype. MCF7 cells transfected with control siRNA (CCR9^{hi}) or CCR9 siRNA (CCR9^{lo}) were co-cultured with survivin TCs for 12 h. Gene microarray was performed with the total RNA extracted from purified T cells after the co-culture. **(A)** Volcano plot illustrating fold change (FC; log₂) in gene expression intensities compared with p-value (-log₂) between CCR9^{hi} and CCR9^{lo} treated TCs. Horizontal bar at y = 4.32 represents a statistical significance of p=0.05 (genes in grey below this line did not reach significance). LogFC cut-off at ± 0.5 is represented by the vertical lines. **(B)** Heatmap representation of the top upregulated (LogFC>0.5) and downregulated (LogFC<-0.85) genes with p≤0.05. Individual replicates per sample group are shown herein. **(C)** GO categories of differentially expressed genes in CCR9^{lo} TCs as determined by DAVID. Percentages of genes within the differentially regulated gene list that are attributed to a certain GO category are represented here with only statistically significant enrichment terms being plotted. **(D)** Differentially regulated genes overlapping in the presented microarray study and a published study comparing gene expression changes in CD8 T cells before and after activation (GSE7572; refer to methods for details) is represented. Significantly up and down regulated genes (top 30%) in both the studies were compared and few of the common gene signatures are summarized in brief.







4.18 Synergistic blockade of immune modulatory pathways: CCR9, PD-L1 and CEACAM-6

Combinatorial inhibition of multiple immune-checkpoint molecules is currently being investigated in the clinics to further strengthen the magnitude of the anti-tumor T cell responses in cancer patients. This study therefore investigated whether any synergy exists between the immune-modulatory pathways mediated by CCR9 and those of other immune-checkpoint molecules, namely PD-L1 and CEACAM-6, so that co-inhibition could result in even heightened immune response against target tumor cells. For this, CCR9 and PD-L1 or CCR9 and CEACAM-6 were co-inhibited in the MDA-MB-231 or PANC-1 tumor cells, respectively, and evaluated for impact on CTL-mediated tumor lysis. Antibody-mediated blockade of PD-L1 or CEACAM-6 on the surface of CCR9 knocked down tumor cells showed no striking additive effect on the anti-tumor T cell responses, however individual blocking of both these immune-checkpoint entities was successful in elevating the cytotoxic potential of the tumor-specific CTLs (Figure 18A, B).

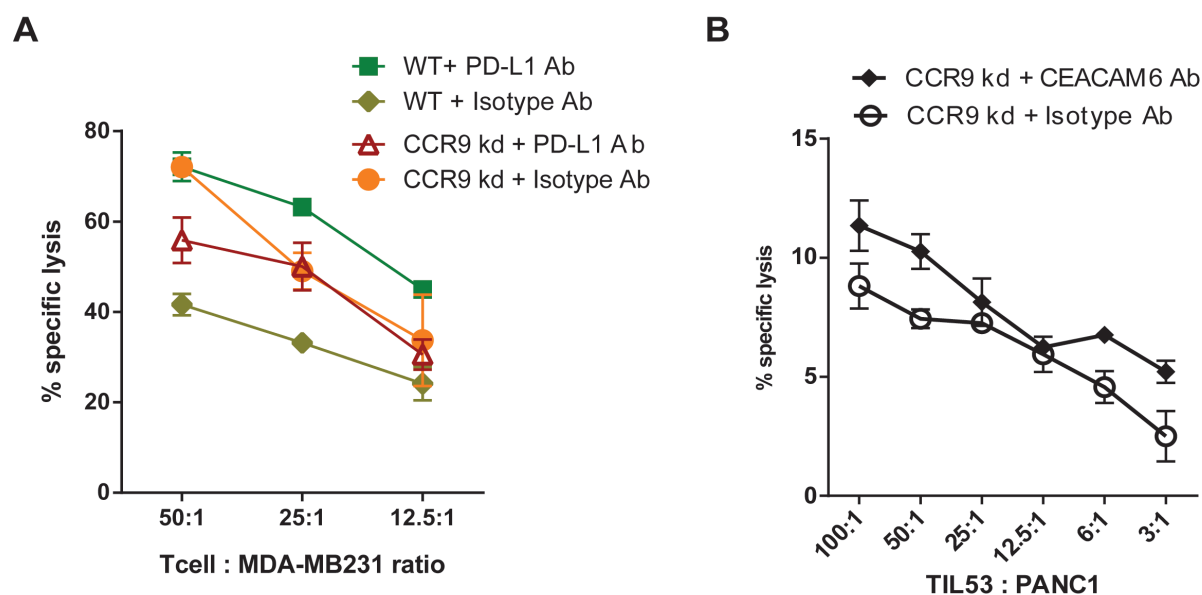


Figure 18. Synergy between CCR9 and PD-L1 or CCR9 and CEACAM-6 mediated immune-suppressive pathways. (A-B) Cr-release cytotoxicity assay showing % specific lysis of MDA-MB-231 cells by survivin-specific CTL (A) or PANC-1 tumor cells by TIL 53 (B) upon CCR9 knockdown along with PD-L1 (A) or CEACAM-6 (B) inhibition. Anti-PD-L1 and anti-CEACAM-6 blocking antibodies, along with respective isotype controls, were used for PD-L1 and CEACAM-6 inhibition on tumor cells. Curve represents the mean and error bars denote +/- SEM.

4.19 Tumor pathways modulated by CCR9

For rational designing of efficient combinatorial therapies for cancer treatment, it is essential to identify whether redundant or divergent signaling pathways underlying the potential immune modulatory function of CCR9 and other immune-checkpoint entities exist, which could then be synergistically targeted. Although intracellular signaling mediated by CCR9 was not found to be critical for its immunosuppressive effect on the T cells, it might still be relevant for its impact on other tumor immune-modulatory pathways and therefore relevant for the design of synergistic approaches. As a preliminary approach in this direction, signaling pathways downstream of CCR9 were characterized using the phospho-protein analysis of major transcription factors in WT versus CCR9 knockdown MCF7 cells. Knockdown of CCR9 resulted in a significantly reduced signaling via Akt and S6-kinase, whereas a potentially compensatory upregulation in the ERK kinase pathway was noted, indicating their involvement in the downstream CCR9 signaling (Figure 19).

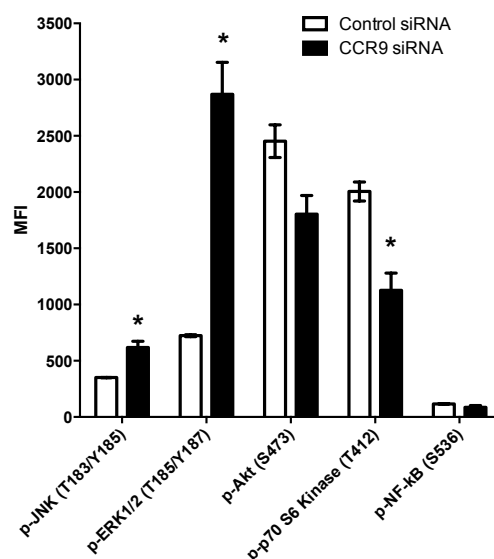


Figure 19. Altered signaling cascades in MCF7 tumor cells upon CCR9 knockdown. MCF7 cells were reverse transfected with control or CCR9-specific siRNA and after 72h protein lysates were used for phospho-plex analysis of the major transcription factors indicated on x-axis (studied phospho-sites are indicated in brackets). Statistical differences between the two groups were analyzed using student's two-sided *t*-test, *n*=3. Error bars represent SEM.

4.20 Blocking antibody for inhibiting CCR9's immunosuppressive effect

Therapeutic targeting of the classical immune-checkpoint nodes such as CTLA4, PD-L1 or PD-1 has gained clinical success owing to the generation of effective blocking antibodies that inhibit the interaction of these negative immune-checkpoint receptors with their respective counterparts on the tumor or T cell surface. Therefore it was next assessed whether any of the commercially available anti-CCR9 monoclonal antibodies could inhibit the tumor immune-resistance phenotype imposed by CCR9 expression. Antibody blockade of CCR9 on MCF7 cells using the two different antibody clones from R&D and Abcam manufacturers failed to induce tumor lysis or IFN- γ secretion by survivin-specific CTLs, irrespective of the dosage (Figure 20A-C). However, the reported blocking properties of the R&D anti-CCR9 antibody clone could not be verified in the transwell migration assay, where the addition of anti-CCR9 antibody did not inhibit the migration of CCR9+ve MDA-MB-231 breast cancer cells towards the chemotactic gradient of the recombinant CCL25 protein (data not shown), leaving open the search for a function blocking CCR9 antibody that could also inhibit its immunosuppressive property.

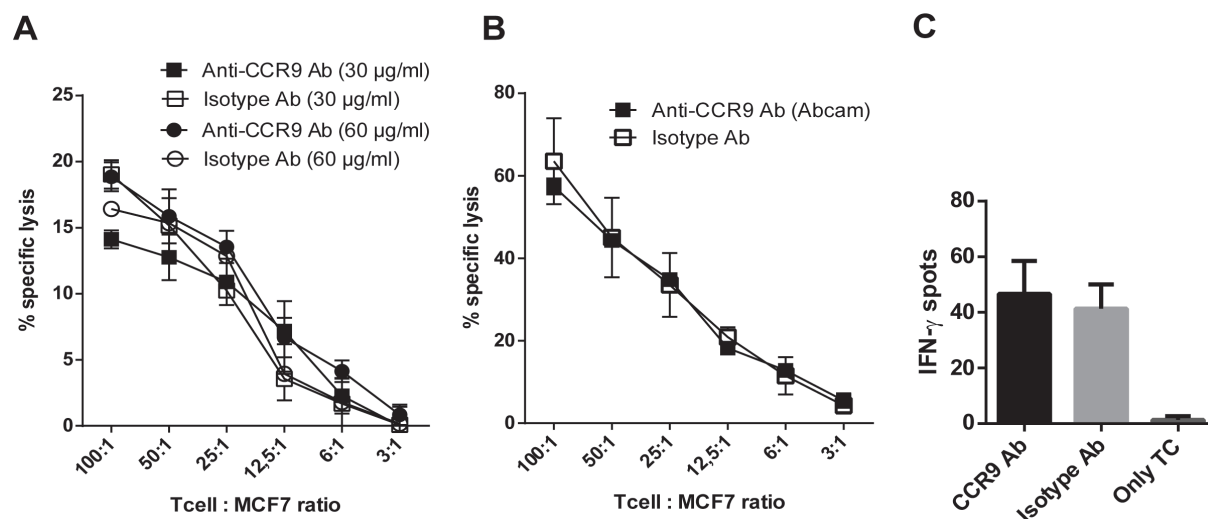


Figure 20. antibody-mediated blockade of CCR9. (A-B) Cr-release assay showing % specific lysis of MCF7 tumor cells by survivin TCs upon CCR9 inhibition using commercial blocking antibodies from R&D systems (A) or Abcam (B) along with the respective isotype controls. Tumor cells were incubated with the respective antibodies for 30 min on ice before being used as target cells in the cytotoxicity assays. (C) ELISpot assay showing IFN- γ secretion by survivin TC as spot numbers in response to MCF7 cells upon CCR9 inhibition using anti-CCR9 Ab (R&D systems) or isotype control Ab. Only T cells (TC) were used as control for unspecific background IFN- γ secretion. Mean \pm SEM are indicated herein.

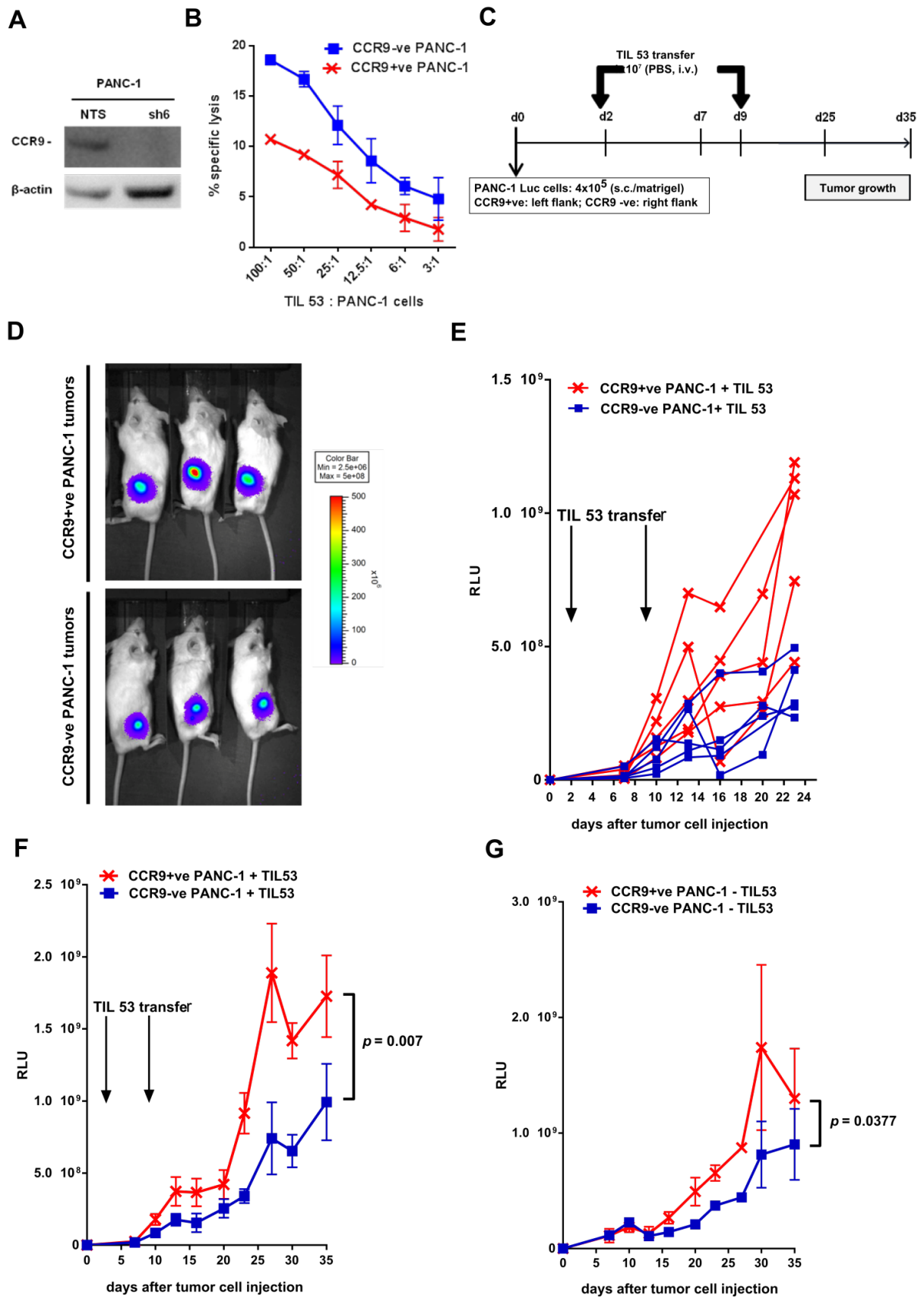
4.21 CCR9 inhibition results in delayed tumor growth *in vivo* upon adoptive T cell transfer in xenograft NSG mouse model

To evaluate the *in vivo* relevance of CCR9 as a tumor-associated immunosuppressive entity, stable CCR9 knockdown variants of the PANC-1 tumor cell line were created which also expressed the luciferase reporter to allow *in vivo* bioluminescent imaging. Figure 21A shows the knockdown efficiency of the lentivirally transduced PANC-1-luc cells using the non-targeting shRNA (NTS) or the CCR9-specific shRNA (shCCR9). As expected, stable CCR9 knocked down cell variants were more susceptible to immune lysis than their counterparts in the *in vitro* chromium release assay (Figure 21B).

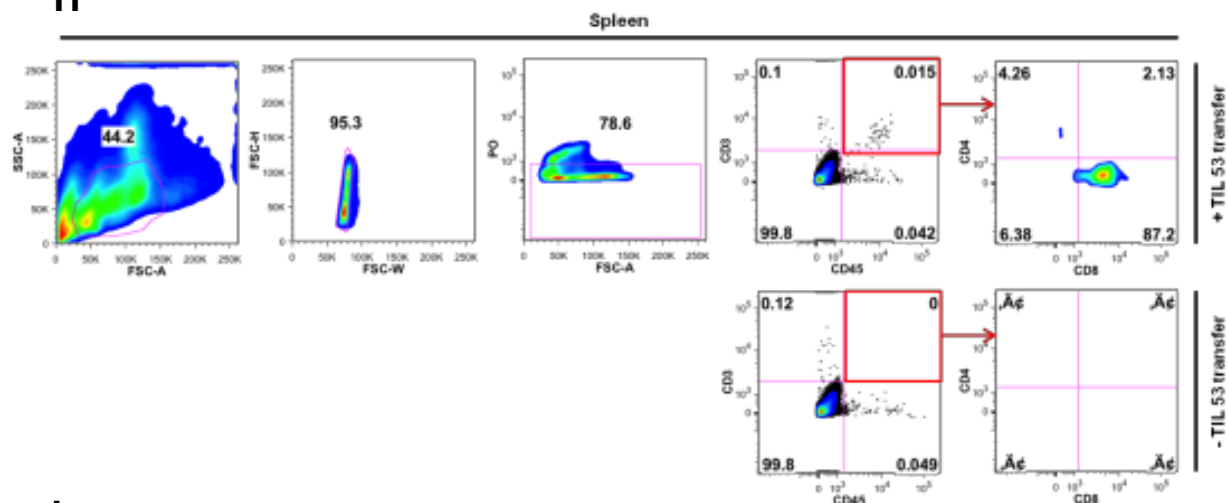
For the preliminary *in vivo* analysis, 4×10^5 cells each of PANC-1-luc-NTS (CCR9+ve) and PANC-1-luc-shCCR9 (CCR9-ve) tumor cell lines were subcutaneously implanted in the left and the right flank respectively of the NOD.Cg-Prkdc^{scid} Il2rg^{tm1Wjl}/SzJ (NSG) immunodeficient mice, which lack mature T, B and NK cell compartments (scheme in Figure 21C). These mice then received intravenous injection of 1×10^7 pancreatic tumor infiltrating

lymphocytes (TIL 53) at day 2 and day 9. Tumor growth was followed using bioluminescent imaging via intraperitoneal injection of the luciferin substrate until day 35 (Figure 21D). As shown in Figure 21E, in the early phases of the tumor growth, CCR9-ve PANC-1 tumors grew much slower in response to the adoptive T cell transfer than the CCR9+ve tumors, indicating that CCR9 suppresses the anti-tumor activity of the transferred T cells *in vivo* as well. Differences in the tumor growth upon T cell therapy remained statistically significant at d35 (Figure 21F). However, towards the later stage, a difference in the tumor growth kinetic between the CCR9+ve and the CCR9-ve tumor cells was also observed in mice that received no T cell transfer, indicating that long term knockdown of CCR9 in itself might confer some growth disadvantage to the growing tumors (Figure 21G). Therefore, this argues for a cautious interpretation of the results. Nevertheless, adoptively transferred human T cells could be detected in the spleen and the tumors of the treated mice even after day 35 as assessed by the CD3/CD45 based flow cytometric analysis of the respective tissue samples (Figure 21H and I). Relative frequency of the detected CD3⁺ CD45⁺ TILs was found to be significantly higher in the tumor bed than in the spleen (Figure 21J), out of which majority of them were CD8⁺ T cells (Figure 21K). This distribution was consistent with the ratio of CD8 and CD4 T cells in the TIL 53 culture before transfer (~ 85% CD8⁺ and ~ 8.5% CD4; Figure 12A).

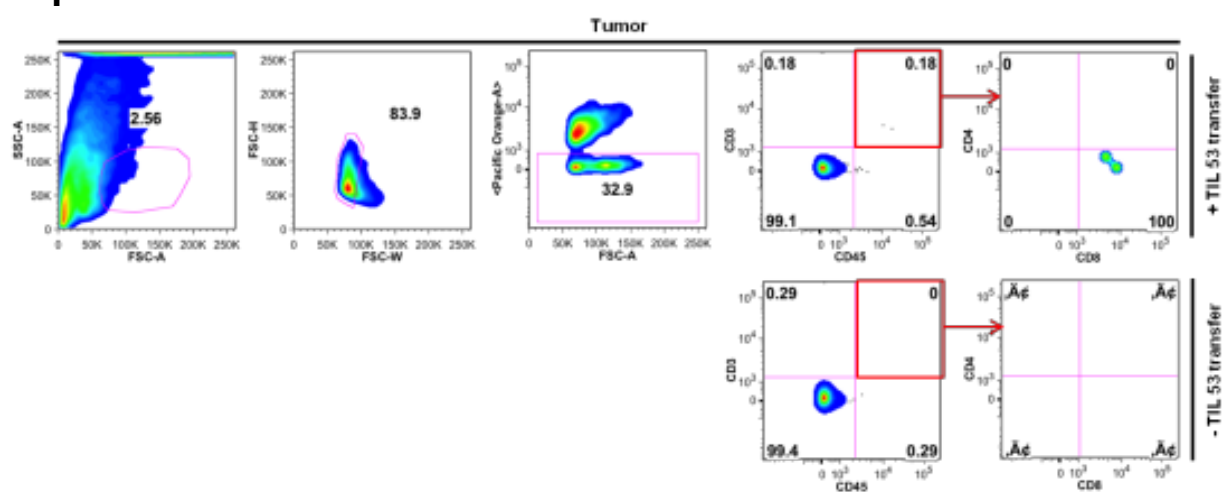
Taken together, these results give a preliminary indication of the *in vivo* relevance of targeting CCR9 as an immune-checkpoint node for application in cancer immunotherapy. These findings need to be replicated for reproducibility with additional improvements implemented to the tumor model.



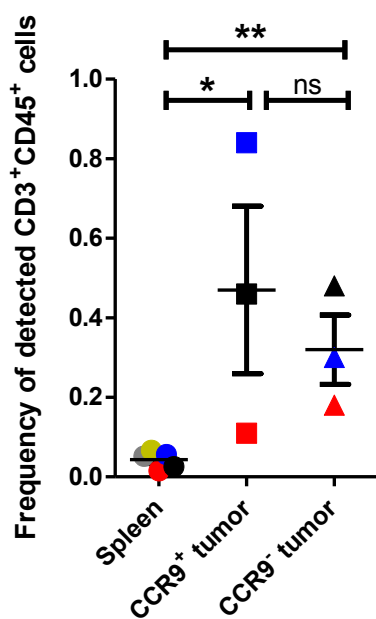
H



I



J



K

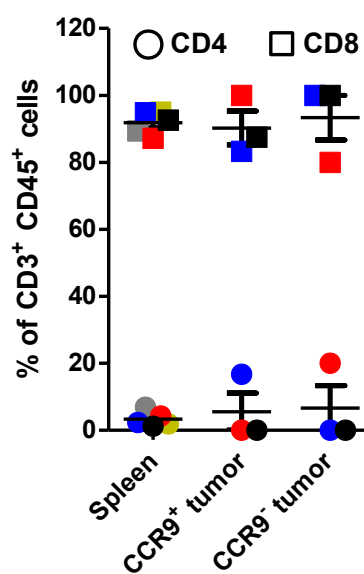


Figure 21. *In vivo* inhibition of CCR9 for adoptive T cell transfer therapy. (A) Immunoblot analysis showing stable knockdown of CCR9 in PANC-1 tumor cells transduced with lentiviral construct coding either CCR9-specific shRNA (sh6) or the non-targeting shRNA (NTS). Immunoblot was probed for beta-actin as control for equal protein loading. (B) Cr-release assay showing TIL 53-mediated lysis of PANC-1 tumor cells upon stable knockdown of CCR9 (CCR9-ve) compared to the control knockdown (CCR9+ve). Mean \pm SEM are plotted herein, n=3. (C) Scheme for the *in vivo* mouse experiment involving the s.c. injection of CCR9+ve or CCR9-ve PANC-1-luc tumor cells in the left and right flank, respectively, of the NSG mice at the beginning of the experiment (d0). Following this, at d2 and d9, mice received i.v. injection of TIL 53 cells (n=5) or no T cells at all (control group for tumor growth; n=3). Mice were imaged for bioluminescence twice every week until d35 to monitor tumor growth upon treatment or without. After d35, mice were sacrificed and organs were harvested for flow cytometric analysis. (D) Representative bioluminescence imaging showing the growth of CCR9+ve and CCR9-ve tumors at d35 of TIL-treated mice. (E) Individual tumor growth per mice (in terms of luciferase units; RLU) is plotted for the first 25 days where maximum immune control of tumors is expected. (F) Mean \pm SEM of tumor growth in terms of luciferase intensity is represented herein for CCR9+ve and CCR9-ve PANC-1 tumors in mice that received adoptive TIL transfer. n=5. (G) Tumor growth curve showing mean \pm SEM of CCR9+ve or CCR9-ve tumors in non-TIL treated mice. n=3. Statistical difference was calculated using paired student's *t*-test. (H-K) Representative dot plots showing the gating strategy to identify CD3⁺ and CD45⁺ human T cells in the spleen (H) and tumor (I) of TIL-treated (or non-treated control) mice after d35. Individual frequency of CD3⁺CD45⁺ T cells in spleen, CCR9+ve and CCR9-ve tumors of each mice are cumulatively shown in J. Percentage of CD4 and CD8 T cells amongst the CD3⁺CD45⁺ T cells are representatively shown on the extreme right in the dot plots (H and I) and the cumulative data is shown in K. Tumors were harvested from 3 mice whereas all 5 mice were used for FACS staining of the spleen. Statistical differences between the test groups were assessed using the paired student's *t*-test. Experiments were designed and supervised by me and executed by Tobias Speck as a part of his Masters thesis.

4.22 Extension of the screening methodology to additional tumor entities

Given that tumors are heterogeneous entities, even in their immune-modulatory profile, it would be essential to elaborate this screening methodology to other tumor entities in order to find tumor-specific immune-modulators that could be targeted for individual cancer types or to find common checkpoint nodes for broader applicability and therapeutic development. Colorectal cancer (CRC) is the third most common cause of cancer worldwide and represents an urgent need for successful translation of immunotherapeutic approaches for better treatment options for patients (127). Therefore, to extend the screen to CRC setting, HLA-A2 positive SW480 colorectal cancer cell line was chosen. Reverse transfection of lethal siRNAs (targeting UBC and PLK-1) using RNAiMAX as the transfection reagent led to a strong decrease in viability of the SW480 cells as demonstrated by the Hoechst dye staining in

Figure 22A-B. Thus SW480 cells could be used for the siRNA-based screening strategy using RNAiMAX as the transfection reagent. For applicability of the SW480 cells in the Luc-CTL assay, plasmid transfection efficacy of these cells was next tested using the pEGFP-Luc plasmid and different transfection reagents. Remarkably, plasmid transfection with Trans-IT, which worked well for the MCF7 cells (Figure 2D), failed to induce luciferase expression in the SW480 cells (Figure 22C). Nevertheless, Lipofectamine LTX-PLUS and GeneJammer transfection reagents could successfully deliver the GFP-Luc plasmid to the SW480 cells as determined by the luciferase activity upon plasmid transfection (Figure 22C). SW480 cells were next tested for whether they could be recognized and lysed by the already established T cell cultures. Both survivin-specific T cell clone and pancreatic cancer derived TIL 53 could recognize and lyse SW480 cells in the chromium-release cytotoxicity assay in a dose-dependent manner, with survivin TCs exhibiting higher cytotoxicity against SW480s. It is indeed known that colorectal cancer in general and SW480s in particular express higher levels of the survivin antigen (128), supporting the observed effect. Both these T cell populations could therefore be used as effector cells against SW480s in an siRNA-based immune screen to uncover CRC-associated immune-modulators.

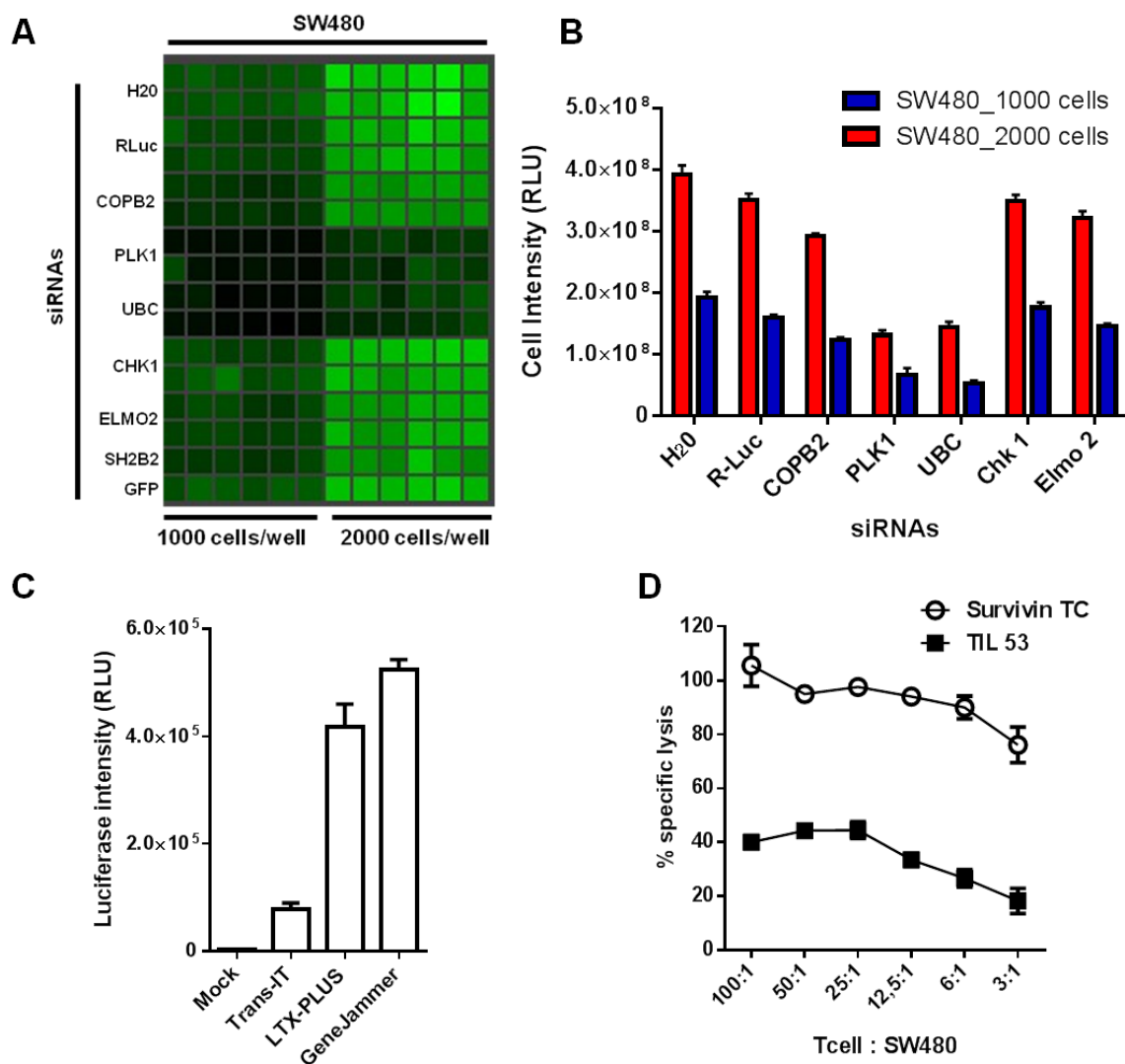


Figure 22. Establishing SW480 colorectal cancer cells for the immune RNAi screen. (A-B) SW480 colorectal cancer cells, seeded at two different concentrations, were reverse transfected with the described control (H2O blank, RLuc) or lethal (UBC, PLK1, COPB2) siRNAs in 384 well plates using RNAiMAX as the transfection reagent. Loss in cell viability was readout 72h later using Hoechst staining with light green representing viable cells and dark green indicating loss in viability (A). Total cellular intensities upon siRNA transfection are enumerated in B. (C) Luciferase activity of SW480 cells upon transfection with pEGFP-Luc plasmid with the indicated transfection reagents. Mock represents addition of no transfection reagent. (D) Cr-release cytotoxicity assay showing % specific lysis of SW480 cells using survivin-specific T cells (○) or pancreatic cancer-derived TIL 53 cells (■) as effector CTLs at titrating E:T ratio. Error bars denote +/- SEM.

5. Discussion

5.1 High-throughput screening for immune modulatory genes

One of the major challenges for the systematic discovery of novel immune modulators has been the lack of a robust and relevant immune-based assay that is suitable for scale up to high-throughput needs. This thesis addresses this problem by establishing and implementing a screening assay which overcomes the current limitations and subsequently proves its efficacy by successful validation of the identified hits. Previous screening strategies to uncover immune modulators have relied on the release of IFN- γ as an indicator of anti-tumor immune cell reactivity (103, 129). However, IFN- γ secretion alone by immune cells does not always correlate with cellular cytotoxicity (130, 131). This could be partly due to the fact that certain tumor cells (for example, LNCaP prostate cancer cells) lack the expression of IFN- γ receptor or have defects in the downstream JAK-STAT signaling pathway, making them insensitive to IFN- γ in the *in vitro* assays (132). This is further reiterated from the observations in the field of viral immunology, where HIV vaccines that predicted T cell responses based on IFN- γ secretion failed to reduce the viral load in infected patients (133). Therefore, in this study direct tumor cell lysis by the T cells was set out as the end-point of the assay readout.

5.1.1 Assessment of cytotoxicity

Quantification of target cell lysis by immune cells has classically relied on the chromium (^{51}Cr)-release based cytotoxicity assay which involves the tagging of target cells with a radioactive salt of chromium, sodium chromate ($\text{Na}_2^{51}\text{CrO}_4$) (113). However, the short half-life and the radioactive nature of the assay itself make this assay unsuitable for an RNAi-based immune screen. Alternatives to the ^{51}Cr -release assay for quantifying immune-mediated cytotoxicity can be broadly classified into the following genres:

1. Fluorescent dye-based assays: These employ tagging of the tumor cells with fluorescent dyes such as calcein (134), BCECF (135), CFSE (136), MUH (137) etc. However, not all target cells take up and retain fluorescent dyes with equal ease and higher spontaneous release of dyes leads to low signal to noise ratio (134).

2. Flow cytometry-based assays: These employ the detection of apoptosis markers, such as annexin V (138), caspase 3 (139), 7-AAD (140), on the target cells at single cell level upon co-culture with immune cells. However, this requires efficient separation of the target and immune cell populations in the flow cytometric set-up, making data analysis time and labor-intensive, along with the requirement for automated acquisition dashboard for flow cytometers for batch sample processing. Moreover, apoptosis marker analysis using flow cytometric staining only captures the cells undergoing apoptosis at the time of staining. This overlooks the impact of immune-mediated lysis during the initial hours of the tumor-T cell co-culture.
3. Reporter enzyme-based assays: These require the tagging of tumor cells with exogenous reporter enzymes, such as luciferase (firefly or renilla), beta-galactosidase or lactate dehydrogenase (LDH), before the co-culture with T cells (111, 134, 141). Tumor cell viability can then be estimated based on the loss or residual enzyme activity. For example, luciferase activity can be quantified by measuring the emitted bioluminescence resulting from the oxidative catalysis of luciferin substrate to oxyluciferin by the tumor-derived luciferase enzyme. Such systems offer the ease of readout desirable for a high-throughput screening approach.

Keeping the above caveats in mind, this study adapted the luciferase-based readout assay from Brown *et al* (107), combined it with the RNAi approach and successfully tested the resulting screening system to identify known as well as novel immune modulators which could be further validated in independent assays. Besides being non-radioactive, the luciferase-based cytotoxicity assay, termed as the Luc-CTL assay in this study, also exhibits: high sensitivity, high signal-to-noise ratio, ease of readout, simplified data analysis and allows batch processing of samples using standard robotics. All of this makes the Luc-CTL assay, in comparison to the other alternatives above, the most suitable assay for high-throughput immune screening needs. Notably, the Luc-CTL assay is based on the detection of the luciferase activity in the leftover live tumor cells upon removal of the dead cells from the culture wells, which assumes the efficient removal of the dead cells upon aspiration of the cell culture supernatant. However, this needs to be controlled and monitored for individual tumor cell lines which might differ in their adhesion properties to the surface of the wells. Accordingly, the Luc-CTL assay would be unsuitable for screening purposes in the suspension cell lines. Besides screening for tumor-associated gene modifiers of CTL

responses, luciferase-based cytotoxicity assay could also be applied to screen for modulators of NK (natural killer) cells, NK-T cells, cytotoxic CD4⁺ T cells and interferon-producing killer DC (IKDC) using the same principle as above.

5.1.2 Gene knockdown for high-throughput approaches

Both siRNA as well as shRNA based formats have been widely employed for high-throughput RNAi screens. Given that the tumor cell lines are generally amenable to transfection with siRNAs and that it doesn't require specialized bio-safety hoods that are necessary for virus-based transductions, this study employed the siRNA-based screening library for its purpose. RNAi screens based on synthetic siRNA duplexes make use of arrayed and pre-spotted siRNAs in individual wells of 384- or 96-well microtiter plates. These, when complexed with RNAi transfection reagent, could reverse transfect the overlaid cells to induce transient gene knockdowns. However, at this stage the right choice of transfection reagent which could successfully deliver the siRNAs to the cells is critical, as not all reagents do the job similarly for all the cell lines and therefore this needs to be carefully optimized for a given cell line. Cationic lipid based transfection of siRNAs is generally employed for successful siRNA delivery in arrayed cell culture systems. Cationic lipids, consisting of positively charged polar head group linked to apolar alkyl chains, interact with the negatively charged phosphate backbone of nucleic acids forming a complex which fuses with the negatively charged cell membrane. The transfection complex enters the cells via endocytosis and once inside, the siRNA diffuses through the cytoplasm, where it is recognized by the cellular RISC machinery and targeted for mRNA inhibition. siRNA duplexes in the endosomes could also be recognized by RNA-sensing Toll-like receptors (TLR), especially TLR-3, -7 and -8; however chemical modifications of nucleosides, such as 2'-O-methyl, are nowadays employed to suppress the immunerecognition of siRNAs (142). Nevertheless, there are numerous cell types and lipid structure that influences the transfection efficiency, case in point being RNAiMAX which could efficiently deliver siRNAs to MCF7 cells but not to KS cells (Figure 2A). This emphasizes the necessity for pre-optimization of siRNA delivery for individual cell types while conducting patient-specific rapid RNAi screening protocols.

5.1.3 T cell recognition format for high-throughput assays

With regard to the nature of the tumor and T cell interaction used for the screen, both antigen-unrestricted as well as antigen-restricted systems were successfully employed. This was done for several reasons. Firstly, this study sought to uncover robust immune modifiers that were not biased based on the use of T cells derived from a single donor. Establishing multiple T cell clones from different donors with the same antigenic specificity is technically challenging and time intensive. Whereas, polyclonal T cells could be easily isolated and expanded from the peripheral blood of multiple donors and used as effector T cells for the screen. Secondly, a genome-wide RNAi screen for immune-modulators would typically require one to ten billion T cells - a number which is difficult to obtain from the expansion of antigen-restricted clones compared to the polyclonal T cells from the peripheral blood. Thirdly, the antigen-unrestricted system using the bi-specific antibody helps to additionally uncover those tumor-associated immune modulatory targets that can be synergistically inhibited to increase the clinical efficacy of the bsAb-based therapy (143). Fourthly, the antigen-restricted system recapitulates the real supramolecular complex structure of the immune synapse involving the TCR-peptide-MHC interaction and the resulting co-stimulatory signals, which is missing from the CD3-mediated activation of the polyclonal T cells. Taking these caveats into consideration, both T cell formats were used so that TCR signaling-dependent as well as -independent immune modifiers could be identified by comparing the two approaches. Indeed, 55% overlapping immune-inhibitory hits from all the three screens were found to be common between the antigen-unrestricted (either of the two screens) and the antigen-restricted screen.

One of the attractive approaches to customize the antigen-specificity of a T cell is by introducing transgenic TCRs which could alleviate the problem of isolating low frequency antigen-specific T cell clones from the patients. However, an important parameter to keep under consideration with the antigen-specific T cell clones is the affinity of their T cell receptor (TCR). High affinity TCR-transgenic T cells bind strongly to their pMHC partners on the tumor targets, but they represent an unlikely and small proportion of the natural repertoire of anti-tumor T cells, since high affinity TCR-bearing T cells that are reactive to tumor-associated antigens (which are mostly dysregulated self-antigens) are subjected to peripheral tolerance mechanisms (144). In accordance with this, it has been observed that most of the naturally occurring anti-tumor T cells isolated from cancer patients bear low-affinity TCRs which possibly escape the strong tolerance mechanism to persist in the

circulation and are favored over the high affinity effector T cells by the tumors themselves (145, 146). Therefore, to keep the *in vitro* RNAi screen as close to the *in vivo* patient scenario as possible, it would be recommended to use low-affinity, naturally occurring anti-tumor T cells rather than strong affinity engineered T cells. The survivin-specific T cell clone used in this study was isolated from the peripheral blood of an HLA-matched (to limit alloreactivity) breast cancer patient bearing a relatively low affinity TCR. In the peptide titration assay, 10^{-7} – 10^{-6} M concentration of survivin_{95–104} peptide loaded onto T2 cells resulted in the half-maximum of IFN- γ secretion by survivin-specific T cells, proving the mild affinity of its TCR (108). Importantly, the inhibition of the identified immune modulatory targets on tumor cells, as shown in the post-validation studies, could enhance the anti-tumor response of even these low-affinity survivin T cells. Additionally, it is important to note that performing a high-throughput genome-wide RNAi screen with antigen-specific CTL clones might also result in true hits being masked or false hits to pop up given that the genes involved in regulating the antigen expression and/or processing itself might be targeted. In such a scenario, post-screen validations with CTL clones of different antigenic specificity than the one used for the initial screen could bypass the problem.

5.1.4 Performance and interpretation of the high-throughput screen

Performance of the established high-throughput screening methodology is reflected by its sensitivity to identify the already established immune-inhibitors (PD-L1, Gal-3, RCAS-1) and immune activators (CXCL9). However, a certain degree of heterogeneity in the performance of the individual genes was noted across the first two screens (e.g., 23 common hits out of the 54 overall hits), as well as in comparison to the third screen. This was expected given their different biological set ups, not only with regard to the different CTL source, but also with regard to the use of genetically engineered MCF7luc cells or wild-type MCF7 cells transiently expressing luciferase. Even though technical replicates within each screen were in the acceptable quality range, more biological replicates would be required to be certain that the observed heterogeneity between the different screens does not represent a technical pitfall, but rather has a biological meaning. On the same note, it is interesting to note the observations from the three different yet similar RNAi screens in which the investigators in each study infected siRNA-transfected HeLa (147, 148) or HEK (149) cells, that expressed HIV receptor CD4, with HIV-1 virus in order to determine the host genes essential for virus replication. Each of these studies yielded more than 200 filtered hits, but when compared to each other,

showed a mutual overlap of only 13-15 genes (150). This limited overlap in rather similar screens emphasizes the importance of doing a biologically mixed screening asking the same question in order to identify high-confidence hits.

Surface-bound immune modulators are easy targets for therapeutic antibody development. G-protein coupled receptors (GPCRs), which represent a sizeable fraction of the surface-bound molecules, were screened in this focused study as a proof-of-concept of the screening methodology. Extension of this approach to all surface-related entities would be an essential step forward for future screening approaches. Unfortunately, none of the current commercial siRNA libraries are uniquely dedicated to the cell surfaceome coverage, therefore custom-designed libraries would need to be produced. With regard to GPCRs, they have been well described to be involved in metastasis, angiogenesis, proliferation and survival among other functions (151). Therefore, it is not surprising that they hold more than 30% of the market share for FDA-approved drugs currently (152). However, the involvement of GPCRs, including the chemokine and chemokine-receptor sub-family, in immune regulation hasn't been investigated in depth before. This study sheds a new light on the role of GPCRs in immune regulation of cancer progression which merits further investigation.

Considering the use of a focused siRNA library in this study, a hit rate of ~10% was noted for identifying potential immune inhibitors. When put in the context of genome-wide screens, this discovery rate might appear high and therefore warrants careful functional validation of the individual candidates. Off-target effects are not uncommon in RNAi-based screenings and could lead to the discovery of false hits (153). They might occur if an siRNA sequence in addition matches to an unintended mRNA sequence, leading to its degradation and creation of a mixed phenotype which might be construed as a false-positive hit (153). Additionally, partial sequence similarity of the seed region of an siRNA to the 3' untranslated region (UTR) of an unrelated mRNA might cause the translational repression of the unintended mRNA, leading to the same consequence as above. Finally, sequence-independent recognition of siRNA duplexes by the cellular sensors, such as Toll-like receptors which can activate type-I interferon signaling, might interfere with the appropriate interpretation of readout assays leading to false-positives (154). Consequently, commercial companies selling siRNA libraries are on a constant look out for unintentional complementarities for their siRNA sequences that are omitted from their databases on a continuing basis. However, it is also plausible that this high discovery rate might indeed represent the complex regulatory networks that govern the

peripheral immune surveillance. Immune response-related genes represent a major proportion of the genome, out of which cell surface signaling proteins, which were already enriched in this study, play a pivotal role in immune modulation (155). Moreover, a previous screen for tumor ligands that modulate NK cell function also revealed a high number of immune-modulatory candidates (103), indicating the complex nature of immune surveillance that possibly involving multiple players.

Besides for CCR9, preliminary experimental validations have been performed for few of the other identified immunosuppressive hits, including GHSR, TRHDE, OR51E2, HTR1D, IL8 and IL8RA. Strong immunosuppression in both luciferase as well as Cr-release based cytotoxicity assays could be demonstrated in breast cancer cell lines using the survivin-specific T cells for GHSR, TRHDE and OR51E2, with mild effects observed for IL8 and IL8RA (preliminary findings, not presented here). Further repetitions and additional analysis of the T cell effector functions (such as cytokine and cytolytic enzyme production) upon target gene knockdown would be required to confirm the immune modulatory role of these candidate genes. Nevertheless, successful validation of these candidate genes in the primary Luc-CTL and the secondary Cr-release assays stresses the robustness of the screening methodology which appears to have a low false-positive hit rate.

Both PD-L1 and CEACAM-6, which were intended as immunosuppressive controls, could be successfully identified as negative modulators of anti-tumor immunity in the RNAi screen. Although PD-L1 is known to mediate immune suppression in breast cancer setting (65), CEACAM-6's involvement in immune modulation of breast cancer has never been reported before. Interestingly, CEACAM-6 is overexpressed on a majority of human breast cancers with expression being correlative to poor prognosis (156). Although not presented here in detail, CEACAM-6 was further validated as a potent immunosuppressor in breast cancer as a sub-project of the presented thesis. CEACAM-6 expression on multiple breast tumor cell lines was found to inhibit antigen-specific tumor lysis by reactive T cells. Moreover, therapeutic inhibition of CEACAM-6 with function-blocking antibody could slow down tumor growth upon adoptive T cell transfer in a breast cancer xenograft mouse model, indicating the therapeutic relevance of targeting CEACAM-6. Notably, the detection of such a valid immune suppressor as a part of the screening methodology further strengthens the biological sensitivity of the screening approach.

5.2 Functional validation of the high-throughput screen

5.2.1 C-C chemokine receptor 9 (CCR9)

CCR9 (previously known as GPR-9-6) is a 42 kDa member of the beta-chemokine receptor family containing the C-C motif. Like most other G-protein coupled receptors, CCR9 is also a seven transmembrane protein with a short extracellular domain. The CCR9 gene is mapped to the chromosome 3 on the p21.3 locus and transcribes two spliced variants: one of which lacks 12 amino acid residues at the N-terminal end (157). Expression of CCR9 is restricted to the intraepithelial lymphocytes (IELs) and to a small subset of the beta7+ T cells in the circulation (158). Along with integrin $\alpha4\beta7$ (or LPAM), CCR9 is one of the key homing receptors of effector T cells, regulating their migration to intestinal mucosa in response to the chemotactic stimulus provided by its ligand CCL25, which is constitutively expressed by the epithelial cells of the intestine (120) (Figure VIII). CCR9 knockout mice show no major effect on the intrathymic T-cell development; however a reduction in the intraepithelial $\gamma\delta$ T cells is noted (159). In cancer, CCR9 has been shown to be overexpressed in breast, ovarian, pancreatic and prostate cancer, aiding in tumor cell migration and invasion (160-162). Its expression positively correlates with the histopathological state of the tumor (162). Recently, CCR9 expression has been shown to mark the tolerogenic plasmacytoid DCs that are capable of suppressing acute graft-versus-host disease (163). However, the exact functional role of CCR9 in defining the tolerogenic phenotype was never elucidated. This study is the first one to point out the functional role of CCR9 in actively suppressing anti-tumor immunity.

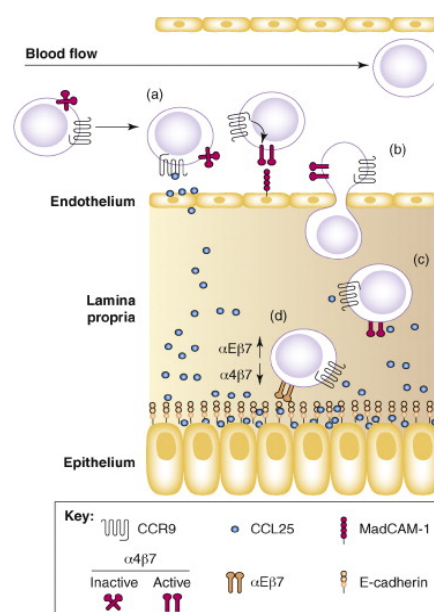


Figure VIII. Role of CCR9 in the homing of IELs. Integrin $\alpha4\beta7$'s expression on the CCR9⁺ T cells facilitate its attachment to mucosal vascular addressin cell adhesion molecule-1 (MadCAM-1) expressed on the small intestinal vascular endothelial cells (a-b). This is followed by the migration of the T cells into the lamina propria in the direction of the CCL25 gradient, expressed constitutively by the intraepithelial cells (c). Adapted from *Agace, 2008* (164).

CCR9 was found to be strongly immunosuppressive in all the three screens. Subsequent validation studies effectively showed that tumor-specific expression of CCR9 inhibited tumor lysis as well as effector Th1 cytokines production by antigen-specific T cells, making CCR9⁺ve tumors highly immune-resistant. Previous studies have demonstrated that triplet production of IFN- γ , IL-2 and TNF- α cohort by virus-specific CD8⁺ T cells correlates with improved virus control *in vitro* as well as *in vivo* (165, 166). The same has been shown for anti-tumor CTL responses whereby secretion of these poly-cytokines is known to be tightly associated with higher peptide sensitivity and superior tumor recognition by antigen-specific CTL clones (167). Similar cytokine release pattern was observed upon CCR9 knockdown which would explain the pro-tumor attack environment generated by disarming the tumor cells of CCR9 expression. Additionally, IL-10, which is known to mediate immune suppression by selectively inhibiting the CD28 co-stimulatory pathway in antigen-specific T cells, was also downregulated upon CCR9 knockdown (168).

Of note, CCR9-mediated immune suppression was found to be comparable, or even stronger in some instances, to PD-L1, making one speculate whether it overtakes and replaces PD-L1 as one of the major immunosuppressive pathway in certain tumors. One reason for the observed effect might be that MCF7 cells, compared to the MDA-MB-231 breast cancer cells, are believed to express lower levels of surface-bound PD-L1 (65). However, even in the MDA-MB-231 cells CCR9 was found to mediate comparable levels of immune suppression as PD-L1 (Figure 18A). CCR9-mediated immunosuppression was noted not only in breast cancer but also in multiple tumor entities, stressing its importance as a key immune regulator. However, the lack of autoimmune phenotype in CCR9 null mouse limits its claim as an important player in the central immune tolerance. Rather, it appears that the deregulated expression of CCR9 is exploited by the tumors to mediate pro-tumor pathways including immunosuppression.

Importantly, this study found out that tumor infiltrating lymphocytes (TILs) derived from melanoma and pancreatic cancer patients are susceptible to CCR9-mediated immunosuppression. Cellular therapy involving isolation, *ex vivo* expansion and autologous adoptive transfer of patient-specific TILs has been shown to induce tumor regression in metastatic melanoma patients with overall response rate of 40-60% (169). But only a fraction of them show durable responses and therefore one of the major challenges that remains to be tackled is to increase the frequency of these durable responses. Two of the doctoral students in our lab (Tillmann Michels and Antonio Sorrentino) have established the *ex vivo* culture and expansion protocol for TILs derived from melanoma and PDAC patients (TIL 412 and TIL 34, TIL53; respectively) and have characterized their exhausted phenotype in culture based on PD-1 and TIM-3 double-positive surface expression. Given, the immune-exhausted phenotype of these TILs in the tumor microenvironment, further enablement of the T cell effector function by targeting the immune-checkpoint nodes would be a promising approach to strengthen the TIL-based therapy. This is even more critical for PDAC-derived TILs, which are known to be less tumor-reactive (170), with TIL 53 showing a weak basal killing of around 10% against syngeneic tumor cell line at 100 to 1 E:T ratio. Additionally, it would be interesting to see whether tumor-specific CCR9 blockade, which reactivates these exhausted TILs to kill again, induces a durable imprinting on the T cells or not.

TCR downstream signaling has been shown to be inhibited upon the engagement of PD-1 receptor on the activated T cells with PD-L1 and is defined as the mode of action of PD-L1 mediated immunosuppression (171). CCR9, however, seemed to act independent of its effect on the TCR signaling, as the level of T cell activation was found to be similar irrespective of tumor's CCR9 expression and even comparable to the superantigen stimulated TCs. This might suggest that a threshold level of activation is already achieved when survivin TCs interact with antigen-bearing MCF7 tumor cells and further fluctuations in TCR signaling upon manipulation of CCR9 expression might be unfeasible. This doesn't come as a surprise as CCR9 was found to mediate strong immunosuppression even in the antigen-unrestricted screen which lacked the TCR interaction. Nevertheless, CCR9 was found to impair the activation of STAT-1 pathway in the encountering T cells. STAT-1 is typically activated upon interferon signaling (especially IFN- γ), following which phospho-STAT dimers translocate to the nucleus and bind to the interferon-stimulated response elements (ISRE) in the promoter region of the target genes (such as CD80, CD40, IL-12, CDKN1A) inducing their expression (126). In accordance with this finding, a previous study has also demonstrated a similar

enhancement in STAT-1 phosphorylation levels upon inhibition of PD-1 signaling in T cells isolated from the HCV-infected patients (172). Moreover, intratumoral exhausted T cells in follicular lymphoma patients also exhibit lower STAT1 signaling upon stimulation compared to the non-exhausted counterparts (173). Given that *Stat1*^{-/-} mice fail to reject immunogenic tumors and their T cells lack cytolytic function (174), inhibition of STAT-1 signaling in CTLs by tumor-specific CCR9 represents an important aspect of its immunosuppressive mechanism. CCR9 inhibition also led to a significant increment in the STAT-2 and slight increases in the STAT-5 signaling. Role of STAT2 in anti-tumor immunity, particularly in CTLs, has been poorly defined. However, it is reported to act along with STAT1 as a part of the heterodimer (175), which might explain its commensurate activation with STAT1 upon CCR9 inhibition. Activated STAT5 signaling, on the other hand, has been clearly shown to correlate with prolonged CTL survival and *in vivo* tumor rejection (176). Taken together, these findings implicate the involvement of deregulated STAT signaling as a part of CCR9's immunosuppressive pathway, but whether they are causally linked to CCR9-mediated immunosuppression remains to be clarified.

Genome-wide transcriptomics analysis in CCR9^{lo} encountering CTLs revealed a distinct pattern of gene signature changes that are mediated by CCR9. Analysis revealed that CCR9-mediated signaling events in the T cells inhibit the expression of genes involved in the gain of T cell effector functions (such as *ITGA2*, *IL2RA*, *LTA*, *SOCS1*, *CISH*); whereas on the other hand it upregulates genes that either inhibit effector functions (such as *ID1*, *TOB1*) or induce immature T cell phenotype (such as *CD24*, *EFNA1*).

Integrins are α/β heterodimeric transmembrane receptors that facilitate cell-to-cell interaction by binding to proteins in the extra cellular matrix (such as collagen), thereby inducing a two-way signaling cascade. Integrin alpha-2 (*ITGA2* or *CD49b*), in heterodimeric interaction with integrin beta-1 (*CD29*), forms the *VLA-2* receptor which mediates the adhesion of activated T lymphocytes to collagen type I in the extracellular matrix (177). *VLA-2* ($\alpha2\beta1$) signaling in T cells acts as a costimulatory signal and augments IFN- γ production (178). Moreover, in a previous study in neuroblastoma it has been demonstrated that upon cell-based vaccination *CD49b* gets upregulated on activated CD8⁺ T cells and that *CD49b*^{hi} CTLs are far more effective in tumor control *in vivo* than the *CD49b*^{lo} counterparts, making *CD49b* expression a marker for superior anti-tumor effector CTLs (179). IL-2 receptor alpha (*IL2RA*) and IL-2 signaling are known to be required for the differentiation of CD8⁺ T cells to cytotoxic

phenotype, as IL2RA-deficient CD8⁺ T cells lack perforin and granzyme B expression *in vivo* and they prematurely express the terminal memory markers CD62L and BCL6 (180). Interestingly, in accordance with the above report, this study also observed a downregulation of BCL6 transcript levels along with IL2RA upregulation in CCR9^{lo} encountering T cells. It would therefore be interesting to assess whether long-term exposure to CCR9 leads to a premature terminal differentiation of the encountering T cells as one of the possible routes to abrogate effective anti-tumor immunity. Fasciculation and elongation protein zeta 1 (FEZ1) was also one of the top upregulated genes found in this study. It is a cytoskeletal transport protein that is involved in axonal guiding. Role of FEZ1 in immune effector functions has not been investigated before, but recent studies have linked the expression of FEZ1 in cultured cells to resistance against viral infection (HIV-1 and MLV) (181), as well as its expression in cancer is known to regulate mitosis (182). It is possible that immune synapse formation might require the involvement of microtubule-associated FEZ-1 in immune cells, a speculation that merits further investigation. Other markers which are typically associated with effector function or prolonged survival of T cells were also found to be upregulated in CCR9^{lo} encountering T cells, for example CISH (183), LTA or TNF-beta (184), SLAMF1 (185). Importantly, many of these upregulated genes, such as CISH, CCND2, IL2RA, SOCS1, IL13, were linked to the JAK-STAT signaling pathway (analyzed via KEGG pathway mapping tool), which was found to be in consistence with the observed upregulation of the phospho-STAT levels upon CCR9 knockdown. Given that many of these gene expression changes noted above correlate with reported enhancement in T cell functionality, it would be interesting to exploit them as functional markers for identifying more effective CTLs that are resistant against immunosuppressive tumors in clinical studies.

Conversely, CCR9 inhibition in tumors resulted in the downregulation of gene signatures associated with immature T cell phenotype, such as KLF4 and ID1 whose expression is known to inhibit the T cell lineage commitment, impair the generation of functional memory CD8⁺ T cells and induce apoptosis by lowering the threshold for TCR activation (186-188). Additional molecules that are known to directly inhibit T cell effector responses or IL-2 mediated signaling, such as TOB1 (189) and EFNA1 (190, 191) were also found to be significantly downregulated in the CCR9^{lo} encountering CTLs. Notably, no significant upregulation in the transcript levels of cytolytic enzymes such as perforin or granzyme B was observed. However, an increase in the lytic enzyme secretion was already detected at protein level in the ELISpot assays 12 hours post target cell and T cell co-culture (Figure 10), which

is the same time-point that was used for the gene-expression analysis. So it is possible that the transcript upregulation for these cytolytic enzymes might have preceded the studied time-point. Consistent with this, an increase in expression of genes that control TCR signaling was also noted at this time-point, such as CEACAM1 (192) and SOCS1 (193), which are generally expressed only in the activated T cells as a fail-safe switch to fine tune the intensity of immune response.

Comparison of the observed gene signatures with another study performed by Wang *et al* (105), where they compared stimulated TCs to unstimulated TCs, confirmed a clear pattern of gene expression changes that correlated with activated T cell phenotype upon tumor-specific CCR9 knockdown. It is relevant to note here that in contrast to the unstimulated peripheral CD8⁺ T cells that were used as the control by Wang *et al*, this study made use of survivin-specific T cells which are not entirely unstimulated as a threshold level of activation occurs upon encounter of wild type survivin-positive MCF7s. Therefore, a significant overlap of differentially regulated gene hits between both these studies might not be expected. However, above and beyond the threshold level of activation, it is encouraging to see many gene signatures overlapping that define activated T cells. Now the question remains that which amongst of these genes falls directly in the line of CCR9-mediated immunosuppressive pathway. Many of the observed changes, such as upregulation of lymphotoxins, shut-down signals or IL-2 signaling related genes, might very well represent the bystander effects of T cell activation upon CCR9 inhibition rather than the causal link for CCR9-mediated suppression. In this regard, it would be interesting to look at the non-overlapping genes between the CCR9^{lo} treated TCs and the polyclonally stimulated TCs, which might represent genes that are unique to the CCR9-mediated pathway. Functional validation studies involving knockdown of these relevant gene hits in T cells would be essential to establish the causal link between tumor-specific CCR9 and induced immunosuppressive pathways in the interacting T cells.

CCL25 (also known as thymus expressed chemokine, TECK) is a 16 kDa CC-chemokine that is primarily expressed in the thymic dendritic cells and mucosal epithelia (194). It serves as a chemoattractant for CCR9-expressing T cells to the mucosal sites. In addition, CCL25 has been shown to be expressed by various tumors, with expression being correlative with histological subtype and metastatic potential (162, 195). Inhibition of CCR9 expression in tumor cells was not found to modulate CCL25's expression. This excluded the possibility of

an autocrine loop mechanism whereby immune-suppression mediated by CCR9 might act via the increase of CCL25 in the tumor-immune cell space as a result of CCR9-CCL25 signaling axis. However, it might still be possible that knockdown of CCR9 on the cell surface leads to increased bioavailability of CCL25 for the interacting T cells in the co-culture, as it is no longer occupied by CCR9, leading to the observed immunosuppressive effects. But to this end, no effect of CCR9 knockdown supernatant or CCL25 *per se* was observed on the suppression of anti-tumor T cell activity, except against melanoma cells which secreted higher levels of CCL25. Therefore, it might be possible that depending on the relative abundance in different tumor types, CCL25 might be involved in shaping the immune response, but whether it does so independently or in concert with CCR9 remains to be established. Although for CCR9 it is clear that its immunosuppressive effect is mediated by non-soluble entities that rather require direct cellular contact with the T cells. Additionally, this immunosuppressive effect also seems to be independent of the intracellular CCR9 signaling as functional blockade of the downstream signaling by pertussis toxin did not have any impact on the immune susceptibility of the treated tumor cells. In contrast, CCR9 knockdown which effectively reduces the surface receptor expression shows an impact.

Together these findings indicate that surface bound CCR9, via its interaction with a putative corresponding ligand on the T cell surface, brings about the immune regulatory phenotype. However, since CCL25 is the only known interaction partner for CCR9 in functional interaction databases, speculating or predicting novel direct or downstream interaction partners seems tedious. It might also be possible that the effect is indirect, wherein CCR9 regulates the expression of another tumor cell surface bound entity that in turn is responsible for relegating the immunosuppressive signals to the interacting T cells. Although such a regulation mediated by CCR9 could be effectively blocked upon long term pertussis toxin treatment (current protocol involved the tumor cell treatment with toxin for only 1 hour before their use in the cytotoxicity assays), it should be avoided as pertussis toxin is an unspecific GPCR blocker affecting other receptors as well. Perhaps stable CCR9 knockdown tumor variants could be employed to investigate the expression changes in the surface proteins upon CCR9 inhibition and assess if they share a causal link to CCR9-mediated suppressive effects on the T cells.

5.2.2 Synergy of CCR9 with other immune-checkpoint pathways

Blockade of multiple immune-checkpoint molecules in several combinations is increasingly being tested in early clinical trials. The recently concluded anti-PD1 plus anti-CTLA4 antibody trial has demonstrated a synergistic advantage (more than 40% objective response rate) of simultaneously targeting multiple immune-checkpoint molecules (70). In this thesis also, synergistic blockade of CCR9-mediated immunosuppressive pathway with other immune-checkpoint molecules was explored. Co-inhibition of PD-L1 or CEACAM-6 with CCR9 resulted in no additive effect upon T cell mediated tumor lysis, however each of these targets in themselves induced a strong suppression on CTL's effector function. In this regard, it is interesting to note that PI3K-Akt and mTOR-S6K1 pathway has been shown to regulate PD-L1's expression in APCs (196), melanoma (197), breast and prostate cancer (198). Inhibition of these pathways leads to a strong downregulation of PD-L1 expression (197, 198). Interestingly, CCR9 knockdown in MCF7 breast tumor cells led to a significant decrease in the activation of the S6 kinase pathway as well as of the Akt pathway, which was in accordance with a previous study showing that CCR9 mediates PI3K/Akt-dependent signaling cascade in prostate cancer cells (199). Therefore, it is possible that CCR9 inhibition leads to the downregulation of PD-L1 expression on tumor cells via the PI3K-AKT-mTOR-S6K pathway, thereby making them insensitive to PD-L1 blockade which might explain the lack of synergy between the two blockade therapies. An additional attribute of Akt activation upon CCR9 signaling that is worth mentioning is that tumor cells with higher, constitutive Akt activation have been shown to be more immune-resistant towards CTL-mediated lysis (200). Therefore, CCR9 inhibition on tumor cells might work partly by interfering with Akt activation and subsequently sensitizing them to immune destruction, although further experimental validation of any direct links between CCR9 expression, AKT activation and immune response are currently required. Similarly, possible mode of co-regulation of CEACAM-6 and CCR9 expression also needs to be further explored.

In this regard, it is relevant to note the findings from a recently published screening strategy which utilized pooled shRNA library for gene knockdowns in OT-I mouse T cells to assess the impact on their accumulation in the tumor of B16-Ova-bearing mice (201). Such a screen revealed interesting immune inhibitory targets on the T cell side whose knockdown facilitated the proliferation and accumulation of reactive T cells in the tumor microenvironment. However, gene expression analysis revealed that out of the five candidate genes studied, none

of them induced a similar gene expression signature in the reactive TILs, indicating that overall enhanced TIL reactivity can be achieved via multiple and more likely complex intracellular routes. A deeper understanding of the underlying mechanisms of immune-checkpoint pathways therefore becomes necessary for rationale designing of combinatorial therapies. The reported screening strategy on T cells investigated and thereby enriched gene knockdowns that facilitated prolonged T cell survival since the readout was based on the detection of shRNA barcodes in tumor-infiltrating T cell populations after a period of time. However, it is to be noted that prolonged survival, which might also result from knocking down cell cycle checkpoints, does not necessarily represent a gain in effector T cell function or better tumor control and therefore the reported hits must be carefully validated to assess true immune-checkpoint entities.

5.2.3 *In vivo* relevance of CCR9 inhibition on anti-tumor immunity

Therapeutic translation of new drug targets requires the proof-of-principle studies in pre-clinical mouse or animal model systems to show their relative effectiveness and anticipated clinical outcome. Various mouse model systems for studying cancer exist, including the xenograft model system whereby human tumors (either established cell line or fresh patient-derived primary tumors) can be implanted (orthotopically or heterotopically) in an immunodeficient mice. Although the lack of the immune system provides an unreal tumour microenvironment in these mice, the xenograft model system is time and cost effective allowing for simple and rapid assessment of response of patient-derived tumors to therapeutic regimen (202). For xenografting of human tumors into the recipient mouse host, several types of immunodeficient mice have been used. Athymic nude mice lack the T cell compartment but retain functional B cells and other immune cells which might interfere with tumor growth. On the other hand, nonobese diabetic/ severe combined immunodeficient (NOD/SCID) mice lack both T and B cell function and are therefore widely used for xenograft experiments. However, they overcompensate for this lack by increase in NK cell and macrophage activity which should be taken into account especially when interpreting the efficacy of adoptive immune cell-based therapy in this model system. Additional null mutation in the interleukin 2 receptor gamma chain (*Il2rg*) gene of the NOD/SCID mice results in the most immunodeficient mice strain, called as NOD/scid gamma or NSG mice, which lacks functional T, B and NK cell compartment (203).

To assess whether tumor-specific CCR9 expression interferes with and suppresses the anti-tumor reactivity of the adoptively transferred T cells, immunodeficient NSG mice were used for transplantation of CCR9+ve or CCR9-ve human PANC-1 pancreatic cancer cell line and subsequently treated with adoptive transfer of pancreatic patient-derived TIL 53 cells. Given the highly immunosuppressive environment of pancreatic tumors and the exhausted state of the patient-derived TIL 53 cells that showed poor anti-tumor cytotoxicity *in vitro*, testing CCR9 inhibition in this setting *in vivo* to reactivate the anti-tumor response in TIL 53 transferred mice constitutes the litmus test for the strength of CCR9-based therapeutics. Bioluminescent *in vivo* imaging was used for monitoring the tumor growth in mice. Besides early detection of small or slow growing tumors, bioluminescent imaging also reduces any user-based biases in tumor measurement, exhibits minimal background luminescence from animal tissue and embodies the 3R principle of ethical animal work by allowing non-invasive and frequent *in vivo* imaging of animals (204). To minimize inter-mouse variability, CCR9+ve and -ve PANC-1-luc cells were xenografted into the right and left flank of the same mice, respectively, thereby also effectively reducing the number of animals per test group to half while keeping the statistically relevant sample size. Given the high sensitivity of the bioluminescent imaging system, one should be aware of the possibility of signal saturation at later time points when tumors have grown out in size which could make comparisons between the test groups difficult.

Adoptive transfer of pancreatic human TIL 53 cells into tumor-bearing immunodeficient mice led to significantly delayed growth of CCR9-ve tumors compared to the CCR9+ve PANC-1 tumors, especially in the early stages. Anti-tumor reactivity of the transferred TILs could only be observed in the CCR9-ve tumors compared to the CCR9+ve tumors during this period. This goes in parallel with the observed poor cytotoxic capacity of TIL 53 in the *in vitro* assays whereby basal lysis of CCR9+ve PANC-1 cells was observed at maximum of 10-20% which effectively doubled upon CCR9 inhibition. However, the *in vivo* delay in tumor growth upon CCR9 inhibition was also noted in the non-TIL treated animal group, indicating that stable knockdown of CCR9 itself retards tumor growth. CCR9-mediated signaling in PANC-1 cells has been shown to be important for cell survival (160), possibly involving the downstream activation of the PI3K-Akt signaling pathway as shown in the prostate cancer cells before (199). This goes in parallel with the findings of this thesis whereby involvement of the Akt pathway in CCR9-mediated signaling was observed in the MCF7 breast cancer cells. Therefore, it is possible that the *in vivo* delay of PANC-1 tumors upon long-term inhibition of

CCR9 might result from defects in the PI3K-Akt pathway. The extent of CCR9's contribution to this pathway and the reliance of different tumor types, such as melanoma or breast tumors, on this pathway for survival is still not clearly known. Preliminary studies in our laboratory using xenotransplantation of control or CCR9 knockdown variants of M579 melanoma cells in NSG mice indicated no difference in tumor growth kinetics between the two cell types when followed until day 35 after tumor injection. Perhaps, the melanoma xenotransplant system, where no growth disadvantage is conferred to tumor cells upon CCR9 inhibition, would be a better model to uncouple the immunosuppressive function of CCR9 from its proliferative function and therefore could be used to independently assess the significance of CCR9 as an immunomodulatory target for adoptive cellular therapy. On the other hand, functional blocking antibody against CCR9, which hinders its interaction with the putative immunosuppressive interacting partner on the T cell without disrupting its intracellular signaling cascade, might be a better tool to inhibit CCR9's immunosuppressive function than the gene knockdown strategy. Commercially available functional blocking antibodies against CCR9 have so far failed to elicit immune-activating response on T cells, stressing the need for undertaking hybridoma panning approach to generate and test multiple antibody clones for the desired effect. Notably, small molecule inhibitors for CCR9 developed by ChemoCentryx (Vercirnon/CCX282 and CCX8037) are being clinically tested in phase III trials for inflammatory bowel disease to inhibit the trafficking of CCR9⁺ IELs to the inflamed bowels (205, 206). These small molecule antagonists could additionally be tested for their potential to inhibit immunosuppressive role of tumor-associated CCR9 in the pre-clinical mouse models.

Interestingly, injected TILs could be detected in the spleen and tumors of the treated mice, although at low frequency, even at 26th day after the last TIL injection. This was observed without any co-administration of cytokines, such as IL-2 or IL-15, which are generally employed in adoptive T cell transfer therapies to facilitate longer persistence of T cells (207, 208). Systemic administration of IL-2 must be cautiously employed in CCR9 inhibition-based therapies as IL-2 and IL-4 have been shown to trigger the internalization of the CCR9 receptor in MOLT-4 human leukemia T cell line (209). Given that central memory T cells (T_{CM}), defined as $CD62L^+ CCR7^+$, are known to proliferate and persist longer *in vivo* upon adoptive transfer compared to the effector memory T cells (T_{EM} ; $CD62L^- CCR7^-$), it would be pertinent to assess the phenotype of the transferred TILs before and after adoptive transfer (210). Selective migration of the T cells to CCR9⁺ or CCR9⁻ tumors was not observed

when assessed at d35, indicating that both the tumors were equally susceptible to immune infiltrate. However, the number of mice was too less to get statistical significance between the two groups and should be thus replicated with larger cohorts. Additionally, time course kinetic needs to be performed to assess whether more TILs infiltrate CCR9-ve tumor during the earlier time-points after adoptive T cell transfer, given that a starker difference in tumor growth is observed during the early stages. It would be even more interesting to evaluate and compare the exhaustion status (via PD-1, TIM-3 staining) and effector functions (IL-2 and IFN- γ secretion capacity, CD107a degranulation marker) of the T cells infiltrating the CCR9+ve and CCR9-ve tumors in a time-course based study and to compare this with the observed tumor regression profile. Even though PANC-1 tumor cells and adoptively transferred TIL 53 immune cells were HLA-matched, one cannot completely exclude the possibility of allogenic T cell reactivity in this non-autologous system. Use of PDX tumor models with tumor and TIL cultures derived from the same patient could address this issue. Nevertheless, the single preliminary *in vivo* experiment presented here needs to be repeated to get more meaningful insights into the relevance of CCR9 as a tumor immune suppressor.

Further development of CCR9 as an immunotherapeutic target for cancer treatment would require toxicological analysis based on the CCR9 knockout mouse model. Besides reduction in the $\gamma\delta$ IELs, CCR9 knockout mouse has been reported to show no adverse side effects (159). However, given that CCR9 is important for the homing of effector T cells to the gut, systemic targeting of CCR9 would be a contraindication for gut-associated tumors. On the other hand, CCR9 was found to be expressed on only a small minority of survivin-specific T cells (~ 6%) and was undetectable on peripheral blood TCs from healthy donors. Its expression in other immune cell subsets and that on healthy tissue remains to be examined.

5.3 Identification of tumor-associated immune activators by the RNAi screen

This study primarily focused on the validation of tumor-associated negative immune regulators that were identified as a result of the screening strategy. An equally interesting and opposite side of the same coin is the discovery of the positive immune regulators from the high-throughput screen, such as CXC-chemokine ligand 9 (CXCL9 or MIG) that facilitate anti-tumor activity of the CTLs. CXCL9 is an IFN- γ -inducible T cell chemoattractant that binds to the chemokine receptor CXCR3 (211). CXCL9 deficient tumors, as well as CXCL9

knockout mice, have been reported to inhibit the activation of tumor-reactive T cells (212, 213). Moreover, tumor-specific expression of CXCL9 has been reported to correlate with higher immune (CD8⁺ T cell) infiltrate and better prognosis in the colorectal cancer patients (214). Identification of such established immune activators lends support to the use of this screening approach for further identification of similar tumor-associated ligands that are vital for anti-tumor immunity. Along this line, GRM4 and GRK5 were found to be positively associated with the anti-tumor immunity in all the three screens.

GRM4 or metabotropic glutamate receptor 4 (mGluR4) is one of the eight receptors belonging to the glutamate receptor family that binds to L-glutamate, a neurotransmitter, which leads to the inhibition of the cyclic AMP cascade. Expression of GRM4 has been reported in non-neuronal tissues recently whereby normal epithelia of the upper respiratory tract, gastrointestinal tracts, breast, uterine cervix, urinary bladder and skin show GRM4 expression whereas thyroid, lung alveoli, liver, testis or prostate lacked any expression (215). Correspondingly, GRM4 expression has also been reported in colorectal cancer, malignant melanoma, laryngeal carcinoma and breast cancer, although expression was found to be associated with poor survival in CRC patients (215). Role of GRM4 in anti-tumor immunity has not been studied so far. However, by using GRM4^{-/-} mice, investigators working on autoimmune encephalomyelitis have shown that the expression of GRM4 on conventional DCs is important for the IFN- γ and IL-2 secretion by WT CD4 T cells upon stimulation (216). Further experimental validations of the role of tumor-specific expression of GRM4 on effector functions of antigen-specific T cells will be necessary in order to shed more light on the matter.

G protein-coupled receptor kinase 5 (GRK5) is a serine/threonine kinase that phosphorylates and deactivates GPCRs by allowing the binding of arrestin proteins that block receptors from activating downstream G protein pathways (217). Besides the regulation of GPCR activity, GRK5 has also been demonstrated to phosphorylate p53 transcription factor, inhibiting p53-mediated apoptotic pathway (218). Lately it has also been shown to positively regulate the NF- κ B signaling pathway by phosphorylating I κ B α (inhibitory κ B; which binds to and represses NF- κ B in the cytoplasm) leading to the release of NF- κ B transcription complex and subsequent activation of the NF- κ B pathway (219). Interestingly, activated NF- κ B in lung tumors of mice has been shown to orchestrate T-cell mediated rejection of immunogenic tumors and a similar correlation between the lung tumor NF- κ B activity and the T cell

infiltration has been documented in patient tumor samples (220). Whether this activation of the NF- κ B activity in tumor samples, which correlates with an enhanced immune surveillance, is dependent on GRK5 remains to be examined.

Further investigations into the role and mechanism of such newly discovered immune-activating ligands and their counterparts on the T cell side would be essential to exploit them as potentially suitable targets for agnostic antibody-based therapy in order to stimulate the anti-tumor immune surveillance in patients.

5.4 Outlook

In this thesis a screening methodology for uncovering novel immune modulators expressed by MCF7 breast tumor cell lines has been described. Given that tumors are heterogeneous, even in their expression of immune modulatory candidates, it would be essential to extend the screening approach to other tumor entities in order to identify overlapping as well as unique immunosuppressive signatures amongst different tumor types. As described in section 4.22, preliminary ground work has been laid down for replicating the screen in colorectal cancer using SW480 as the target cell line. Furthermore, application of the Luc-CTL assay to uncover immune-modulome in metastatic melanoma and pancreatic carcinoma have been undertaken in our laboratory by Tillmann Michels and Antonio Sorrentino, respectively, under my supervision. To adapt the screen as close to the patient setting as possible, tumor infiltrating lymphocyte cultures, established from melanoma and pancreatic cancer patients (TIL 412 and TIL 53 from the respective tumor types; described in section 4.11 and 4.12), were used as effector cells in the RNAi screen. TILs, which directly encounter the immunosuppressive tumor microenvironment, represent one of the best suited models for studying the dependency of T cell's cytotoxic capacity in response to tumor-specific expression of immune modulators. In a step further, primary melanoma cell cultures have been established from resected tumor of syngeneic patient and used as targets cells for the melanoma screen. Using siRNA libraries enriched in surface receptors and kinases that covered a total of 2800 gene targets, both the screens have identified a range of novel immunomodulatory candidates along with the well-reported immunosuppressors, such as JAK2 (103) and LPA (221), lending strength to the sensitivity and the detection capacity of the screening approach. Furthermore, CCR9 popped up as a strongly immunosuppressive hit

in the melanoma screen as well, while in-depth analysis of the pancreatic cancer screen is currently underway. Further functional validations of the novel candidate genes identified from both the screens are required and is being actively pursued.

Systematic dissection of the rather complex immune regulatory circuit mediated by different tumor types offers a great promise for therapeutic translation. The possibility and feasibility of using patient-derived pairs of primary tumor and T cells for immune-modulatory screening ushers this approach to the frontline of personalized medicine. In such a setting, tumor samples from a post-operative patient could be screened for relevant immunosuppressors which affect patient-specific anti-tumor immune response and these could then be targeted clinically to induce durable and protective responses in the patients. Nevertheless, increased immune reactivity upon checkpoint blockade requires a pre-existing immune response. Therefore, combining checkpoint blockade with immune response-inducing therapies, such as vaccination strategies, chemotherapy or radiotherapy that facilitate the mounting of T cell responses, would be an effective way for future treatments. Homing of the effector T cells to the tumor site might be improved by employing gene modified T cells (such as chimeric antigen receptor bearing T cells or CART cells expressing homing chemokine receptors) that are especially equipped to migrate to the tumor niche. Toxicities, which might be a limiting factor for the success of such immune-stimulatory approaches, might be restricted by considering local administration over systemic therapy, as has been demonstrated in the case of anti-CTLA4 antibody to control autoimmunity (222). Based on the above rationales, multi-combinatorial trials employing a cocktail of different therapeutic options are currently being tested with great vigor to maximize the therapeutic advantage for the patients.

Concluding remarks

Despite the capacity of the immune system to recognize and eliminate cancerous cells, effective immunotherapy based on the adoptive transfer of reactive T cells is opposed by the immunosuppressive interactions between the tumor and the T cells. Findings from the presented thesis have added to the functional characterization of the immunosuppressive nature of the tumor cells by establishing an immune function-based RNAi screen that systematically uncovers the repertoire of immune modulatory surface ligands on the tumor cells. This could serve as a great diagnostic tool for identifying patients that are best suited to benefit from a particular checkpoint blockade therapy or a cocktail of it thereof based on the expression of the repertoire of checkpoint candidates identified as a result of this screening system. Personalized immune screening in the future for tumor immune modulators could be employed to rapidly assess the patient-specific immune-modulome before devising immunotherapeutic treatment strategies. As a proof-of-principle of the screening methodology, the novel involvement of CCR9 - one of the top hits identified from the screening approach - in mediating immune suppression via differential regulation of the STAT pathways in antigen-experienced T cells is highlighted in this study. Given that CCR9 is well reported to be involved in cancer metastasis and in some instances tumor growth, targeting it clinically would mean hitting three birds with one stone: tumor growth, tumor metastasis and immune-resistance, making it an attractive target for further clinical and pharmaceutical investigations.

6. References:

1. Ferlay J SI, Ervik M, Dikshit R, Eser S, Mathers C, Rebelo M, Parkin DM, Forman D, Bray, F. (2013) Cancer Incidence and Mortality Worldwide: IARC CancerBase No. 11 [Internet]. *GLOBOCAN 2012 v1.0, Lyon, France: International Agency for Research on Cancer*. Available from: <http://globocan.iarc.fr>, (accessed on 09/04/2014.).
2. Hanahan D & Weinberg RA (2000) The hallmarks of cancer. *Cell* 100(1):57-70.
3. Hanahan D & Weinberg RA (2011) Hallmarks of cancer: the next generation. *Cell* 144(5):646-674.
4. Burnet FM (1970) The concept of immunological surveillance. *Progress in experimental tumor research* 13:1-27.
5. Clemente CG, *et al.* (1996) Prognostic value of tumor infiltrating lymphocytes in the vertical growth phase of primary cutaneous melanoma. *Cancer* 77(7):1303-1310.
6. Galon J, *et al.* (2006) Type, density, and location of immune cells within human colorectal tumors predict clinical outcome. *Science* 313(5795):1960-1964.
7. Chen DS & Mellman I (2013) Oncology meets immunology: the cancer-immunity cycle. *Immunity* 39(1):1-10.
8. Ferguson TA, Choi J, & Green DR (2011) Armed response: how dying cells influence T-cell functions. *Immunological reviews* 241(1):77-88.
9. Robbins PF, *et al.* (2013) Mining exomic sequencing data to identify mutated antigens recognized by adoptively transferred tumor-reactive T cells. *Nature medicine* 19(6):747-752.
10. Lee W, *et al.* (2010) The mutation spectrum revealed by paired genome sequences from a lung cancer patient. *Nature* 465(7297):473-477.
11. Alexandrov LB, *et al.* (2013) Signatures of mutational processes in human cancer. *Nature* 500(7463):415-421.
12. Franciszkievicz K, Boissonnas A, Boutet M, Combadiere C, & Mami-Chouaib F (2012) Role of chemokines and chemokine receptors in shaping the effector phase of the antitumor immune response. *Cancer research* 72(24):6325-6332.
13. Dudley ME & Rosenberg SA (2003) Adoptive-cell-transfer therapy for the treatment of patients with cancer. *Nature reviews. Cancer* 3(9):666-675.
14. Dunn GP, Bruce AT, Ikeda H, Old LJ, & Schreiber RD (2002) Cancer immunoediting: from immunosurveillance to tumor escape. *Nature immunology* 3(11):991-998.
15. Khong HT & Restifo NP (2002) Natural selection of tumor variants in the generation of "tumor escape" phenotypes. *Nature immunology* 3(11):999-1005.

16. Bicknell DC, Rowan A, & Bodmer WF (1994) Beta 2-microglobulin gene mutations: a study of established colorectal cell lines and fresh tumors. *Proceedings of the National Academy of Sciences of the United States of America* 91(11):4751-4755.
17. Hicklin DJ, Marincola FM, & Ferrone S (1999) HLA class I antigen downregulation in human cancers: T-cell immunotherapy revives an old story. *Molecular medicine today* 5(4):178-186.
18. Marincola FM, Jaffee EM, Hicklin DJ, & Ferrone S (2000) Escape of human solid tumors from T-cell recognition: molecular mechanisms and functional significance. *Advances in immunology* 74:181-273.
19. Hinrichs CS & Restifo NP (2013) Reassessing target antigens for adoptive T-cell therapy. *Nature biotechnology* 31(11):999-1008.
20. Thomas DA & Massague J (2005) TGF-beta directly targets cytotoxic T cell functions during tumor evasion of immune surveillance. *Cancer cell* 8(5):369-380.
21. Bouzin C, Brouet A, De Vriese J, Dewever J, & Feron O (2007) Effects of vascular endothelial growth factor on the lymphocyte-endothelium interactions: identification of caveolin-1 and nitric oxide as control points of endothelial cell anergy. *Journal of immunology* 178(3):1505-1511.
22. Sato T, *et al.* (2011) Interleukin 10 in the tumor microenvironment: a target for anticancer immunotherapy. *Immunologic research* 51(2-3):170-182.
23. Kalinski P (2012) Regulation of immune responses by prostaglandin E2. *Journal of immunology* 188(1):21-28.
24. Uyttenhove C, *et al.* (2003) Evidence for a tumoral immune resistance mechanism based on tryptophan degradation by indoleamine 2,3-dioxygenase. *Nature medicine* 9(10):1269-1274.
25. Munder M (2009) Arginase: an emerging key player in the mammalian immune system. *British journal of pharmacology* 158(3):638-651.
26. Curiel TJ, *et al.* (2004) Specific recruitment of regulatory T cells in ovarian carcinoma fosters immune privilege and predicts reduced survival. *Nature medicine* 10(9):942-949.
27. Kono K, *et al.* (2006) CD4(+)CD25high regulatory T cells increase with tumor stage in patients with gastric and esophageal cancers. *Cancer immunology, immunotherapy : CII* 55(9):1064-1071.
28. Liu F, *et al.* (2011) CD8(+) cytotoxic T cell and FOXP3(+) regulatory T cell infiltration in relation to breast cancer survival and molecular subtypes. *Breast cancer research and treatment* 130(2):645-655.
29. Schmidt HH, *et al.* (2013) HLA Class II tetramers reveal tissue-specific regulatory T cells that suppress T-cell responses in breast carcinoma patients. *Oncoimmunology* 2(6):e24962.

30. Oleinika K, Nibbs RJ, Graham GJ, & Fraser AR (2013) Suppression, subversion and escape: the role of regulatory T cells in cancer progression. *Clinical and experimental immunology* 171(1):36-45.
31. Caridade M, Graca L, & Ribeiro RM (2013) Mechanisms Underlying CD4+ Treg Immune Regulation in the Adult: From Experiments to Models. *Frontiers in immunology* 4:378.
32. Enk AH, Jonuleit H, Saloga J, & Knop J (1997) Dendritic cells as mediators of tumor-induced tolerance in metastatic melanoma. *International journal of cancer. Journal international du cancer* 73(3):309-316.
33. Troy AJ, Summers KL, Davidson PJ, Atkinson CH, & Hart DN (1998) Minimal recruitment and activation of dendritic cells within renal cell carcinoma. *Clinical cancer research : an official journal of the American Association for Cancer Research* 4(3):585-593.
34. Colonna M, Trinchieri G, & Liu YJ (2004) Plasmacytoid dendritic cells in immunity. *Nature immunology* 5(12):1219-1226.
35. Hartmann E, *et al.* (2003) Identification and functional analysis of tumor-infiltrating plasmacytoid dendritic cells in head and neck cancer. *Cancer research* 63(19):6478-6487.
36. Montero AJ, Diaz-Montero CM, Kyriakopoulos CE, Bronte V, & Mandruzzato S (2012) Myeloid-derived suppressor cells in cancer patients: a clinical perspective. *Journal of immunotherapy* 35(2):107-115.
37. Gabitass RF, Annels NE, Stocken DD, Pandha HA, & Middleton GW (2011) Elevated myeloid-derived suppressor cells in pancreatic, esophageal and gastric cancer are an independent prognostic factor and are associated with significant elevation of the Th2 cytokine interleukin-13. *Cancer immunology, immunotherapy : CII* 60(10):1419-1430.
38. Pittenger MF, *et al.* (1999) Multilineage potential of adult human mesenchymal stem cells. *Science* 284(5411):143-147.
39. Ljubic B, *et al.* (2013) Human mesenchymal stem cells creating an immunosuppressive environment and promote breast cancer in mice. *Scientific reports* 3:2298.
40. Aggarwal S & Pittenger MF (2005) Human mesenchymal stem cells modulate allogeneic immune cell responses. *Blood* 105(4):1815-1822.
41. Mantovani A & Locati M (2013) Tumor-associated macrophages as a paradigm of macrophage plasticity, diversity, and polarization: lessons and open questions. *Arteriosclerosis, thrombosis, and vascular biology* 33(7):1478-1483.
42. al-Sarireh B & Eremin O (2000) Tumour-associated macrophages (TAMS): disordered function, immune suppression and progressive tumour growth. *Journal of the Royal College of Surgeons of Edinburgh* 45(1):1-16.
43. Pardoll DM (2012) The blockade of immune checkpoints in cancer immunotherapy. *Nature reviews. Cancer* 12(4):252-264.

44. Brunet JF, *et al.* (1987) A new member of the immunoglobulin superfamily--CTLA-4. *Nature* 328(6127):267-270.
45. Linsley PS, *et al.* (1991) CTLA-4 is a second receptor for the B cell activation antigen B7. *The Journal of experimental medicine* 174(3):561-569.
46. Waterhouse P, *et al.* (1995) Lymphoproliferative disorders with early lethality in mice deficient in Ctl4-4. *Science* 270(5238):985-988.
47. Tivol EA, *et al.* (1995) Loss of CTLA-4 leads to massive lymphoproliferation and fatal multiorgan tissue destruction, revealing a critical negative regulatory role of CTLA-4. *Immunity* 3(5):541-547.
48. Townsend SE, Su FW, Atherton JM, & Allison JP (1994) Specificity and longevity of antitumor immune responses induced by B7-transfected tumors. *Cancer research* 54(24):6477-6483.
49. Leach DR, Krummel MF, & Allison JP (1996) Enhancement of antitumor immunity by CTLA-4 blockade. *Science* 271(5256):1734-1736.
50. Wing K, *et al.* (2008) CTLA-4 control over Foxp3+ regulatory T cell function. *Science* 322(5899):271-275.
51. Hodi FS, *et al.* (2010) Improved survival with ipilimumab in patients with metastatic melanoma. *The New England journal of medicine* 363(8):711-723.
52. Korn EL, *et al.* (2008) Meta-analysis of phase II cooperative group trials in metastatic stage IV melanoma to determine progression-free and overall survival benchmarks for future phase II trials. *Journal of clinical oncology : official journal of the American Society of Clinical Oncology* 26(4):527-534.
53. FDA (2011) FDA approves new treatment for a type of late-stage skin cancer. *The U.S. Food and Drug Administration*. March 25, 2011.
54. Attia P, *et al.* (2005) Autoimmunity correlates with tumor regression in patients with metastatic melanoma treated with anti-cytotoxic T-lymphocyte antigen-4. *Journal of clinical oncology : official journal of the American Society of Clinical Oncology* 23(25):6043-6053.
55. Wolchok JD, *et al.* (2009) Guidelines for the evaluation of immune therapy activity in solid tumors: immune-related response criteria. *Clinical cancer research : an official journal of the American Association for Cancer Research* 15(23):7412-7420.
56. Mellman I, Coukos G, & Dranoff G (2011) Cancer immunotherapy comes of age. *Nature* 480(7378):480-489.
57. Agata Y, *et al.* (1996) Expression of the PD-1 antigen on the surface of stimulated mouse T and B lymphocytes. *Int Immunol* 8(5):765-772.
58. Mazanet MM & Hughes CC (2002) B7-H1 is expressed by human endothelial cells and suppresses T cell cytokine synthesis. *Journal of immunology* 169(7):3581-3588.

59. Topalian SL, Drake CG, & Pardoll DM (2012) Targeting the PD-1/B7-H1(PD-L1) pathway to activate anti-tumor immunity. *Current opinion in immunology* 24(2):207-212.
60. Dong H, *et al.* (2002) Tumor-associated B7-H1 promotes T-cell apoptosis: a potential mechanism of immune evasion. *Nature medicine* 8(8):793-800.
61. Parsa AT, *et al.* (2007) Loss of tumor suppressor PTEN function increases B7-H1 expression and immunoresistance in glioma. *Nature medicine* 13(1):84-88.
62. Spranger S, *et al.* (2013) Up-regulation of PD-L1, IDO, and T(regs) in the melanoma tumor microenvironment is driven by CD8(+) T cells. *Science translational medicine* 5(200):200ra116.
63. Hino R, *et al.* (2010) Tumor cell expression of programmed cell death-1 ligand 1 is a prognostic factor for malignant melanoma. *Cancer* 116(7):1757-1766.
64. Liu J, *et al.* (2007) Plasma cells from multiple myeloma patients express B7-H1 (PD-L1) and increase expression after stimulation with IFN- γ and TLR ligands via a MyD88-, TRAF6-, and MEK-dependent pathway. *Blood* 110(1):296-304.
65. Ghebeh H, *et al.* (2006) The B7-H1 (PD-L1) T lymphocyte-inhibitory molecule is expressed in breast cancer patients with infiltrating ductal carcinoma: correlation with important high-risk prognostic factors. *Neoplasia* 8(3):190-198.
66. Sznol M & Chen L (2013) Antagonist antibodies to PD-1 and B7-H1 (PD-L1) in the treatment of advanced human cancer. *Clinical cancer research : an official journal of the American Association for Cancer Research* 19(5):1021-1034.
67. Amarnath S, *et al.* (2011) The PDL1-PD1 axis converts human TH1 cells into regulatory T cells. *Science translational medicine* 3(111):111ra120.
68. Blank C, *et al.* (2006) Blockade of PD-L1 (B7-H1) augments human tumor-specific T cell responses in vitro. *International journal of cancer. Journal international du cancer* 119(2):317-327.
69. Topalian SL, *et al.* (2012) Safety, activity, and immune correlates of anti-PD-1 antibody in cancer. *The New England journal of medicine* 366(26):2443-2454.
70. Wolchok JD, *et al.* (2013) Nivolumab plus ipilimumab in advanced melanoma. *The New England journal of medicine* 369(2):122-133.
71. Dhein J, Walczak H, Baumler C, Debatin KM, & Krammer PH (1995) Autocrine T-cell suicide mediated by APO-1/(Fas/CD95). *Nature* 373(6513):438-441.
72. Igney FH & Krammer PH (2005) Tumor counterattack: fact or fiction? *Cancer immunology, immunotherapy : CII* 54(11):1127-1136.
73. Liu FT & Rabinovich GA (2005) Galectins as modulators of tumour progression. *Nature reviews. Cancer* 5(1):29-41.

-
74. Perillo NL, Pace KE, Seilhamer JJ, & Baum LG (1995) Apoptosis of T cells mediated by galectin-1. *Nature* 378(6558):736-739.
 75. Peng W, Wang HY, Miyahara Y, Peng G, & Wang RF (2008) Tumor-associated galectin-3 modulates the function of tumor-reactive T cells. *Cancer research* 68(17):7228-7236.
 76. Demetriou M, Granovsky M, Quaggin S, & Dennis JW (2001) Negative regulation of T-cell activation and autoimmunity by Mgat5 N-glycosylation. *Nature* 409(6821):733-739.
 77. Zhu C, *et al.* (2005) The Tim-3 ligand galectin-9 negatively regulates T helper type 1 immunity. *Nature immunology* 6(12):1245-1252.
 78. Leitner J, *et al.* (2013) TIM-3 does not act as a receptor for galectin-9. *PLoS pathogens* 9(3):e1003253.
 79. Huang CT, *et al.* (2004) Role of LAG-3 in regulatory T cells. *Immunity* 21(4):503-513.
 80. Grosso JF, *et al.* (2007) LAG-3 regulates CD8+ T cell accumulation and effector function in murine self- and tumor-tolerance systems. *The Journal of clinical investigation* 117(11):3383-3392.
 81. Woo SR, *et al.* (2012) Immune inhibitory molecules LAG-3 and PD-1 synergistically regulate T-cell function to promote tumoral immune escape. *Cancer research* 72(4):917-927.
 82. Kuespert K, Pils S, & Hauck CR (2006) CEACAMs: their role in physiology and pathophysiology. *Current opinion in cell biology* 18(5):565-571.
 83. Gray-Owen SD & Blumberg RS (2006) CEACAM1: contact-dependent control of immunity. *Nature reviews. Immunology* 6(6):433-446.
 84. Witzens-Harig M, *et al.* (2013) Tumor cells in multiple myeloma patients inhibit myeloma-reactive T cells through carcinoembryonic-antigen-related cell adhesion molecule-6. *Blood*.
 85. Nakashima M, Sonoda K, & Watanabe T (1999) Inhibition of cell growth and induction of apoptotic cell death by the human tumor-associated antigen RCAS1. *Nature medicine* 5(8):938-942.
 86. Radvanyi L, *et al.* (2013) Antagonist antibodies to PD-1 and B7-H1 (PD-L1) in the treatment of advanced human cancer--letter. *Clinical cancer research : an official journal of the American Association for Cancer Research* 19(19):5541.
 87. Herbst RS (2013) A study of MPDL3280A, an engineered PD-L1 antibody in patients with locally advanced or metastatic tumors. *J Clin Oncol.* 31, (suppl; abstr 3000).
 88. Blackburn SD, *et al.* (2009) Coregulation of CD8+ T cell exhaustion by multiple inhibitory receptors during chronic viral infection. *Nature immunology* 10(1):29-37.

89. Boutros M & Ahringer J (2008) The art and design of genetic screens: RNA interference. *Nature reviews. Genetics* 9(7):554-566.
90. Fire A, *et al.* (1998) Potent and specific genetic interference by double-stranded RNA in *Caenorhabditis elegans*. *Nature* 391(6669):806-811.
91. Dorsett Y & Tuschl T (2004) siRNAs: applications in functional genomics and potential as therapeutics. *Nature reviews. Drug discovery* 3(4):318-329.
92. Hannon GJ (2002) RNA interference. *Nature* 418(6894):244-251.
93. de Fougerolles A, Vornlocher HP, Maraganore J, & Lieberman J (2007) Interfering with disease: a progress report on siRNA-based therapeutics. *Nature reviews. Drug discovery* 6(6):443-453.
94. Singel SM, *et al.* (2013) A targeted RNAi screen of the breast cancer genome identifies KIF14 and TLN1 as genes that modulate docetaxel chemosensitivity in triple-negative breast cancer. *Clinical cancer research : an official journal of the American Association for Cancer Research* 19(8):2061-2070.
95. Berns K, *et al.* (2007) A functional genetic approach identifies the PI3K pathway as a major determinant of trastuzumab resistance in breast cancer. *Cancer cell* 12(4):395-402.
96. Lara R, *et al.* (2011) An siRNA screen identifies RSK1 as a key modulator of lung cancer metastasis. *Oncogene* 30(32):3513-3521.
97. Pelz O, Gilsdorf M, & Boutros M (2010) web cellHTS2: a web-application for the analysis of high-throughput screening data. *BMC bioinformatics* 11:185.
98. Rieber N, Knapp B, Eils R, & Kaderali L (2009) RNAither, an automated pipeline for the statistical analysis of high-throughput RNAi screens. *Bioinformatics* 25(5):678-679.
99. Goktug AN, Ong SS, & Chen T (2012) GUItars: a GUI tool for analysis of high-throughput RNA interference screening data. *PloS one* 7(11):e49386.
100. Birmingham A, *et al.* (2009) Statistical methods for analysis of high-throughput RNA interference screens. *Nature methods* 6(8):569-575.
101. Boutros M, Bras LP, & Huber W (2006) Analysis of cell-based RNAi screens. *Genome biology* 7(7):R66.
102. Moita CF, Chora A, Hacohen N, & Moita LF (2012) RNAi screen for kinases and phosphatases that play a role in antigen presentation by dendritic cells. *European journal of immunology* 42(7):1843-1849.
103. Bellucci R, *et al.* (2012) Tyrosine kinase pathways modulate tumor susceptibility to natural killer cells. *The Journal of clinical investigation* 122(7):2369-2383.

104. Machlenkin A, *et al.* (2008) Capture of tumor cell membranes by trogocytosis facilitates detection and isolation of tumor-specific functional CTLs. *Cancer research* 68(6):2006-2013.
105. Wang M, Windgassen D, & Papoutsakis ET (2008) A global transcriptional view of apoptosis in human T-cell activation. *BMC medical genomics* 1:53.
106. Gilbert DF, *et al.* (2011) A novel multiplex cell viability assay for high-throughput RNAi screening. *PloS one* 6(12):e28338.
107. Brown CE, *et al.* (2005) Biophotonic cytotoxicity assay for high-throughput screening of cytolytic killing. *Journal of immunological methods* 297(1-2):39-52.
108. Brackertz B, *et al.* (2011) FLT3-regulated antigens as targets for leukemia-reactive cytotoxic T lymphocytes. *Blood cancer journal* 1(3):e11.
109. Dudley ME, *et al.* (2010) CD8+ enriched "young" tumor infiltrating lymphocytes can mediate regression of metastatic melanoma. *Clinical cancer research : an official journal of the American Association for Cancer Research* 16(24):6122-6131.
110. Dudley ME, Wunderlich JR, Shelton TE, Even J, & Rosenberg SA (2003) Generation of tumor-infiltrating lymphocyte cultures for use in adoptive transfer therapy for melanoma patients. *J Immunother* 26(4):332-342.
111. Schafer H, Schafer A, Kiderlen AF, Masihi KN, & Burger R (1997) A highly sensitive cytotoxicity assay based on the release of reporter enzymes, from stably transfected cell lines. *Journal of immunological methods* 204(1):89-98.
112. Fu X, *et al.* (2010) A simple and sensitive method for measuring tumor-specific T cell cytotoxicity. *PloS one* 5(7):e11867.
113. Brunner KT, Mael J, Cerottini JC, & Chapuis B (1968) Quantitative assay of the lytic action of immune lymphoid cells on 51-Cr-labelled allogeneic target cells in vitro; inhibition by isoantibody and by drugs. *Immunology* 14(2):181-196.
114. Stein JA, Adler A, Efraim SB, & Maor M (1976) Immunocompetence, immunosuppression, and human breast cancer. I. An analysis of their relationship by known parameters of cell-mediated immunity in well-defined clinical stages of disease. *Cancer* 38(3):1171-1187.
115. Simms PE & Ellis TM (1996) Utility of flow cytometric detection of CD69 expression as a rapid method for determining poly- and oligoclonal lymphocyte activation. *Clinical and diagnostic laboratory immunology* 3(3):301-304.
116. Hoffmann SC, Wabnitz GH, Samstag Y, Moldenhauer G, & Ludwig T (2011) Functional analysis of bispecific antibody (EpCAMxCD3)-mediated T-lymphocyte and cancer cell interaction by single-cell force spectroscopy. *International journal of cancer. Journal international du cancer* 128(9):2096-2104.
117. Witzens-Harig M, *et al.* (2013) Tumor cells in multiple myeloma patients inhibit myeloma-reactive T cells through carcinoembryonic antigen-related cell adhesion molecule-6. *Blood* 121(22):4493-4503.

118. Henkart PA (1996) ICE Family Proteases: Mediators of All Apoptotic Cell Death? *Immunity* 4(3):195-201.
119. Boldin MP, Goncharov TM, Goltseve YV, & Wallach D (1996) Involvement of MACH, a Novel MORT1/FADD-Interacting Protease, in Fas/APO-1- and TNF Receptor-Induced Cell Death. *Cell* 85(6):803-815.
120. Wurbel MA, *et al.* (2000) The chemokine TECK is expressed by thymic and intestinal epithelial cells and attracts double- and single-positive thymocytes expressing the TECK receptor CCR9. *European journal of immunology* 30(1):262-271.
121. Fan Z & Zhang Q (2005) Molecular mechanisms of lymphocyte-mediated cytotoxicity. *Cellular & molecular immunology* 2(4):259-264.
122. Jin HT, *et al.* (2010) Cooperation of Tim-3 and PD-1 in CD8 T-cell exhaustion during chronic viral infection. *Proceedings of the National Academy of Sciences of the United States of America* 107(33):14733-14738.
123. Sakuishi K, *et al.* (2010) Targeting Tim-3 and PD-1 pathways to reverse T cell exhaustion and restore anti-tumor immunity. *The Journal of experimental medicine* 207(10):2187-2194.
124. Society AC (2010) Cancer Facts & Figures 2010. *Atlanta: American Cancer Society.*
125. von Bernstorff W, *et al.* (2001) Systemic and local immunosuppression in pancreatic cancer patients. *Clinical cancer research : an official journal of the American Association for Cancer Research* 7(3 Suppl):925s-932s.
126. Yu H, Pardoll D, & Jove R (2009) STATs in cancer inflammation and immunity: a leading role for STAT3. *Nature reviews. Cancer* 9(11):798-809.
127. Koido S, *et al.* (2013) Immunotherapy for colorectal cancer. *World journal of gastroenterology : WJG* 19(46):8531-8542.
128. Rodel C, *et al.* (2003) Spontaneous and radiation-induced apoptosis in colorectal carcinoma cells with different intrinsic radiosensitivities: survivin as a radioresistance factor. *International journal of radiation oncology, biology, physics* 55(5):1341-1347.
129. Hill HR & Martins TB (2006) The flow cytometric analysis of cytokines using multi-analyte fluorescence microarray technology. *Methods* 38(4):312-316.
130. Bachmann MF, Barner M, Viola A, & Kopf M (1999) Distinct kinetics of cytokine production and cytolysis in effector and memory T cells after viral infection. *European journal of immunology* 29(1):291-299.
131. Slifka MK, Rodriguez F, & Whitton JL (1999) Rapid on/off cycling of cytokine production by virus-specific CD8+ T cells. *Nature* 401(6748):76-79.
132. Dunn GP, Sheehan KC, Old LJ, & Schreiber RD (2005) IFN unresponsiveness in LNCaP cells due to the lack of JAK1 gene expression. *Cancer research* 65(8):3447-3453.

133. Koup RA, Graham BS, & Douek DC (2011) The quest for a T cell-based immune correlate of protection against HIV: a story of trials and errors. *Nature reviews. Immunology* 11(1):65-70.
134. Lichtenfels R, Biddison WE, Schulz H, Vogt AB, & Martin R (1994) CARE-LASS (calcein-release-assay), an improved fluorescence-based test system to measure cytotoxic T lymphocyte activity. *Journal of immunological methods* 172(2):227-239.
135. Kolber MA, Quinones RR, Gress RE, & Henkart PA (1988) Measurement of cytotoxicity by target cell release and retention of the fluorescent dye bis-carboxyethyl-carboxyfluorescein (BCECF). *Journal of immunological methods* 108(1-2):255-264.
136. Sheehy ME, McDermott AB, Furlan SN, Klenerman P, & Nixon DF (2001) A novel technique for the fluorometric assessment of T lymphocyte antigen specific lysis. *Journal of immunological methods* 249(1-2):99-110.
137. Virag L, Kerekgyarto C, & Facht J (1995) A simple, rapid and sensitive fluorimetric assay for the measurement of cell-mediated cytotoxicity. *Journal of immunological methods* 185(2):199-208.
138. Aubry JP, *et al.* (1999) Annexin V used for measuring apoptosis in the early events of cellular cytotoxicity. *Cytometry* 37(3):197-204.
139. Jerome KR, Sloan DD, & Aubert M (2003) Measurement of CTL-induced cytotoxicity: the caspase 3 assay. *Apoptosis : an international journal on programmed cell death* 8(6):563-571.
140. Lecoeur H, Fevrier M, Garcia S, Riviere Y, & Gougeon ML (2001) A novel flow cytometric assay for quantitation and multiparametric characterization of cell-mediated cytotoxicity. *Journal of immunological methods* 253(1-2):177-187.
141. Sepp A, Binns RM, & Lechler RI (1996) Improved protocol for colorimetric detection of complement-mediated cytotoxicity based on the measurement of cytoplasmic lactate dehydrogenase activity. *Journal of immunological methods* 196(2):175-180.
142. Schlee M, Hornung V, & Hartmann G (2006) siRNA and isRNA: two edges of one sword. *Molecular therapy : the journal of the American Society of Gene Therapy* 14(4):463-470.
143. Thakur A & Lum LG (2010) Cancer therapy with bispecific antibodies: Clinical experience. *Current opinion in molecular therapeutics* 12(3):340-349.
144. Corse E, Gottschalk RA, Krogsgaard M, & Allison JP (2010) Attenuated T cell responses to a high-potency ligand in vivo. *PLoS biology* 8(9).
145. Zhong S, *et al.* (2013) T-cell receptor affinity and avidity defines antitumor response and autoimmunity in T-cell immunotherapy. *Proceedings of the National Academy of Sciences of the United States of America* 110(17):6973-6978.

146. Gehring AJ, *et al.* (2009) Profile of tumor antigen-specific CD8 T cells in patients with hepatitis B virus-related hepatocellular carcinoma. *Gastroenterology* 137(2):682-690.
147. Zhou H, *et al.* (2008) Genome-scale RNAi screen for host factors required for HIV replication. *Cell host & microbe* 4(5):495-504.
148. Brass AL, *et al.* (2008) Identification of host proteins required for HIV infection through a functional genomic screen. *Science* 319(5865):921-926.
149. Konig R, *et al.* (2008) Global analysis of host-pathogen interactions that regulate early-stage HIV-1 replication. *Cell* 135(1):49-60.
150. Goff SP (2008) Knockdown screens to knockout HIV-1. *Cell* 135(3):417-420.
151. Dorsam RT & Gutkind JS (2007) G-protein-coupled receptors and cancer. *Nature reviews. Cancer* 7(2):79-94.
152. Hopkins AL & Groom CR (2002) The druggable genome. *Nature reviews. Drug discovery* 1(9):727-730.
153. Echeverri CJ, *et al.* (2006) Minimizing the risk of reporting false positives in large-scale RNAi screens. *Nature methods* 3(10):777-779.
154. Sledz CA & Williams BR (2004) RNA interference and double-stranded-RNA-activated pathways. *Biochemical Society transactions* 32(Pt 6):952-956.
155. Zhu Y, Yao S, & Chen L (2011) Cell surface signaling molecules in the control of immune responses: a tide model. *Immunity* 34(4):466-478.
156. Maraqa L, *et al.* (2008) Carcinoembryonic antigen cell adhesion molecule 6 predicts breast cancer recurrence following adjuvant tamoxifen. *Clinical cancer research : an official journal of the American Association for Cancer Research* 14(2):405-411.
157. Zaballos A, Gutierrez J, Varona R, Ardavin C, & Marquez G (1999) Cutting edge: identification of the orphan chemokine receptor GPR-9-6 as CCR9, the receptor for the chemokine TECK. *Journal of immunology* 162(10):5671-5675.
158. Zabel BA, *et al.* (1999) Human G protein-coupled receptor GPR-9-6/CC chemokine receptor 9 is selectively expressed on intestinal homing T lymphocytes, mucosal lymphocytes, and thymocytes and is required for thymus-expressed chemokine-mediated chemotaxis. *The Journal of experimental medicine* 190(9):1241-1256.
159. Wurbel MA, *et al.* (2001) Mice lacking the CCR9 CC-chemokine receptor show a mild impairment of early T- and B-cell development and a reduction in T-cell receptor gammadelta(+) gut intraepithelial lymphocytes. *Blood* 98(9):2626-2632.
160. Shen X, *et al.* (2009) CC chemokine receptor 9 enhances proliferation in pancreatic intraepithelial neoplasia and pancreatic cancer cells. *Journal of gastrointestinal surgery : official journal of the Society for Surgery of the Alimentary Tract* 13(11):1955-1962; discussion 1962.

161. Johnson-Holiday C, *et al.* (2011) CCL25 mediates migration, invasion and matrix metalloproteinase expression by breast cancer cells in a CCR9-dependent fashion. *International journal of oncology* 38(5):1279-1285.
162. Singh R, Stockard CR, Grizzle WE, Lillard JW, Jr., & Singh S (2011) Expression and histopathological correlation of CCR9 and CCL25 in ovarian cancer. *International journal of oncology* 39(2):373-381.
163. Hadeiba H, *et al.* (2008) CCR9 expression defines tolerogenic plasmacytoid dendritic cells able to suppress acute graft-versus-host disease. *Nature immunology* 9(11):1253-1260.
164. Agace WW (2008) T-cell recruitment to the intestinal mucosa. *Trends in immunology* 29(11):514-522.
165. Almeida JR, *et al.* (2009) Antigen sensitivity is a major determinant of CD8+ T-cell polyfunctionality and HIV-suppressive activity. *Blood* 113(25):6351-6360.
166. La Gruta NL, Turner SJ, & Doherty PC (2004) Hierarchies in cytokine expression profiles for acute and resolving influenza virus-specific CD8+ T cell responses: correlation of cytokine profile and TCR avidity. *J Immunol* 172(9):5553-5560.
167. Wilde S, *et al.* (2012) Human antitumor CD8+ T cells producing Th1 polycytokines show superior antigen sensitivity and tumor recognition. *J Immunol* 189(2):598-605.
168. Akdis CA & Blaser K (2001) Mechanisms of interleukin-10-mediated immune suppression. *Immunology* 103(2):131-136.
169. Rosenberg SA, *et al.* (2011) Durable complete responses in heavily pretreated patients with metastatic melanoma using T-cell transfer immunotherapy. *Clinical cancer research : an official journal of the American Association for Cancer Research* 17(13):4550-4557.
170. Turcotte S, *et al.* (2013) Phenotype and function of T cells infiltrating visceral metastases from gastrointestinal cancers and melanoma: implications for adoptive cell transfer therapy. *J Immunol* 191(5):2217-2225.
171. Freeman GJ, *et al.* (2000) Engagement of the PD-1 immunoinhibitory receptor by a novel B7 family member leads to negative regulation of lymphocyte activation. *The Journal of experimental medicine* 192(7):1027-1034.
172. Frazier AD, *et al.* (2010) Programmed death-1 affects suppressor of cytokine signaling-1 expression in T cells during hepatitis C infection. *Viral immunology* 23(5):487-495.
173. Yang ZZ, *et al.* (2012) IL-12 upregulates TIM-3 expression and induces T cell exhaustion in patients with follicular B cell non-Hodgkin lymphoma. *The Journal of clinical investigation* 122(4):1271-1282.
174. Fallarino F & Gajewski TF (1999) Cutting edge: differentiation of antitumor CTL in vivo requires host expression of Stat1. *J Immunol* 163(8):4109-4113.

175. Li X, Leung S, Qureshi S, Darnell JE, Jr., & Stark GR (1996) Formation of STAT1-STAT2 heterodimers and their role in the activation of IRF-1 gene transcription by interferon-alpha. *The Journal of biological chemistry* 271(10):5790-5794.
176. Grange M, *et al.* (2012) Activated STAT5 promotes long-lived cytotoxic CD8+ T cells that induce regression of autochthonous melanoma. *Cancer research* 72(1):76-87.
177. Campanero MR, *et al.* (1992) Functional role of alpha 2/beta 1 and alpha 4/beta 1 integrins in leukocyte intercellular adhesion induced through the common beta 1 subunit. *European journal of immunology* 22(12):3111-3119.
178. Boisvert M, Gendron S, Chetoui N, & Aoudjit F (2007) Alpha2 beta1 integrin signaling augments T cell receptor-dependent production of interferon-gamma in human T cells. *Molecular immunology* 44(15):3732-3740.
179. Yan X, Johnson BD, & Orentas RJ (2008) Induction of a VLA-2 (CD49b)-expressing effector T cell population by a cell-based neuroblastoma vaccine expressing CD137L. *J Immunol* 181(7):4621-4631.
180. Pipkin ME, *et al.* (2010) Interleukin-2 and inflammation induce distinct transcriptional programs that promote the differentiation of effector cytolytic T cells. *Immunity* 32(1):79-90.
181. Naghavi MH, Hatzioannou T, Gao G, & Goff SP (2005) Overexpression of fasciculation and elongation protein zeta-1 (FEZ1) induces a post-entry block to retroviruses in cultured cells. *Genes & development* 19(9):1105-1115.
182. Ishii H, *et al.* (2001) FEZ1/LZTS1 gene at 8p22 suppresses cancer cell growth and regulates mitosis. *Proceedings of the National Academy of Sciences of the United States of America* 98(18):10374-10379.
183. Li S, *et al.* (2000) Cytokine-induced Src homology 2 protein (CIS) promotes T cell receptor-mediated proliferation and prolongs survival of activated T cells. *The Journal of experimental medicine* 191(6):985-994.
184. Dobrzanski MJ, Reome JB, Hollenbaugh JA, Hyland JC, & Dutton RW (2004) Effector cell-derived lymphotoxin alpha and Fas ligand, but not perforin, promote Tc1 and Tc2 effector cell-mediated tumor therapy in established pulmonary metastases. *Cancer research* 64(1):406-414.
185. Mehrle S, Schmidt J, Buchler MW, Watzl C, & Marten A (2008) Enhancement of anti-tumor activity in vitro and in vivo by CD150 and SAP. *Molecular immunology* 45(3):796-804.
186. Mamonkin M, *et al.* (2013) Differential roles of KLF4 in the development and differentiation of CD8+ T cells. *Immunology letters* 156(1-2):94-101.
187. Wen X, Liu H, Xiao G, & Liu X (2011) Downregulation of the transcription factor KLF4 is required for the lineage commitment of T cells. *Cell research* 21(12):1701-1710.

188. Qi Z & Sun XH (2004) Hyperresponse to T-cell receptor signaling and apoptosis of Id1 transgenic thymocytes. *Molecular and cellular biology* 24(17):7313-7323.
189. Tzachanis D, *et al.* (2001) Tob is a negative regulator of activation that is expressed in anergic and quiescent T cells. *Nature immunology* 2(12):1174-1182.
190. Luo H, Wan X, Wu Y, & Wu J (2001) Cross-linking of EphB6 resulting in signal transduction and apoptosis in Jurkat cells. *J Immunol* 167(3):1362-1370.
191. Abouzahr S, *et al.* (2006) Identification of target actin content and polymerization status as a mechanism of tumor resistance after cytolytic T lymphocyte pressure. *Proceedings of the National Academy of Sciences of the United States of America* 103(5):1428-1433.
192. Chen Z, Chen L, Qiao SW, Nagaishi T, & Blumberg RS (2008) Carcinoembryonic antigen-related cell adhesion molecule 1 inhibits proximal TCR signaling by targeting ZAP-70. *J Immunol* 180(9):6085-6093.
193. Yoshimura A, Naka T, & Kubo M (2007) SOCS proteins, cytokine signalling and immune regulation. *Nature reviews. Immunology* 7(6):454-465.
194. Vicari AP, *et al.* (1997) TECK: a novel CC chemokine specifically expressed by thymic dendritic cells and potentially involved in T cell development. *Immunity* 7(2):291-301.
195. Shailesh Singh PS, Rajesh Singh and William Grizzle (2010) Role of CCR9-CCL25 axis in Prostate Cancer Metastasis. *The Journal of Immunology* 184 (Meeting Abstract Supplement) (133.7).
196. Muthumani K, *et al.* (2011) HIV-mediated phosphatidylinositol 3-kinase/serine-threonine kinase activation in APCs leads to programmed death-1 ligand upregulation and suppression of HIV-specific CD8 T cells. *J Immunol* 187(6):2932-2943.
197. Jiang X, Zhou J, Giobbie-Hurder A, Wargo J, & Hodi FS (2013) The activation of MAPK in melanoma cells resistant to BRAF inhibition promotes PD-L1 expression that is reversible by MEK and PI3K inhibition. *Clinical cancer research : an official journal of the American Association for Cancer Research* 19(3):598-609.
198. Crane CA, *et al.* (2009) PI(3) kinase is associated with a mechanism of immunoresistance in breast and prostate cancer. *Oncogene* 28(2):306-312.
199. Sharma PK, *et al.* (2010) CCR9 mediates PI3K/AKT-dependent antiapoptotic signals in prostate cancer cells and inhibition of CCR9-CCL25 interaction enhances the cytotoxic effects of etoposide. *International journal of cancer. Journal international du cancer* 127(9):2020-2030.
200. Hahnel PS, *et al.* (2008) Targeting AKT signaling sensitizes cancer to cellular immunotherapy. *Cancer research* 68(10):3899-3906.
201. Zhou P, *et al.* (2014) In vivo discovery of immunotherapy targets in the tumour microenvironment. *Nature* 506(7486):52-57.

-
202. Richmond A & Su Y (2008) Mouse xenograft models vs GEM models for human cancer therapeutics. *Disease models & mechanisms* 1(2-3):78-82.
 203. Ito M, *et al.* (2002) NOD/SCID/gamma(c)(null) mouse: an excellent recipient mouse model for engraftment of human cells. *Blood* 100(9):3175-3182.
 204. Kim JB, *et al.* (2010) Non-invasive detection of a small number of bioluminescent cancer cells in vivo. *PloS one* 5(2):e9364.
 205. Keshav S, *et al.* (2013) A randomized controlled trial of the efficacy and safety of CCX282-B, an orally-administered blocker of chemokine receptor CCR9, for patients with Crohn's disease. *PloS one* 8(3):e60094.
 206. Tubo NJ, *et al.* (2012) A systemically-administered small molecule antagonist of CCR9 acts as a tissue-selective inhibitor of lymphocyte trafficking. *PloS one* 7(11):e50498.
 207. Klebanoff CA, *et al.* (2005) Central memory self/tumor-reactive CD8+ T cells confer superior antitumor immunity compared with effector memory T cells. *Proceedings of the National Academy of Sciences of the United States of America* 102(27):9571-9576.
 208. Yee C, *et al.* (2002) Adoptive T cell therapy using antigen-specific CD8+ T cell clones for the treatment of patients with metastatic melanoma: in vivo persistence, migration, and antitumor effect of transferred T cells. *Proceedings of the National Academy of Sciences of the United States of America* 99(25):16168-16173.
 209. Tong X, *et al.* (2009) The mechanism of chemokine receptor 9 internalization triggered by interleukin 2 and interleukin 4. *Cellular & molecular immunology* 6(3):181-189.
 210. Berger C, *et al.* (2008) Adoptive transfer of effector CD8+ T cells derived from central memory cells establishes persistent T cell memory in primates. *The Journal of clinical investigation* 118(1):294-305.
 211. Tensen CP, *et al.* (1999) Human IP-9: A keratinocyte-derived high affinity CXC-chemokine ligand for the IP-10/Mig receptor (CXCR3). *The Journal of investigative dermatology* 112(5):716-722.
 212. Petro M, *et al.* (2013) Cutaneous tumors cease CXCL9/Mig production as a result of IFN-gamma-mediated immunoediting. *J Immunol* 190(2):832-841.
 213. Anton Gorbachev DK, Marianne Petro and Robert Fairchild (2012) Distinct functions of CXCL9/Mig and CXCL10/IP-10 in the priming of tumor-specific IFN-g producing effector T cells. *The Journal of Immunology*. 188 (Meeting Abstract Supplement) 46.2.
 214. Mlecnik B, *et al.* (2010) Biomolecular network reconstruction identifies T-cell homing factors associated with survival in colorectal cancer. *Gastroenterology* 138(4):1429-1440.

-
215. Chang HJ, *et al.* (2005) Metabotropic glutamate receptor 4 expression in colorectal carcinoma and its prognostic significance. *Clinical cancer research : an official journal of the American Association for Cancer Research* 11(9):3288-3295.
 216. Fallarino F, *et al.* (2010) Metabotropic glutamate receptor-4 modulates adaptive immunity and restrains neuroinflammation. *Nature medicine* 16(8):897-902.
 217. Premont RT & Gainetdinov RR (2007) Physiological roles of G protein-coupled receptor kinases and arrestins. *Annual review of physiology* 69:511-534.
 218. Chen X, *et al.* (2010) G-protein-coupled receptor kinase 5 phosphorylates p53 and inhibits DNA damage-induced apoptosis. *The Journal of biological chemistry* 285(17):12823-12830.
 219. Patial S, Luo J, Porter KJ, Benovic JL, & Parameswaran N (2010) G-protein-coupled-receptor kinases mediate TNFalpha-induced NFkappaB signalling via direct interaction with and phosphorylation of IkappaBalpha. *The Biochemical journal* 425(1):169-178.
 220. Hopewell EL, *et al.* (2013) Lung tumor NF-kappaB signaling promotes T cell-mediated immune surveillance. *The Journal of clinical investigation* 123(6):2509-2522.
 221. Oda SK, *et al.* (2013) Lysophosphatidic Acid inhibits CD8 T cell activation and control of tumor progression. *Cancer immunology research* 1:245-255.
 222. Sandin LC, *et al.* (2014) Local CTLA4 blockade effectively restrains experimental pancreatic adenocarcinoma growth in vivo. *Oncoimmunology* 3(1):e27614.

Declaration

I, Nisit Khandelwal, herewith declare that I have completed this thesis single-handedly without any unauthorized help of a second party. Any help that I have received in my research work or in the preparation of this thesis has been duly acknowledged.

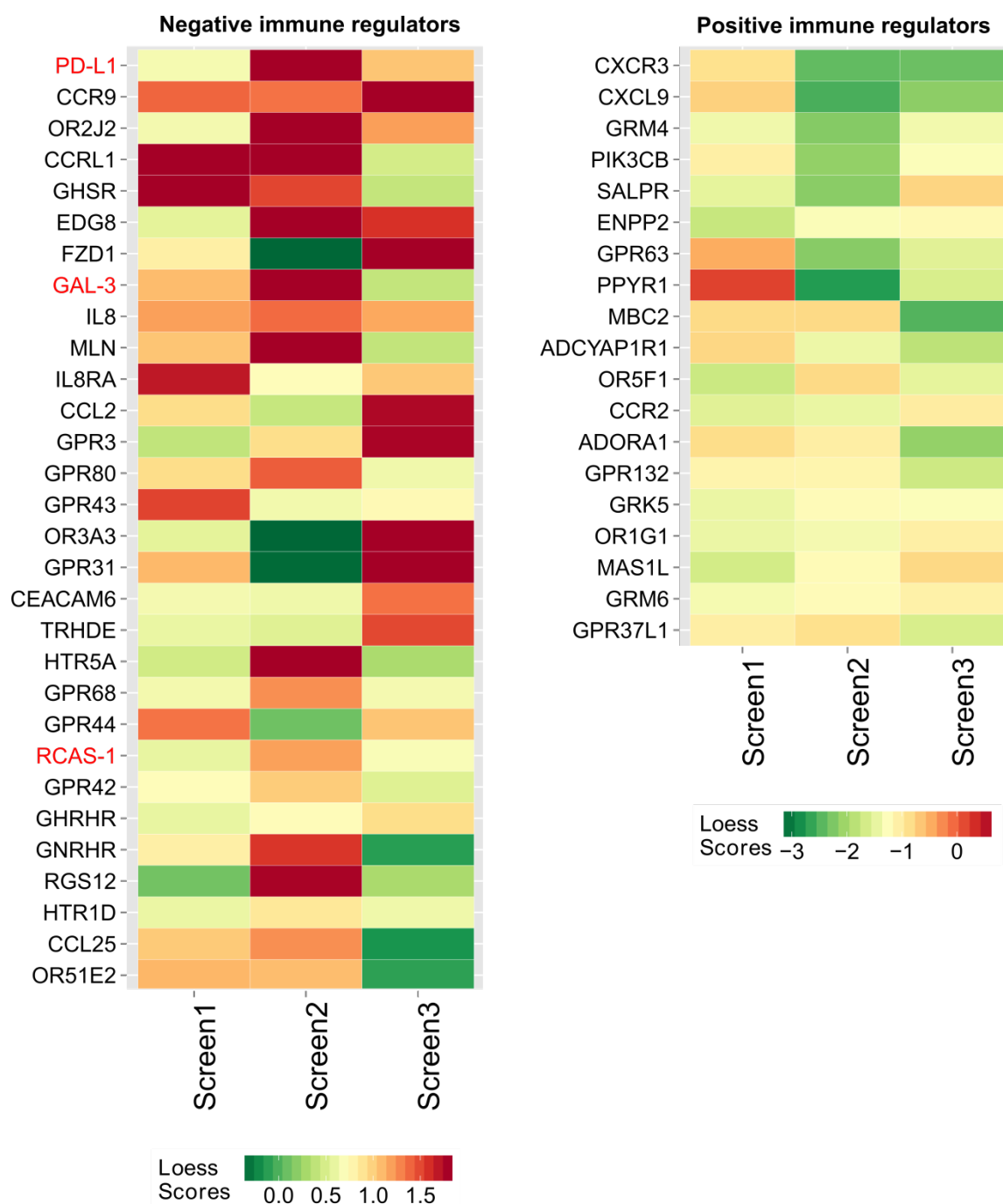
Heidelberg, 05.06.2014

Nisit Khandelwal

7. Appendix

Supplementary Table 1: Lethal siRNAs used as viability controls with reported function of their targeted genes

siRNA Target	Function
COPB2	Constitutes the coat of nonclathrin-coated vesicles and is essential for Golgi budding, vesicular trafficking.
PLK1	Serine/threonine-protein kinase that regulates centrosome maturation and spindle assembly.
UBC	Polyubiquitin precursor, involved in DNA repair, cell-cycle regulation, protein degradation.
CHK1	Required for checkpoint mediated cell cycle arrest in response to DNA damage.
ELMO2	Involved in cytoskeletal rearrangements required for phagocytosis of apoptotic cells.



Supplementary Figure 1. Filtered hit-list of candidate immune modulatory genes identified from the RNAi screen. Genes that satisfied the screen-specific threshold criteria (detailed in text and methods) for the toxicity and the viability values in two screens or more were shortlisted and the sum of their loess differential score in all three screens was calculated. Based on this sum, genes were ranked for their immunomodulatory strength and defined as negative ($\Sigma\text{loess} > 2.0$) or positive ($\Sigma\text{loess} < -3.3$) immune regulatory candidates. The individual loess scores of the shortlisted candidate genes across the three different screen setups are represented herein as heatmaps. Note the difference in the coloring scales of the individual heatmaps used for highlighting the relative performance of candidate genes across the three setups.

8. Abbreviations and definitions

%	percentage	CTL(s)	cytotoxic T cell(s)
~	approximately	CTLA-4	cytotoxic T lymphocyte associated antigen 4
°C	degree celsius	d	day(s)
⁵¹ Cr	radioactive chromium isotope 51	DC	dendritic cells
7-AAD	7-amino actinomycin D	ddH ₂ O	double distilled water
AB	human serum type AB	DKFZ	German Cancer Research Center
ACK	ammonium chloride potassium phosphate	DMEM	dulbecco's modified Eagle's medium
APC	antigen presenting cell	DMSO	dimethyl sulfoxide
ATCC	American Type Culture Collection	DNA	deoxyribonucleic acid
BCECF	2',7'-bis-(2-carboxyethyl)-5-(and-6)-carboxyfluorescein	DTT	dithiothreitol
BD	Becton Dickinson	<i>E. coli</i>	<i>Escherichia coli</i>
bp(s)	base pair(s)	E:T	effector to target ratio
BSA	bovine serum albumin	ECL	enhanced chemiluminescent
bsAb	bi-specific antibody	EDTA	ethylenediaminetetraacetic acid
Ca ²⁺	calcium	EFNA1	ephrin-A1
CCL25	chemokine (C-C motif) ligand 25	EGFP	enhanced green fluorescent protein
CCR9	chemokine (C-C motif) receptor 9	ELISpot	enzyme-linked immunospot assay
CD	cluster of differentiation	env	envelope proteins gene
cDNA	complementary DNA	EpCAM	epithelial cell adhesion molecule
CEACAM	carcinoembryonic antigen related cell adhesion molecule	et al.	Latin " <i>et alii</i> ", - "and others"
CFSE	carboxyfluorescein succinimidyl ester	FACS	fluorescence activated cell sorting/flow cytometry
CISH	cytokine inducible SH2-containing protein	FCS	fetal calf serum
CLM	complete lymphoma medium	FDA	Food and Drug Administration
cm ²	square centimeter	Fluc	firefly luciferase
CO ₂	carbon dioxide	Foxp3	forkhead box P3
CTG	CellTiter-Glo	g	gram(s)

G protein	guanosine nucleotide binding proteins	mAb(s)	monoclonal antibody(ies)
G418	geneticin sulfate	MART-1	melanocytic differentiation antigen
gag	group antigens gene	MDSC	myeloid-derived suppressor cells
GM-CSF	granulocyte macrophage colony-stimulating factor	mg	milligram
gp100	glycoprotein 100	Mg ²⁺	magnesium
GPCR	G protein-coupled receptor	MHC	major histocompatibility complex
h	hour(s)	min	minute(s)
HEPES	2-[4-(2-hydroxyethyl)piperazin-1-yl]ethanesulfonic acid	miRNA	micro-RNA
HLA-A2	human leukocyte antigen A2	ml	milliliter
HRP	horseradish peroxidase	mm	millimeter
HRP	horseradish peroxidase	mM	millimolar
hu	human	mRNA	messenger RNA
i.v.	intravenous	MUH	4-Methylumbelliferyl heptanoate
ID1	inhibitor of DNA binding 1	n	number
IDO	indoleamine 2,3-dioxygenase	NEAA	non-essential amino acid
IFN	interferon	NF- κ B	nuclear factor 'kappa-light-chain-enhancer "of activated B-cells)
IgG	immunoglobulin G	NK	natural killer
IL	interleukin	nm	nanometer
IL2RA	Interleukin-2 receptor alpha	NOD	non-obese diabetic
ITGA2	integrin, alpha 2	ns	not significant
IVC	individually ventilated cages	NSG	NOD <i>scid</i> gamma
kb	kilobase	nt	nucleotides
kd	knockdown	OKT-3	Muromonab-CD3
kDa	kilodalton	p	p-value
L	liter	P/S	penicillin/streptomycin
LAG3	lymphocyte-activation gene 3	PAGE	polyacrylamide gel electrophoresis
LTA	Lymphotoxin alpha	PBMC	peripheral blood mononuclear cells
luc	luciferase	PBS	phosphate buffered saline
M	molar	PBS-T	PBS-Tween
mA	milliampere		

PCR	polymerase chain reaction	TH1	T helper type-I
PD-1	programmed cell death 1	TIL(s)	tumor infiltrating lymphocyte(s)
PD-L1	programmed cell death 1 ligand 1	TOB1	transducer of ERBB2, 1
PerCPCy5.5	peridinin-chlorophyllprotein-complex-cyanine	TRAIL	TNF-related apoptosis inducing ligand
pH	Latin " <i>potentia hydrogenii</i> "	Treg	regulatory T cells
pol	reverse transcriptase, RNase H and integrase gene	U	unit
PTX	pertussis toxin	UV	ultraviolet
PVDF	polyvinylidene difluoride	V	volt
r	recombinant	VEGF	vascular endothelial growth factor
RFP	red fluorescent protein	VSV-G	vesicular stomatitis indiana virus-G protein
RLU	relative luminescence units	w/v	weight/volume
RNA	ribonucleic acid	WB	western blot
RNAi	RNA interference	WHO	World Health Organization
rpm	rounds per minute	wt	wild type
RPMI	Roswell park memorial institute	X	x-fold
RT	room temperature	α	alpha
s.c.	subcutaneous	β	beta
S.O.C.	super optimal broth medium with catabolite repression	γ	gamma
SCID	severe combined immunodeficient	μg	microgram
SDS	sodium dodecyl sulfate	μm	micrometer
SEM	standard error of the mean		
shRNA	short hairpin RNA		
siRNA	small interfering RNA		
SOCS1	suppressor of cytokine signaling 1		
STAT	signal transducers and activators of transcription		
TAE	Tris-Acetate-EDTA		
TAP	transporter associated with antigen processing		
TCR	T cell receptor		